DET NORSKE VIDENSKAPS-AKADEMI I OSLO

GEOFYSISKE PUBLIKASJONER
GEOPHYSICA NORVEGICA

Vol. XXVIII. No. 4 February 1972

PER B. STOREBØ

Steady State Aerosols

OSLO 1972
UNIVERSITETSFORLAGET

GEOFYSISKE PUBLIKASJONER

GEOPHYSICA NORVEGICA

VOL. XXVIII NO. 4

STEADY STATE AEROSOLS

By

Per B. Storebø

FREMLAGT I VIDENSKAPS-AKADEMIETS MØTE DEN 16. APRIL 1971 AV HESSTVEDT.

Summary. In the search for causal relationship between aerosol formation parameters and aerosol characteristics, calculations on models are presented. Formation parameters treated are supply mass, mode and spread, dilution with pure air, and particle removal. Coagulation within the aerosol is treated as a continuous phenomenon concerning all particle size combinations present. The effect is a sort of inverse relationship between distribution density of particles at medium/large and at small sizes.

A number of resulting size distributions are shown. Aerosols are classified in two groups. Aerosols with slow coagulation have low mass and contain either few particles or have a narrow size distribution, preferably at small sizes. Aerosols with faster coagulation display a distinct medium size particle mode, and they have few small particles.

The distribution of individual elements of natural radioactivity on particle size is also presented. Simple aerosol age estimates based on radioactivity measurements are shown to be questionable.

1. Introduction. For any aerosol, the particle size distribution is the result of 1) a continuous particle supply to the air, 2) solid mass production from vapours or gases in the air, 3) mass flow from small to large particles caused by coagulation, 4) removal of particles, and 5) admixture of new air to the aerosol. Since weather is variable, since none of the processes mentioned are constant, and since most conditions change when air moves from place to place, the immediate size distribution of particles in an aerosol does not necessarily reflect a steady state.

The steady state size distribution is nevertheless the desired distribution, and as such, should be of particular interest. In an earlier paper (7) an attempt was made to calculate this distribution when parameters for supply, production, and removal were known.

Since the parameters involved have no universal value, the applicability of such calculations is restricted by the model chosen. In this paper the method has been improved, and a wider range of aerosols is examined. Furthermore, dilution of the aerosol due to air exchanges has been included, and the steady-state distributions of natural radioactivity on the particles are treated.

2. Method of computation. The radii of the particles of interest are spread over a wide size range, and calculation of pertinent numbers for sizes spaced evenly on a logarithmic scale seems to be most appropriate.

The smallest particle radius considered in this study was $6 \cdot 10^{-8}$ cm, in the size range of a free atom with air molecules attached (6). The largest size considered was $5 \cdot 10^{-3}$ cm radius, i.e. 50μ, and well above the peak of the size distributions normally encountered in the atmosphere.

Since no distribution could have particles above this size, the model implies an absolute sink for such particles. Only small resultant errors are expected.

Within each size decade calculations were performed for approximately 10 fixed sizes, and the distribution was represented by the concentration of particles per logarithmic unit of size for the sizes chosen.

The steady state distribution was approximated step by step in conciliation with the instantaneous parameters for supply, coagulation, dilution, and removal of particles.

2.1 Specification of parameters. If N is the total particle concentration in the aerosol, the concentration density per logarithmic size unit at radius r_j is

$$n_j = \left(\frac{dN}{d\log r/r_0}\right)_j$$

where r is measured in units of r_0.

Production of molecular size particles within the aerosol, presumably by radioactive, chemical, or photochemical processes, was assumed to occur at a rate of c_1 particles per second per cm^3. These particles were supposed to be of the smallest size considered, and conversion to concentration density was performed in a way that gave the correct rate of supply, when that quantity was computed by integration from the input distribution:

$$\frac{dn_1}{dt} = \frac{c_1}{\log r_1/r_2} \tag{2.1}$$

where index 1 indicates the lower limit of the computation interval, while index 2 refers to the next size for which calculations were made.

The numerical value of c_1 was normally chosen as 100.

The size distribution for the rest of the particles supplied to an aerosol from sources outside the aerosol may be highly variable. A log-normal distribution was chosen to represent the concentration density versus radius. It does not necessarily express the supply correctly, but the procedure allows for a wide variability in mode, spread, and rate of supply.

The change due to supply is thus

$$\frac{dn_j}{dt} = \phi \cdot n_{j0} \tag{2.2}$$

where ϕ is a constant for supply.

Since (2.2) represents a matrix without reference to the distribution formula, it will be assumed in the further treatment that (2.1) has been included in this matrix.

Removal of particles was supposed to increase with the radius according to a power function

$$\frac{dn_j}{dt} = -\alpha \cdot n_j \cdot \left(\frac{r_j}{r_p}\right)^g \qquad (2.3)$$

where α is the removal coefficient for size r_p, and g is the removal exponent. In this paper $r_p = 1\mu$, and α is thus the removed fraction per second of particles of 1μ radius.

Based on fall velocity as the removing agent, g should be equal to 2 in the Stoke regime. For smaller particles, fall velocity is so small that modifications in the formula are of no practical value.

Since ultimate removal takes place at the earth's surface, additional transport processes to the surface should be considered. It is obvious that some sort of circulation, either orderly or of an interchange nature, occurs in most aerosols. This will work in the same manner on all particles and smooth out differences in size-dependent displacement, i.e., g will decrease below 2.

The actual deposition on the ground is more likely to occur by inertial impaction, i.e. the particles strike against obstacles, or for the very small particles by deposition on surfaces due to Brownian motion. This implies a very complicated and variable size dependence.

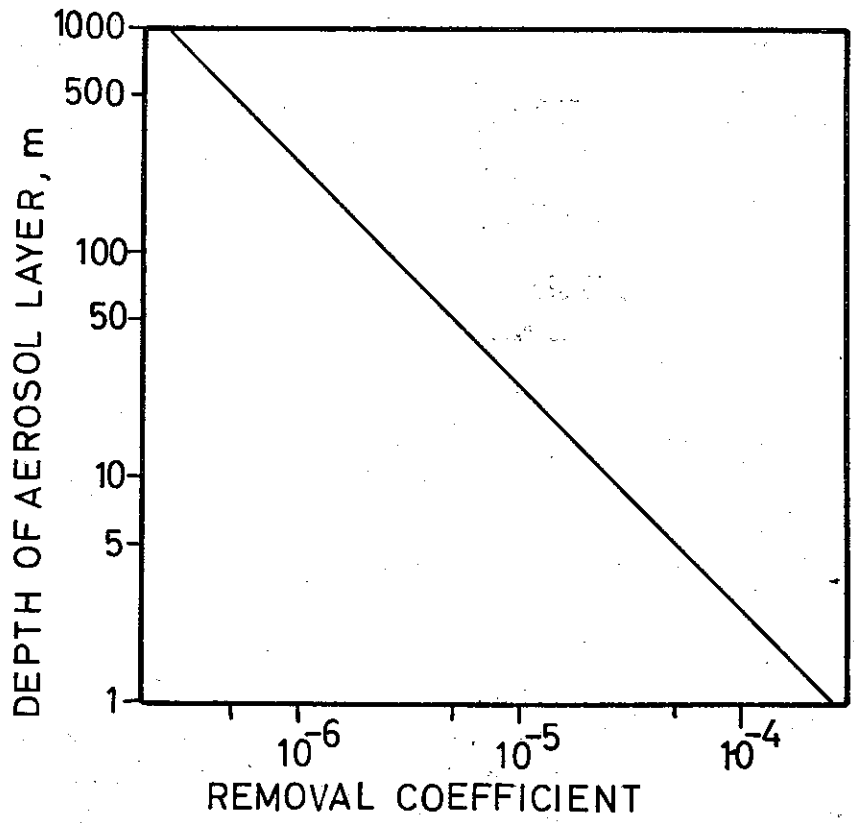

Fig. 2.1. *Minimum value of removal coefficient.*

However, the formation of dense aerosol layers over cities only, seems to indicate that the surface works as a rather good sink. The bottle-neck in the removal process is then the downward transport, giving g a value between 0 and 2.

Calculation based on particle fall thus constitutes a minimum removal rate. Figure 2.1 shows the connection between depth of an aerosol layer and the minimum value of the removal coefficient, i.e. the removal rate for a 1μ radius particle. It is based on particle fall time from the middle of the aerosol layer.

Mixing of outside air with an aerosol layer should also be taken into account. It is hardly possible to find an aerosol where no exchange takes place with the environment. In this paper it is assumed that the environment consists of pure air, with pure dilution as a result. The intensity of the dilution is expressed by the air replacement time T, i.e. the time necessary to replace the whole air mass in the aerosol at the constant rate of mixing. The effect on the particle concentration is given by:

$$\frac{dn_j}{dt} = -\frac{n_j}{T} = -\gamma \cdot n_j \tag{2.4}$$

where γ is the coefficient of dilution.

2.2 Internal change due to coagulation. With regard to coagulation it was assumed that formulas valid for spherical particles were sufficiently accurate for the purpose. Since most particles are loosely bound aggregates, coagulation should not result in compound particles with forms or properties radically different from those of the parent particles. The specific density for such particles was assumed to be 1.

The rate of formation of coagulated particles, consisting of one particle with radius r_i and another with radius r_j when concentrations were n_i and n_j, was determined by

$$\frac{dn}{dt} = 4\pi(r_i + r_j) \cdot (D_i + D_j) \cdot n_i \cdot n_j \cdot \beta_{ij} = K_{i,j} \cdot n_i \cdot n_j \tag{2.5}$$

where the D's are particle diffusion coefficients, β_{ij} is Fuchs' correction term (3), and $K_{i,j}$ is the coagulation coefficient between the two particle sizes.

For the diffusion coefficients an empirical formula was used, the constants of which are presented by Fuchs (3).

$$D_j = \frac{k \cdot T}{6\pi\eta r_i}\left(1 + 1.246\frac{\lambda}{r_i} + 0.42\frac{\lambda}{r_i} \cdot \exp\left(-0.87\frac{r_i}{\lambda}\right)\right) \tag{2.6}$$

where k is Boltzmann's constant, T is absolute temperature, η is air viscosity, and λ is the mean free path of air molecules.

The basic philosophy for Fuchs' correction term β is as follows: When particle size is close to basic step-length for the motions, the diffusion process cannot be considered continuous close to the surface. Basic step-length is defined by a quantity l, which should be the average distance covered by a particle before its original direction is completely changed. This is the same as the distance covered by a particle in a viscous medium due to a start velocity equal to its thermal equilibrium velocity

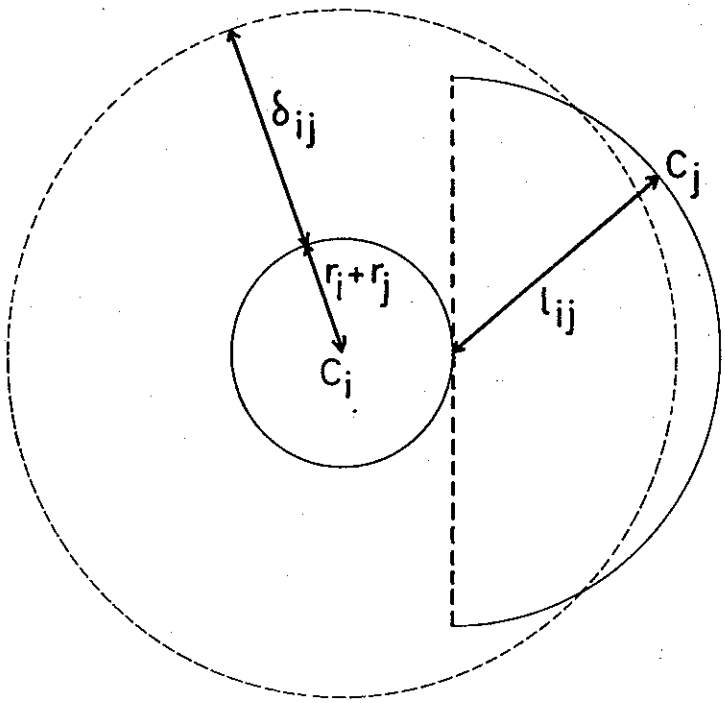

Fig. 2.2. *Quantities in Fuchs' coagulation treatment.*

$$l=\frac{2r^2\rho}{9\eta}\cdot\left(\frac{8kT}{\pi m}\right)^{\frac{1}{2}}\cdot\left(1+1.246\frac{\lambda}{r}+0.42\frac{\lambda}{r}\cdot\exp\left(-0.87\cdot\frac{r}{\lambda}\right)\right) \tag{2.7}$$

where r, ρ, and m are particle radius, density, and mass; η, T and λ are medium viscosity, temperature, and mean free molecular path, while k is the Bolzmann constant.

Based on the basic step-length and the particle radii r_i and r_j, a distance δ_{ij} from the particle surfaces is defined, inside which microscopic diffusion considerations exist, and outside which macroscopic conditions prevail.

The situation is sketched in Figure 2.2. Two particles with radii r_i and r_j have their centres at C_i and C_j, and the figure is meant to represent the situation one step before coagulation occurs. Both particles are in relative motion, but the reasoning may proceed as though one particle were at rest if basic step-lengths l_i and l_j are substituted by relative step-length

$$l_{ij}=(l_i^2+l_j^2)^{\frac{1}{2}} \tag{2.8}$$

When C_j coincides with the surface of the contact sphere around C_i with radius r_i+r_j, the two particles are in contact and by definition coagulate. δ_{ij} is thus the mean distance between the surface of the contact sphere and the surface of a hemisphere with radius l_{ij}, centred on the surface of the contact sphere:

$$\delta_{ij}=\frac{(r_i+r_j+l_{ij})^3-\{(r_i+r_j)^2+l_{ij}^2\}^{3/2}}{3(r_i+r_j)\cdot l_{ij}} \tag{2.9}$$

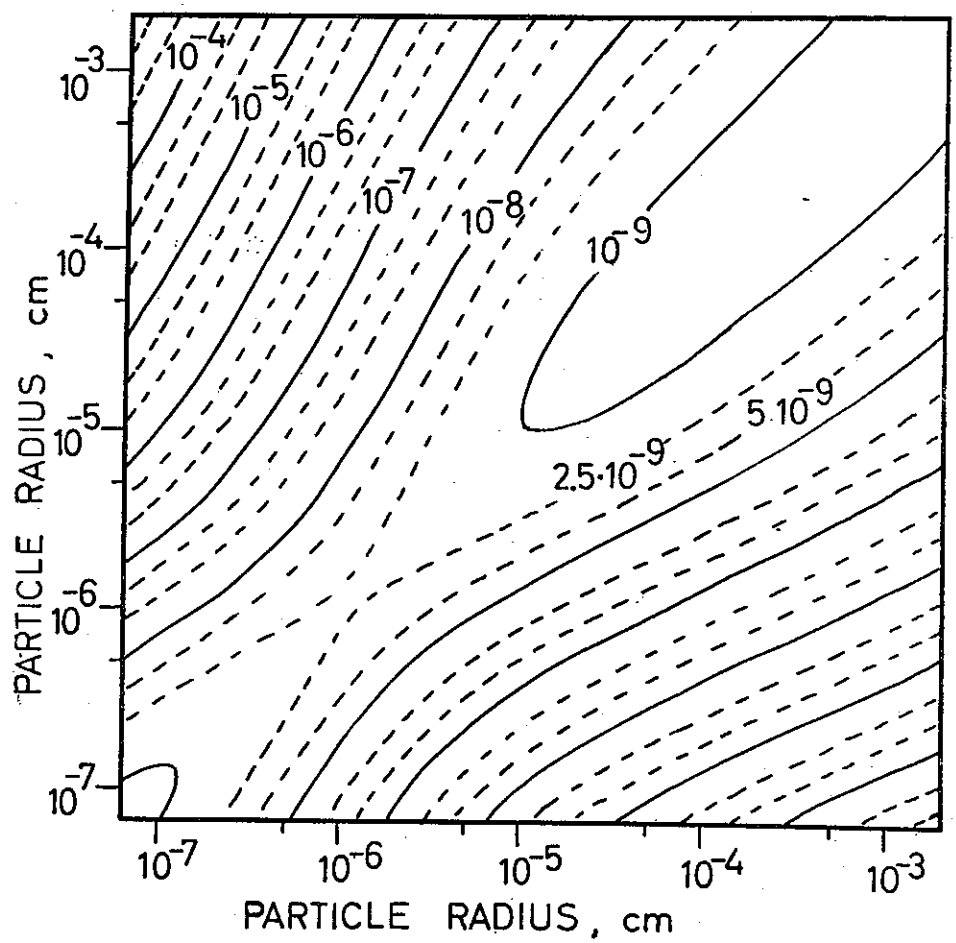

Fig. 2.3. *Coagulation coefficient*, 293 K and 1013 mb.

If the particle concentration at the surface of the sphere with radius $r_i+r_j+\delta_{ij}$ is n_j' and far away n_j, the particle flow towards C_i is determined by macroscopic diffusion considerations:

$$\frac{dn}{dt}=4\pi\cdot(r_i+r_j+\delta_{ij})\cdot(D_i+D_j)\cdot(n_j-n_j') \tag{2.10}$$

Further in towards the contact sphere the particles move in straight lines, and if it is assumed that no type of reflection occurs at contact

$$\frac{dn}{dt}=4\pi\cdot(r_i+r_j)^2\cdot n_j'\cdot\frac{G_{ij}}{4} \tag{2.11}$$

where G_{ij} is the relative thermal velocity of the particles:

$$G_{ij}=\left\{\frac{8kT}{\pi}\left(\frac{1}{m_i}+\frac{1}{m_j}\right)\right\}^{\frac{1}{2}} \tag{2.12}$$

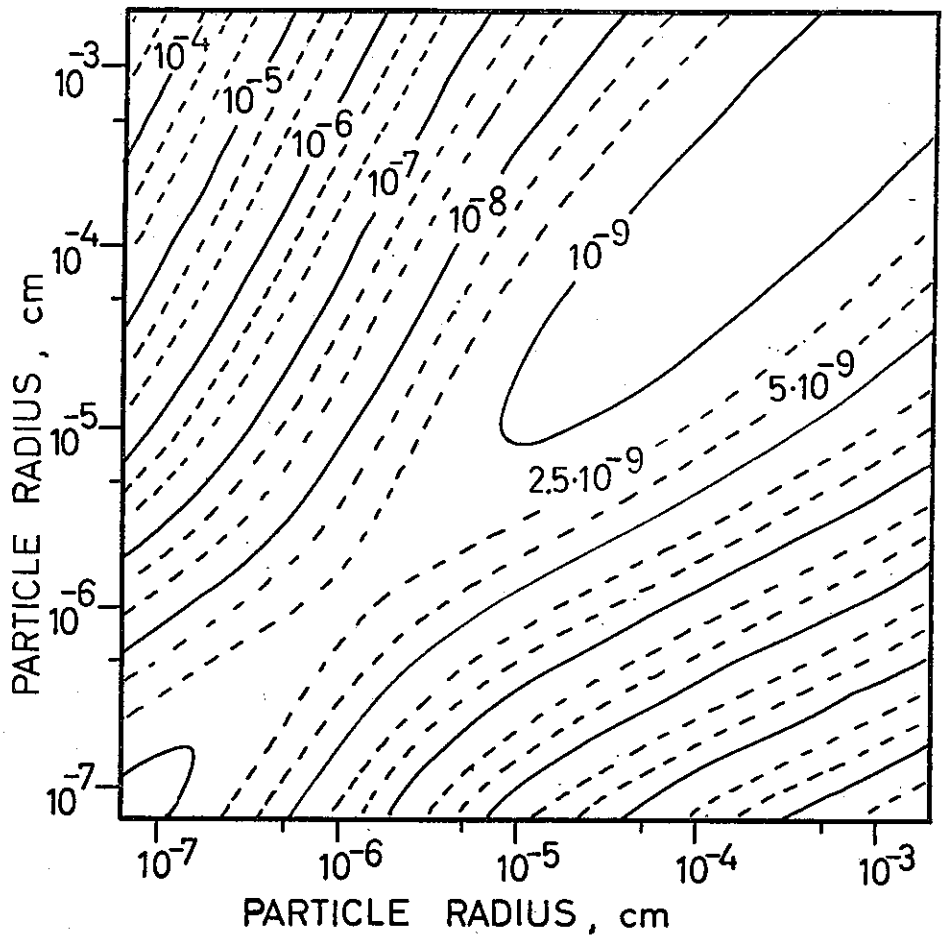

Fig. 2.4. *Coagulation coefficient*, 253 K and 1013 mb.

Elimination of n_j' between the two particle flow expressions (2.10) and (2.11) leads to Fuchs' correction term for coagulation

$$\beta_{ij} = \frac{(r_i + r_j + \delta_{ij}) \cdot G_{ij} \cdot (r_i + r_j)}{G_{ij}(r_i + r)^2 + 4(D_i + D_j) \cdot (r_i + r_j + \delta_{ij})} \tag{2.13}$$

The resulting values for the coagulation coefficients over the whole region of computation are shown in Figure 2.3. Computation is performed for 293 K and 1013.25 mb. Absolute values increase slightly with temperature and pressure, and Figures 2.4 and 2.5 show the coagulation coefficient for 253 K and 800 mb respectively.

When coagulation coefficients for different combinations are studied, the striking feature is the similar values obtained when relative sizes only are invariant. For the strength of coagulation a size shift of the whole distribution has little importance, as long as the relative distribution, as it appears on a $dN/d\log r/r_0$ diagram, is of the same shape.

Coagulation of particles causes redistribution of mass or volume among the different particle sizes. With volume as independent variable, the change in the particle density distribution can easily be seen to follow (3)

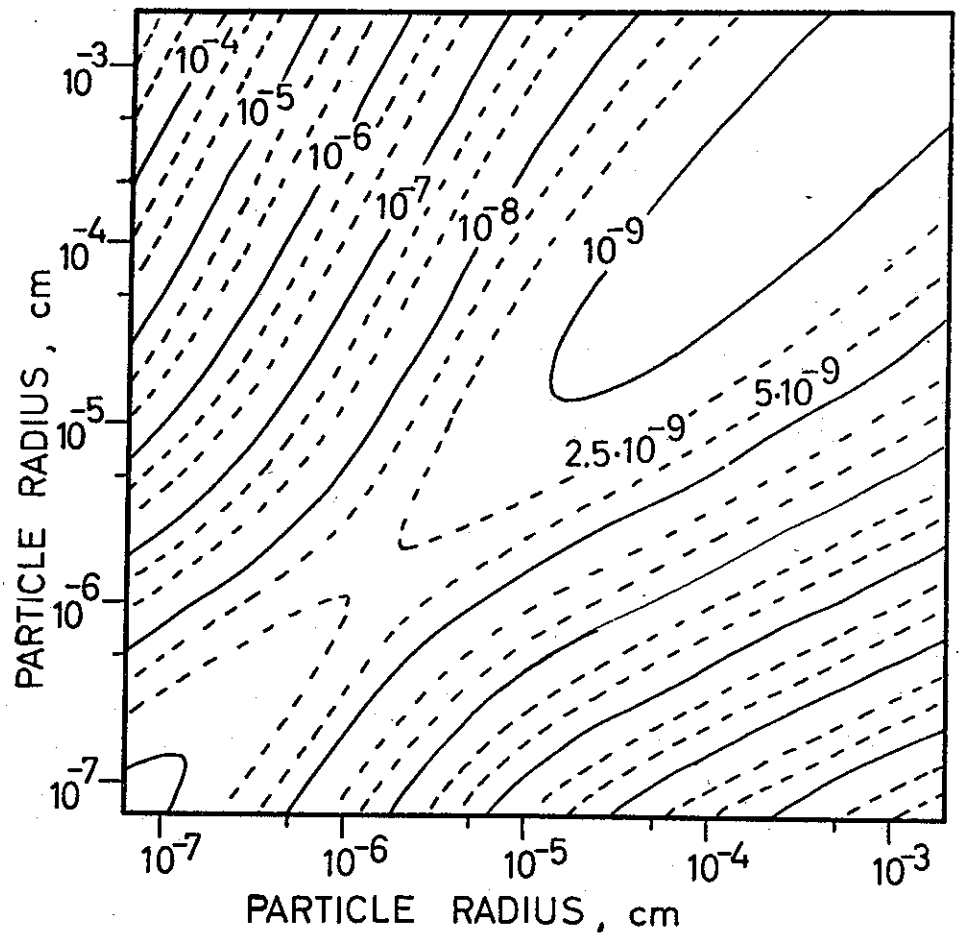

Fig. 2.5. *Coagulation coefficient.* 293 K and 800 mb.

$$\frac{dn(v_j)}{dt} = \int_{v_{min}}^{v_j/2} K_{i,j-i} \cdot n(v_i) \cdot n(v_j - v_i) \cdot dv_i - n(v_j) \cdot \int_{v_{min}}^{\infty} K_{i,j} \cdot n(v_i) \cdot dv_i \quad (2.14)$$

where $n(v)$ is the concentration density of particles per unit volume interval at volume v, and v_{min} is the volume of the smallest particle in the aerosol.

If log$r$ is used as independent variable, the equation reads

$$\frac{dn_j}{dt} = \int_{r_{min}}^{r_j \cdot 2^{-1/3}} K_{i,k} \cdot n_i \cdot n_k \cdot \frac{r_j^3}{r_k^3} \cdot d\log\frac{r_i}{r_0} - n_j \cdot \int_{r_{min}}^{\infty} K_{i,j} \cdot n_i \cdot d\log\frac{r_i}{r_0} \quad (2.15)$$

where index k indicates the complementary size of i, i.e. $v_k + v_i = v_j$.

Regarding the first integral, the computational work is much facilitated if account of particle concentration is kept for intervals in size so that particle volume is doubled from one size to the next higher up. As indicated in Figure 2.6, formation of new particles of size r_j then occurs when one particle from a size lower than r_{j-1} coagulates with one particle of size between r_j and r_{j-1}, the boundary case being two particles of size

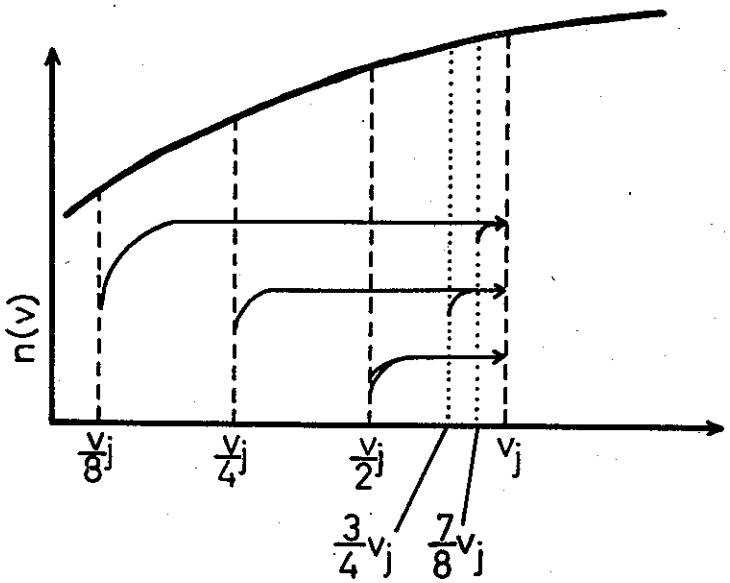

Fig. 2.6. *Particle combinations during coagulation calculation.*

r_{j-1} forming one particle of size r_j. This was the system chosen for the calculations. It leads to the distribution being expressed by nearly 10 numbers per decade of size.

During computation, all interpolations of products of n and K were performed linearly on a log$r$ scale. For integration, the trapezoidal method on the n-logr/r_0-diagram was used.

2.3 Steady state conditions. In an aerosol on which all the processes mentioned are at work, the particle concentration per logarithmic unit of size is determined by:

$$\frac{dn_j}{dt} = \phi \cdot n_{j0} + \int_{r_{min}}^{r_j \cdot 2^{-1/s}} K_{i,k} \cdot n_i \cdot n_k \cdot \frac{r_j^3}{r_k^3} \cdot d\log\frac{r_i}{r_0} -$$

$$n_j \cdot \left\{ \int_{r_{min}}^{\infty} K_{i,j} \cdot n_i \cdot d\log\frac{r_i}{r_0} + \alpha \cdot \left(\frac{r_j}{r_p}\right)^g + \gamma \right\} \qquad (2.16)$$

where the first term on the right-hand side expresses supply of particles to the aerosol, the second term particle transfer to the size in question due to coagulation of smaller particles in the distribution, while the third term expresses reduction in particle concentration due to coagulation, removal from the aerosol and exchange of part of the aerosol with pure air.

A steady state approximation for n_j is found from a start-distribution by requiring that the right-hand side of (2.16) be zero. Since considerable feed-back is present due to the two integration terms, and since 50 interdependent matrix numbers are present, the steady state was approximated step by step.

The direct expression from (2.16) does not lead to a rapid convergence. During computation it was therefore incorporated in a method in which successive values

were assumed to lie on a hyperbola branch, so that the value of the asymptote was the one to be sought. In general, the steady state was considered found when none of the n_j's describing the distribution was reset by more than 0.001 of the value in the previous step.

In order to avoid corrections due solely to wrong mass, a normalization procedure was used after each step. If it is assumed that all numbers in the distribution must be multiplied by a factor F in order to secure a mass balance, F may be found by equating the mass loss per unit of time

$$F \cdot \rho \cdot \alpha \cdot \int_{r_{min}}^{r_{max}} n_j \cdot v_j \cdot \left(\frac{r_j}{r_p}\right)^g d\log\frac{r_i}{r_0} + F^2 \cdot n_{max} \cdot v_{max} \cdot \rho \cdot \int_{r_{min}}^{r_{max}} K_{j,max} \cdot n_j \cdot d\log\frac{r_i}{r_0}$$

to the mass supply

$$\phi \cdot \rho \cdot \int_{r_{min}}^{r_{max}} n_{j0} \cdot v_j \cdot d\log\frac{r_i}{r_0}$$

Although close to 1, the factor F is seldom identical with 1 during the calculations. It is believed that smaller computation intervals would improve the accuracy. However, it is not believed that the general results would be altered.

3. Internal transfer in steady-state aerosols. Once a steady state is found, several quantities describing the steady state are of interest and can be computed. Aerosol mass concentration is

$$M = \int_{r_{min}}^{\infty} \frac{4}{3}\pi \cdot r_i^3 \cdot \rho \cdot n_i \cdot d\log\frac{r_i}{r_0}$$

where ρ is the aerosol density, in this paper set to 1.

Mass turnover time (i.e. the mean residence time of the mass in the aerosol) is the ratio between M and the corresponding quantity in the rate of supply matrix:

$$T = \frac{M}{\phi \cdot \int_{r_{min}}^{\infty} \frac{4}{3}\pi \cdot r_i^3 \cdot \rho \cdot n_{0i} \cdot d\log\frac{r_i}{r_0}} \tag{3.1}$$

An analogous quantity for a specific particle size may be called relaxation time, i.e. the mean time necessary for exchanging all the particles of one particular size. The relaxation time may be expressed as the ratio between the concentration and rate of disappearance for that particular size:

$$t_j = \frac{1}{\int_{r_{min}}^{\infty} K_{i,j} \cdot n_i \cdot d\log\frac{r_i}{r_0} + \alpha \cdot \left(\frac{r_j}{r_p}\right)^g + \gamma} \tag{3.2}$$

The variation with size in the effect of the different supply and removal processes is of some interest for the understanding of the working mechanism in an aerosol. The ratio between mass entering due to coagulation of smaller particles and mass entering due to supply is

$$s_j = \frac{\int_{r_{min}}^{r_j \cdot 2^{-1/3}} K_{i,k} \cdot n_i \cdot n_k \cdot \left(\frac{r_j}{r_k}\right)^3 \cdot d\log\frac{r_i}{r_0}}{n_{j0}} \tag{3.3}$$

The ratio between mass removed by coagulation and mass removed by deposition on the ground

$$p_j = \frac{\int_{r_{min}}^{\infty} K_{i,j} \cdot n_i \cdot d\log\frac{r_i}{r_0}}{\alpha \cdot \left(\frac{r_j}{r_p}\right)^g} \tag{3.4}$$

The instantaneous transfer of mass within an aerosol due to coagulation is of considerable interest. Two quantities have been computed in this paper. The fraction of the mass entering a size m, which comes from a size l is

$$U_{l\to m} = \frac{r_l^3 \cdot K_{l,k1} \cdot n_l \cdot n_{k1} \cdot \left(\frac{r_m}{r_{k1}}\right)^3}{r_m^3 \cdot \int_{r_{min}}^{r_j \cdot 2^{-1/3}} K_{i,k} \cdot n_i \cdot n_k \cdot \left(\frac{r_j}{r_k}\right)^3 \cdot d\log\frac{r_i}{r_0}} \tag{3.5}$$

where $U_{l\to m}$ is normalized to give the fraction transferred per logarithmic unit of r/r_0 (i. e., per decade for 10 as logarithmic base). In this expression $l<m$. The index $k1$ indicates that $v_l + v_k = v_m$, while k is reserved for the general case $v_i + v_k = v_m$.

The fraction of the particles (or the mass) which, because of coagulation, leaves a size m and goes to a size l, is

$$V_{m\to l} = \frac{K_{m,k2} \cdot n_{k2} \cdot \left(\frac{r_j}{r_{k2}}\right)^3}{\int_{r_{min}}^{\infty} K_{i,m} \cdot n_i \cdot d\log\frac{r}{r_0}} \tag{3.6}$$

Index k2 indicates that $v_m + v_{k2} = v_l$.

$V_{m\to l}$ is normalized to give the fraction transferred to each logarithmic unit of r.

4. General features of aerosol size distributions. Steady-state aerosol size distributions seem to fall into two classes. The first class shows distribution characteristics leading to slow coagulation. In the second class coagulation is much more vigorous, and a distinct mode is always present in the middle part of the distribution.

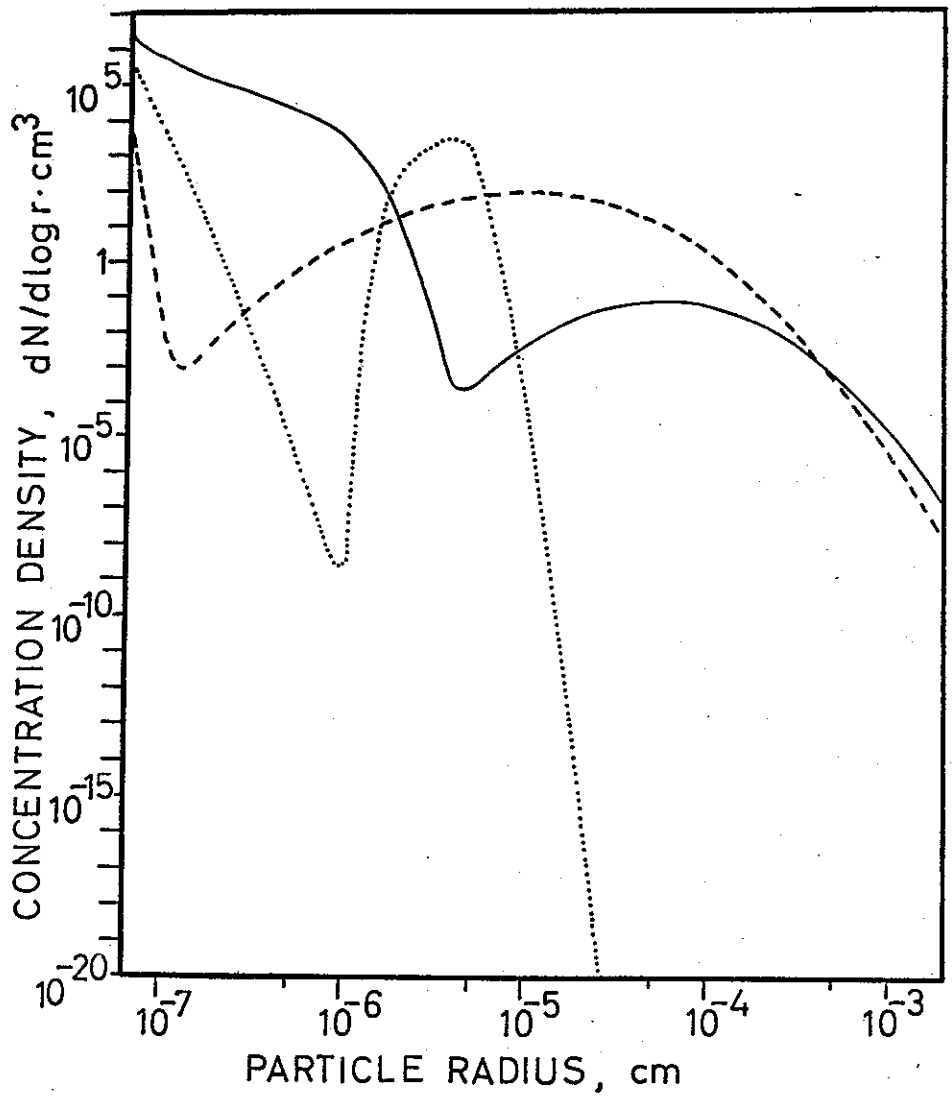

Fig. 4.1. *Type 1. size distribution.* Parameters for solid curve: small-particle supply 100 $cm^{-3}s^{-1}$, other supply $10^{-14}gcm^{-3}s^{-1}$ with mode 10^{-4}cm and $\sigma = 2$, removal coefficient 10^{-4} and exponent 1.8, air replacement time 24 hrs. Corresponding numbers for broken curve: 0.1, 10^{-15}, 10^{-5}, 2.5, 10^{-4}, 1.75, 3 and for dotted curve: 10, 0, —, —, 10^{-6}, 1.75, 5000.

When input parameters are gradually varied, a fairly abrupt replacement of the one by the other takes place. An explanation of the phenomenon may be that, in principle, the rate of coagulation increases with the square of the particle concentration, which makes the relative effect of coagulation influence highly sensitive to the distribution. Apparently two stable types of aerosol size distributions exist, while a distribution in-between may easily be broken down by slight changes in supply and removal conditions.

4.1 Distribution type 1: Slow coagulation. Steady-state aerosols with slow coagulation have typically a mass less than 10^{-11} g/cm³, contain either few particles or have a narrow size distribution, preferably at small sizes. The latter type may have a

high particle number concentration. This type of distribution is presented in Figure 4.1. In the $dN/d\log r/r_0$-presentation it usually falls rapidly off towards larger particle sizes. There may, however, be secondary maxima or slope changes due to changes in the coagulation coefficient or the supply distribution.

Abel, Winkler and Junge (1) have presented measurements from the Canary Islands which are in accord with these characteristics.

This type of distribution is normally found when some supply of small particles takes place, while the introduction of medium particles is small.

It is also established when the mode of the larger particles supplied to the aerosol is found at too large a size. Such particles are apparently removed so fast as to be hardly noticeable in the aerosol distribution. If the supply distribution has a geometric standard deviation of 2.5 or more, a mode particle size larger than 10^{-4} cm produces type 1 distribution.

When the supply mode is down to some 10^{-5} cm radius, it will be displayed as a distinct hump in the aerosol distribution.

Mass turn-over time is not a good parameter to describe type 1 distributions. The important factor for this quantity is the number of large size particles, and when the bulk of the particles are small the meaning of this parameter becomes doubtful and perhaps somewhat fortuitous.

The particle number in the distribution depends on the supply parameters. When 100 particles of minimum size were introduced per cm^3 per second, total particle number could exceed 400,000 cm^{-3} with aerosol mass lower than some 10^{-12} gcm^{-3}. On the other hand, introduction of 0.001 small-size particles per cm^3 per second and nothing else, produced a concentration of 1300 cm^{-3}.

4.2 Distribution type 2: Vigorous coagulation. When coagulation is more vigorous, aerosol mass is of the order of 10^{-10} gcm^{-3} or higher, and the steady state size distribution shows a pronounced mode for a medium size. This type of distribution is presented in Figure 4.2.

The particle concentration density for low sizes is normally very low. When the supply distribution showed a peak at the lower end, which it often did during the computations, the peak was sharply reflected in the aerosol. The peak increased in height with low aerosol mass, but the sharpness of the peak in terms of the slope towards larger particle sizes was greatest when the aerosol mass was high.

The small-particle concentration density varied with other parameters. It was low with narrow supply distribution and long mass turn-over time.

For an aerosol mass less than 10^{-8} gcm^{-3}, the supply mode corresponds fairly well with the aerosol mode, provided the former is not much higher than 10^{-5} cm. A supply mode of the order of 10^{-4} cm usually resulted in a slightly lower aerosol mode. Large mass supply usually resulted in a very high aerosol mass with some upward shift in the mode. Some size distributions of this category are presented in Figure 4.3.

The concentration at mode size was from 10^3 to 10^6 cm^{-3} per decade of the radius.

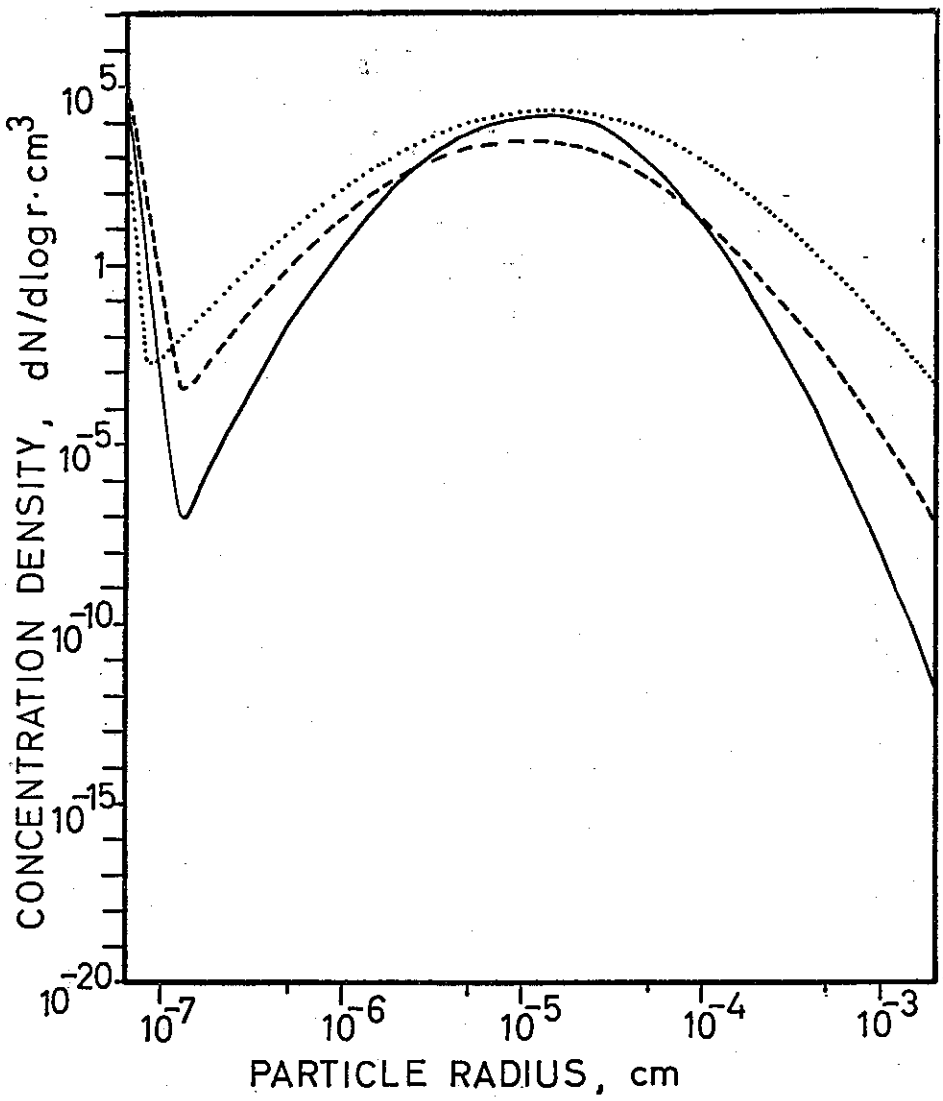

Fig. 4.2. *Type 2 size distributions, normal mass aerosols.* Parameters for solid curve: small-particle supply 100 $cm^{-3}s^{-1}$, other supply $10^{-14}gcm^{-3}s^{-1}$ with mode $10^{-5}cm$ and $\sigma = 2$, removal coefficient 10^{-4} and exponent 2, air replacement time 24 hrs. Corresponding numbers for broken curve: 100, 10^{-14}, 10^{-5}, 2.5, 10^{-4}, 2, 24 and for dotted curve: 10, 10^{-12}, 10^{-5}, 3, 10^{-4}, 1.75, 12.

The lower number is close to a transition to the first type of distribution, the upper number seems to be a limit set by the increase in coagulation at high particle concentrations.

The width of the mode peak seemed to some degree to be determined by the width in the supply mode.

The slope on the upper side of the aerosol mode seemed to increase with air exchange time, sharpness of supply and removal constant. In general, the slope increased with increasing distance from the mode.

The distribution at about 1μ radius has been measured by Junge (4) to follow a formula

$$\frac{dN}{d\log r/r_0} = c \cdot r^{-3}$$

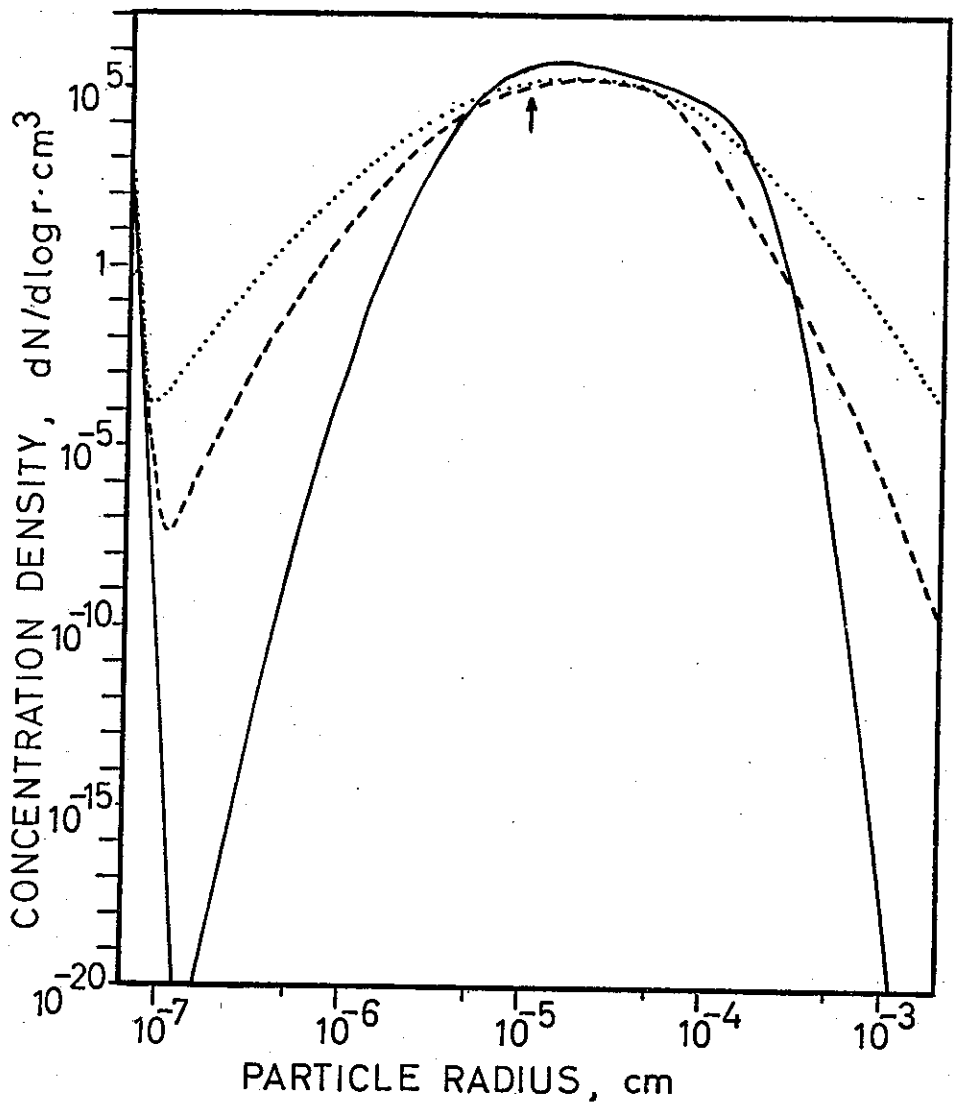

Fig. 4.3. *Type 2 size distributions, dense aerosols.* Supply modes are indicated by arrow. Parameters for solid curve: small-particle supply 100 $cm^{-3}s^{-1}$, other supply $10^{-12}gcm^{-3}s^{-1}$ with mode 10^{-5} cm and $\sigma = 1.5$, removal coefficient 10^{-5} and exponent 2, air replacement time 48 hrs. Corresponding numbers for broken curve: 100, 10^{-12}, 10^{-5}, 2, 10^{-4}, 2, 24 and for dotted curve: 100, 10^{-11}, 10^{-5}, 2.5, 10^{-4}, 1.75, 3.

With the restrictions in supply parameters given by the log-normal distribution, the exponent -3 was difficult to achieve. The normal exponent for a reasonably broad supply distribution varied from -7 to -3.5, i.e. a steeper slope than that found by Junge. It is probable that his distribution will more easily be reproduced if the log-normal distribution of supply is replaced by a suitable power function above the mode.

With a small-particle supply of 100 $cm^{-3}s^{-1}$, total particle number for this type of distribution seemed to have a minimum of the order of 10,000 cm^{-3}, most frequently found for aerosol masses between $5 \cdot 10^{-11}$ and 10^{-9} gcm^{-3}. For very dense aerosols the concentration increased markedly. A concentration of 500,000 cm^{-3} seems possible for a mass of 10^{-7} gcm^{-3}.

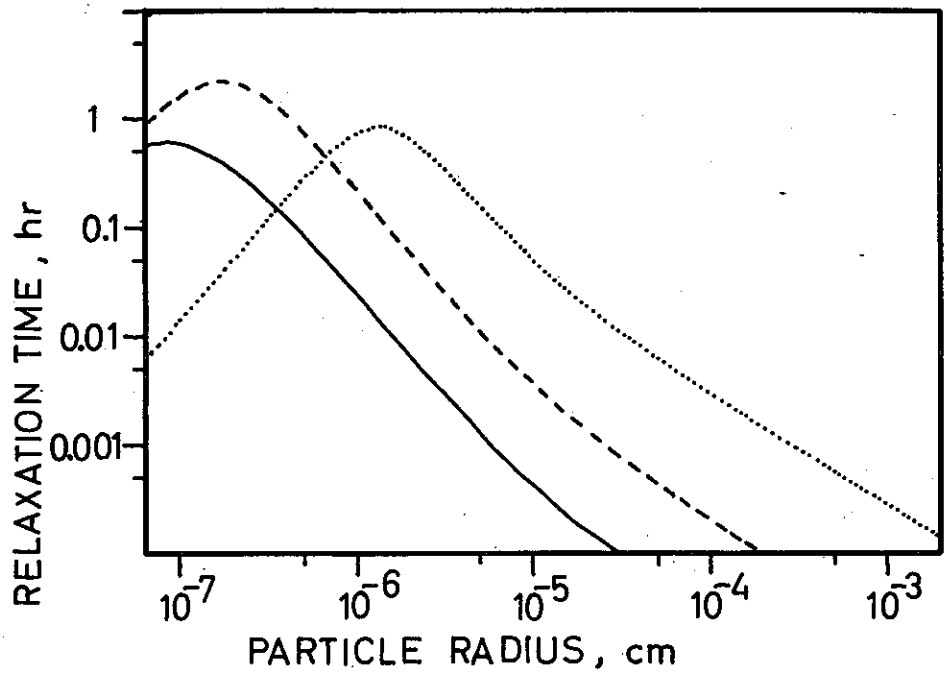

Fig. 4.4. *Time of relaxation.* Parameters for solid curve: small-particle supply 100 $cm^{-3}s^{-1}$, other supply $10^{-14}gcm^{-3}s^{-1}$ with mode 10^{-4} cm and $\sigma = 2$, removal coefficient 10^{-4} and exponent 1.8, air replacetime ment 24 hrs. Corresponding numbers for broken curve: 10, 0, —, —, 10^{-6}, 1.75, 5000 and for dotted curve: 10, 10^{-14}, 10^{-5}, 2, 10^{-4}, 2, 24.

4.3 Time of relaxation. Time of relaxation is defined as the time used for replacing all particles of a certain size. Typical results are shown in Figure 4.4. The time of relaxation has a maximum which is not normally found at a central place in the distribution. If the bulk of the particles is found at the lower end of the distribution, this is also where replacement of particles is slowest.

When the particle distribution has a mode in the medium particle size range, the maximum in relaxation time is generally found for considerably smaller particles, typically at about 1/10 of the mode radius. The relaxation time maximum is found closer to the mode for dense aerosols and may coincide when the mass is high enough. This is illustrated in Figure 4.5. The relaxation time normally falls off rapidly for sizes off the maximum point, typically with a factor of 0.2—0.1 per decade in radius.

When few small particles are present in the aerosol, the relaxation time becomes fairly high and the maximum less peaked. Figure 4.6 shows the change occurring when the small-particle supply increases from practically 0 to 100 per cm^3 per second.

The relaxation time does not indicate the degree of change in the replaced particles, and the numerical time found is therefore very dependent on the particle distribution. Many small particles may lead to a short time of relaxation, even though larger particles only are changed to a negligible degree by coagulation. Lack of small particles may, on the other hand, lead to a long relaxation time.

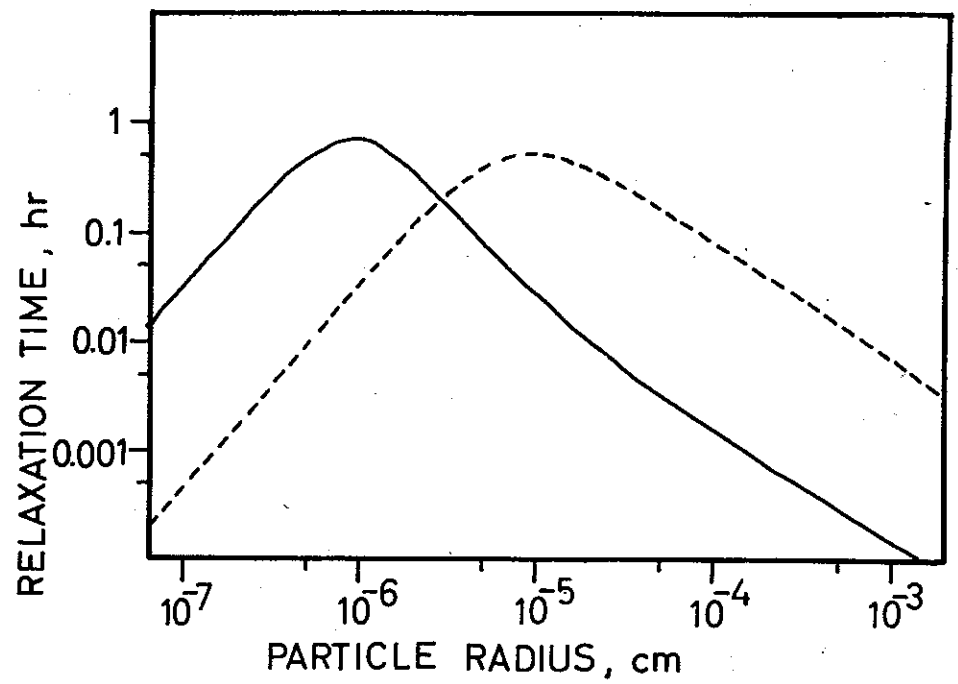

Fig. 4.5. *Time of relaxation, dense aerosols.* Parameters for solid curve: small-particle supply 100 $cm^{-3}s^{-1}$, other supply $10^{-13}gcm^{-3}s^{-1}$ with mode 10^{-5} cm and $\sigma = 2.5$, removal coefficient 10^{-4} and exponent 1.75, air replacement time 3 hrs. Except for increase of mass supply to $10^{-11}gcm^{-3}s^{-1}$ for the broken curve, parameters remain unchanged.

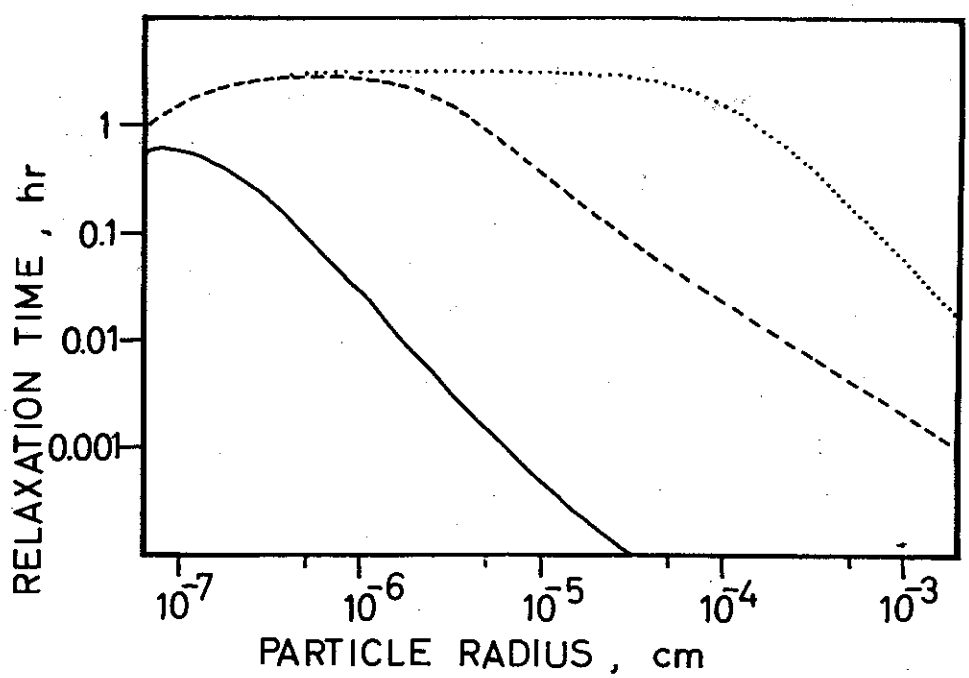

Fig. 4.6. *Time of relaxation, small particle variation.* Parameters for solid curve: small-particle supply 100 $cm^{-3}s^{-1}$, other supply $10^{-15}gcm^{-3}s^{-1}$ with mode 10^{-5} cm and $\sigma = 2.5$, removal coefficient 10^{-4} and exponent 1.75, air replacement time 3 hrs. Except for decrease in small-particle supply to 0.1 $cm^{-3}s^{-1}$ for the broken curve and to 0 for the dotted curve, parameters remain unchanged.

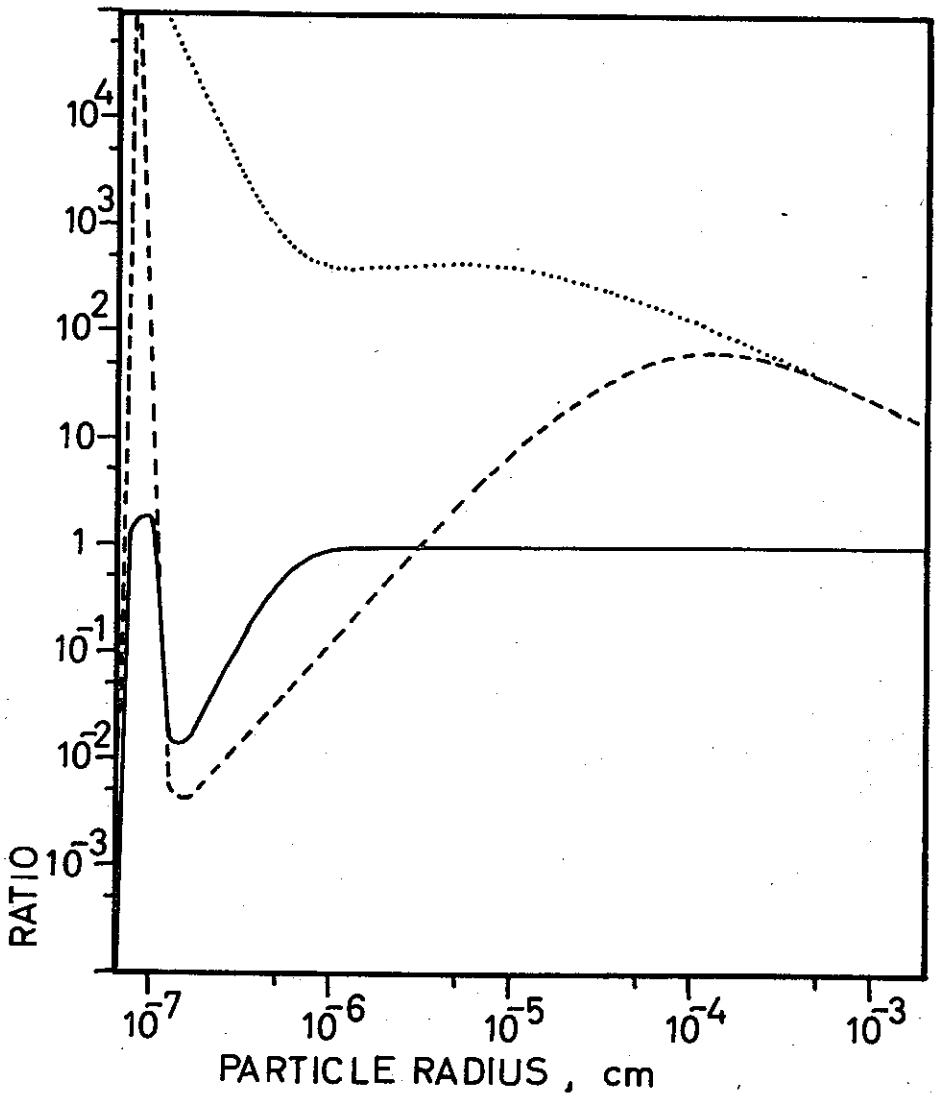

Fig. 4.7. *Coagulation effects versus supply and removal, aerosol type 1.* Solid curve shows the ratio between coagulation accumulation and coagulation removal, broken curve between coagulation accumulation and outside supply and dotted curve between coagulation removal and removal from the aerosol. Parameters for the aerosol: small-particle supply 0.1 $cm^{-3}s^{-1}$, other supply $10^{-15}gcm^{-3}s^{-1}$ with mode 10^{-5} cm and $\sigma = 2.5$, removal coefficient 10^{-4} and exponent 1.75, air replacement time 3 hrs.

Mass turn-over time has little immediate relationship to relaxation time. It depends mostly on the particle amount in the upper part of the size range, and will always be much longer than the relaxation time for the large particles.

4.4 Coagulation mass transfer. For any particle size, coagulation removes some particles and adds others. In a steady state distribution the differences in the rates of a certain size must be made up by other types of addition or removal for that size. Most of the computations seem to indicate that with ample small-particle supply, the distribution in the steady state will adjust itself at such a level, that approximate equilibrium exists between coagulation accumulation and removal from those sizes

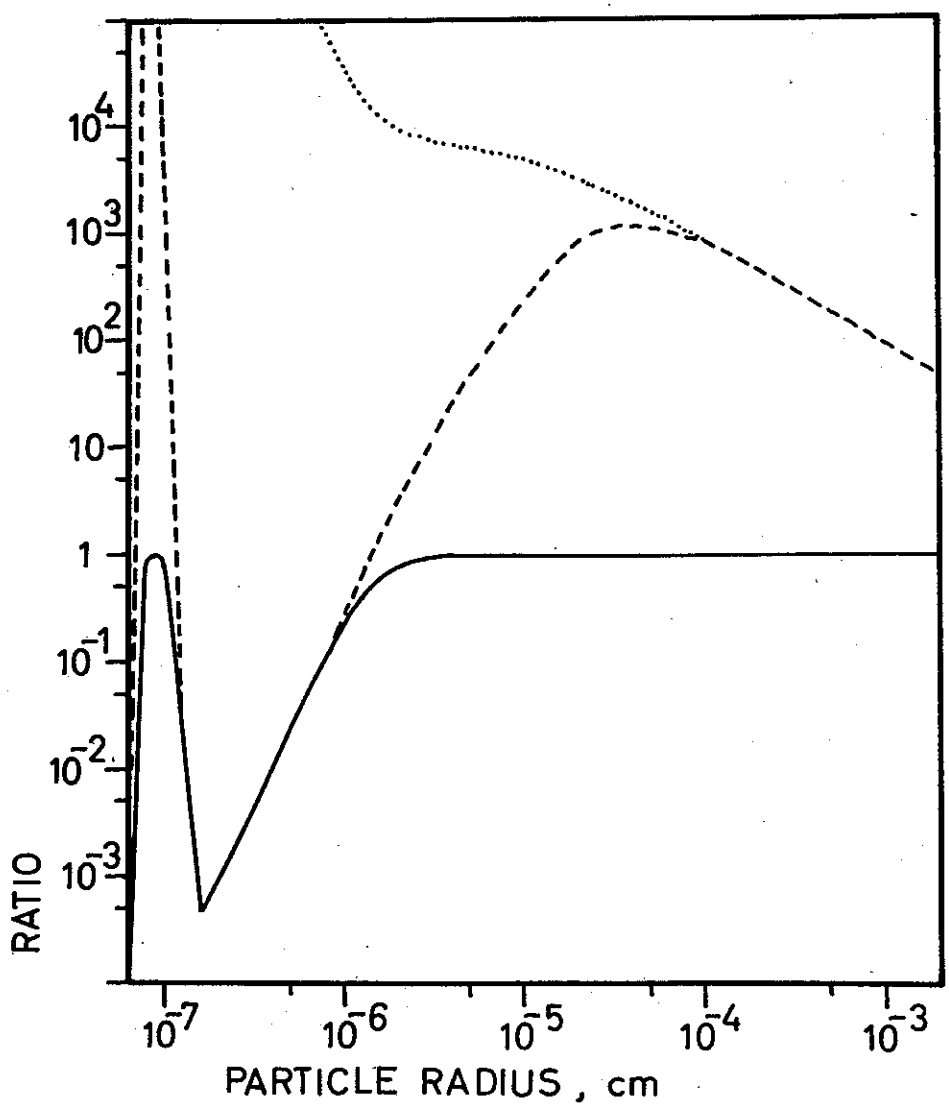

Fig. 4.8. *Coagulation effects versus supply and removal, aerosol type 2.* Solid curve shows the ratio between coagulation accumulation and coagulation removal, broken curve between coagulation accumulation and outside supply and dotted curve between coagulation removal and removal from the aerosol. Parameters for the aerosol: small-particle supply 100 $cm^{-3}s^{-1}$, other supply $10^{-14}gcm^{-3}s^{-1}$ with mode 10^{-5} cm and $\sigma = 2$, removal coefficient 10^{-4} and exponent 2, air replacement time 24 hrs.

in which the bulk of the particles are found. Results from two different distributions are shown in Figures 4.7 and 4.8.

Figure 4.7 illustrates the situation for a distribution where the bulk of the particles is in the low size range. In this case coagulation removal is far stronger than particle removal all over the size distribution. In the lower size region accumulation by coagulation is, in part, smaller than supply. In this region the balance between outside supply and removal determines the distribution.

Figure 4.8 illustrates the situation for a distribution where a distinct mode is found in the medium particle size range. The only deviation from equilibrium between coagulation accumulation and removal is found for very small particle sizes, where

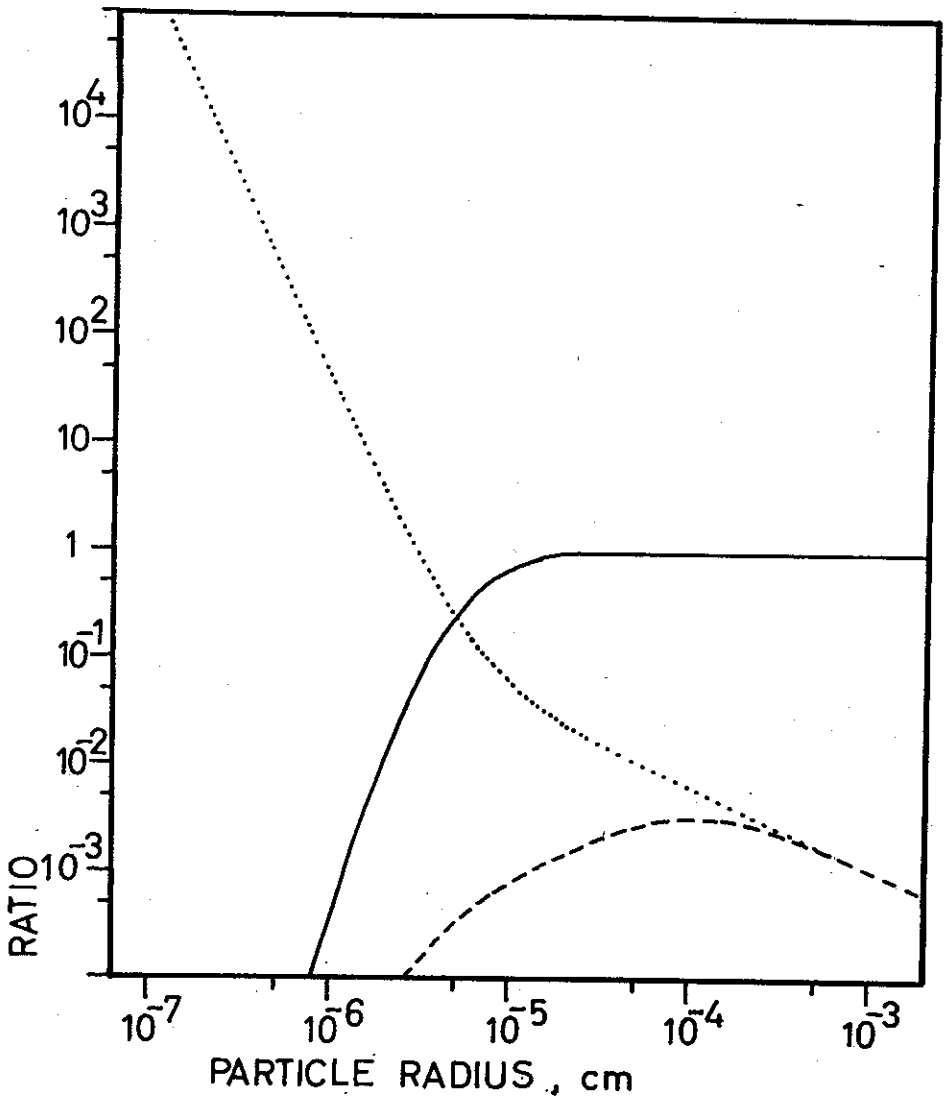

Fig. 4.9. *Coagulation effects versus supply and removal, no small-particle supply.* Solid curve shows the ratio between coagulation accumulation and coagulation removal, broken curve between coagulation accumulation and outside supply, and dotted curve between coagulation removal and removal from the aerosol. Parameters for the aerosol: small-particle supply 0 $cm^{-3}s^{-1}$, other supply $10^{-15}gcm^{-3}s^{-1}$ with mode 10^{-5} cm and $\sigma = 2.5$, removal coefficient 10^{-4} and exponent 1.75, air replacement time 3 hrs.

particle concentration is low. In this region coagulation removal far outweighs the accumulation, and the balance is maintained by supply to the aerosol. This can be seen by the approximate agreement between the coagulation-accumulation/removal curve and the accumulation/supply curve. Elsewhere coagulation accumulation far outweighs supply and coagulation removal far outweighs removal of particles from the aerosol.

When few small particles are present, coagulation accumulation or removal may mean considerably less than other supply or removal agents. Figure 4.9 shows an example with no supply of small particles, in which coagulation plays a minor role, especially for the larger sizes.

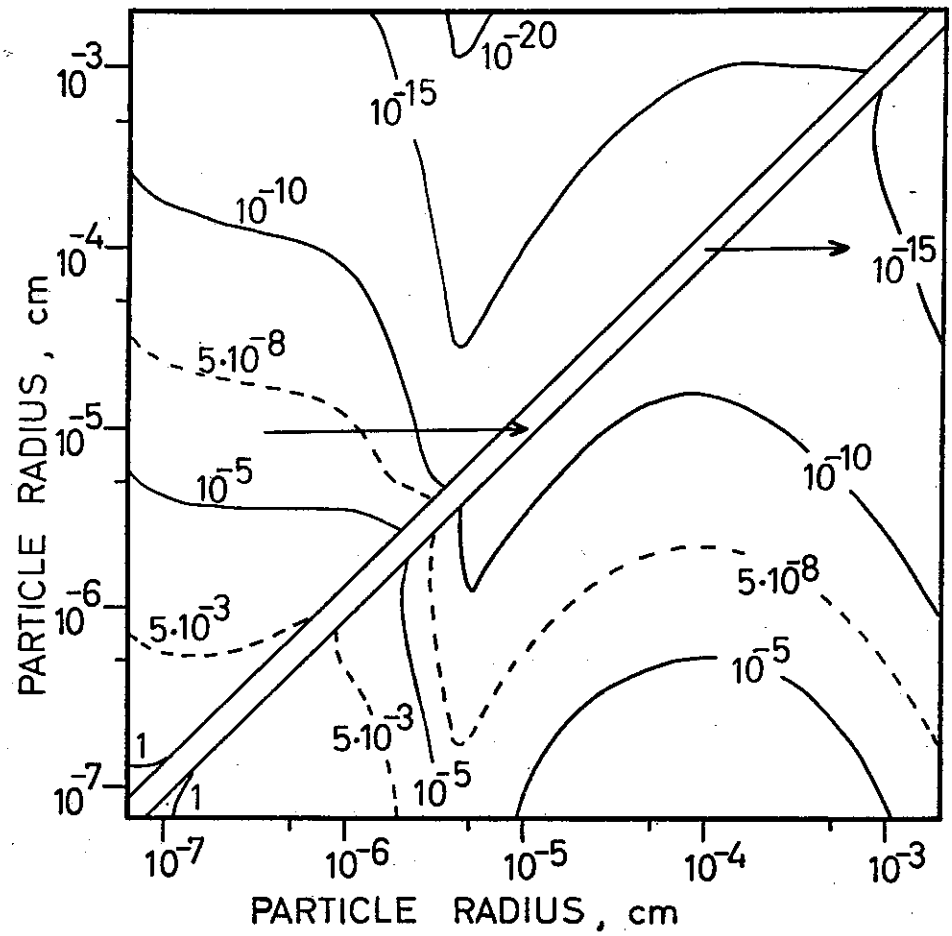

Fig. 4.10. *Coagulation mass transfer, aerosol type 1.* Lower right: Fractional mass transfer from the ordinate to a decade in particle radius at abscissa values. Upper left: Fractional mass transfer to the ordinate from a decade in particle radius at abscissa values. Parameters for the aerosol: small-particle supply 100 $cm^{-3}s^{-1}$, other supply $10^{-14}gcm^{-3}s^{-1}$ with mode 10^{-4} cm and $\sigma = 2$, removal coefficient 10^{-4} and exponent 1.8, air replacement time 24 hrs.

Coagulation mass transfer is probably best studied by help of the diagram in Figure 4.10, which is based on formulas (3.5) and (3.6).

The lower right-hand part shows the distribution of the mass leaving a certain size region. The abscissae in the diagram express size of recipients, while the ordinate (or the diagonal) expresses the supply size. The particle distribution, to which the diagram refers, is of type 1. Small particles can coagulate with an abundance of other small particles, giving a maximum in mass transfer at low sizes. Under such circumstances the bulk of the particles is present at low sizes, and the lower mass transfer maximum is the main one, even though mass transfer to secondary maxima in larger size regions of the distribution may be pronounced.

The diagram does not contain transfer fractions for coagulation between particles leading to size shifts less than the computation interval, i.e. for less than volume doubling. Since integration horizontally should result in 1, the small numbers elsewhere show

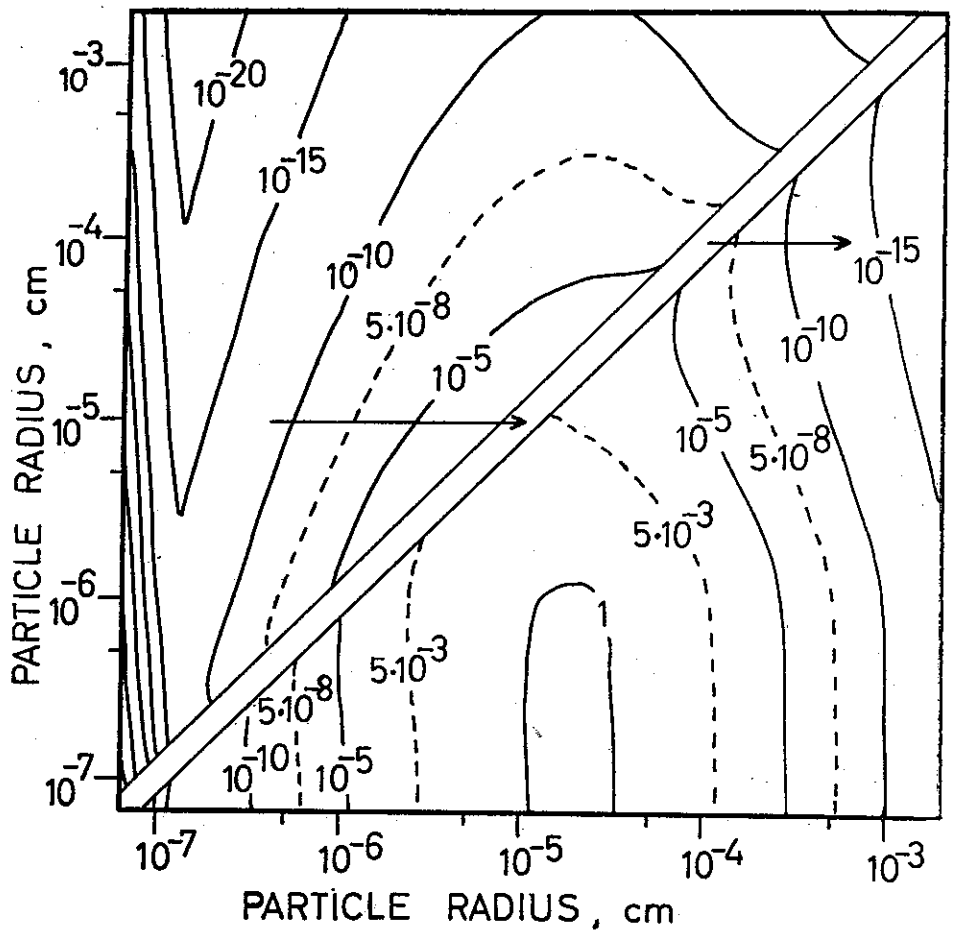

Fig. 4.11. *Coagulation mass transfer, aerosol type 2.* Lower right: Fractional mass transfer from the ordinate to a decade in particle radius at abscissa values. Upper left: Fractional mass transfer to the ordinate from a decade in particle radius at abscissa values. Parameters for the aerosol: small-particle supply 100 $cm^{-3}s^{-1}$, other supply $10^{-14}gcm^{-3}s^{-1}$ with mode $10^{-5}cm$ and $\sigma = 2$, removal coefficient 10^{-4} and exponent 2, air replacement time 24 hrs.

that coagulation leading to very small size shifts must be important in that type of distribution. Coagulation with large particles exists, and a secondary maximum even is seen in the diagram for the lower half of the size region, but the fraction of particles undergoing this type of coagulation is very low.

When a pronounced medium size mode is present in the aerosol size distribution, as in Figures 4.11 and 4.12, the transfer of small particles to this region, or slightly shifted towards larger sizes, is the dominant one. Under these conditions the general fate of small particles is coagulation with very much bigger ones, and this type of mass flow increases in importance with increasing aerosol mass. By comparison, coagulation between the small particles is next to non-existent.

For the larger particles in the distribution, the fractional mass transfer outlined in the diagrams is considerably less than unity. These particles therefore grow by coagulation with small size increments, which means they do in general coagulate with the small particles.

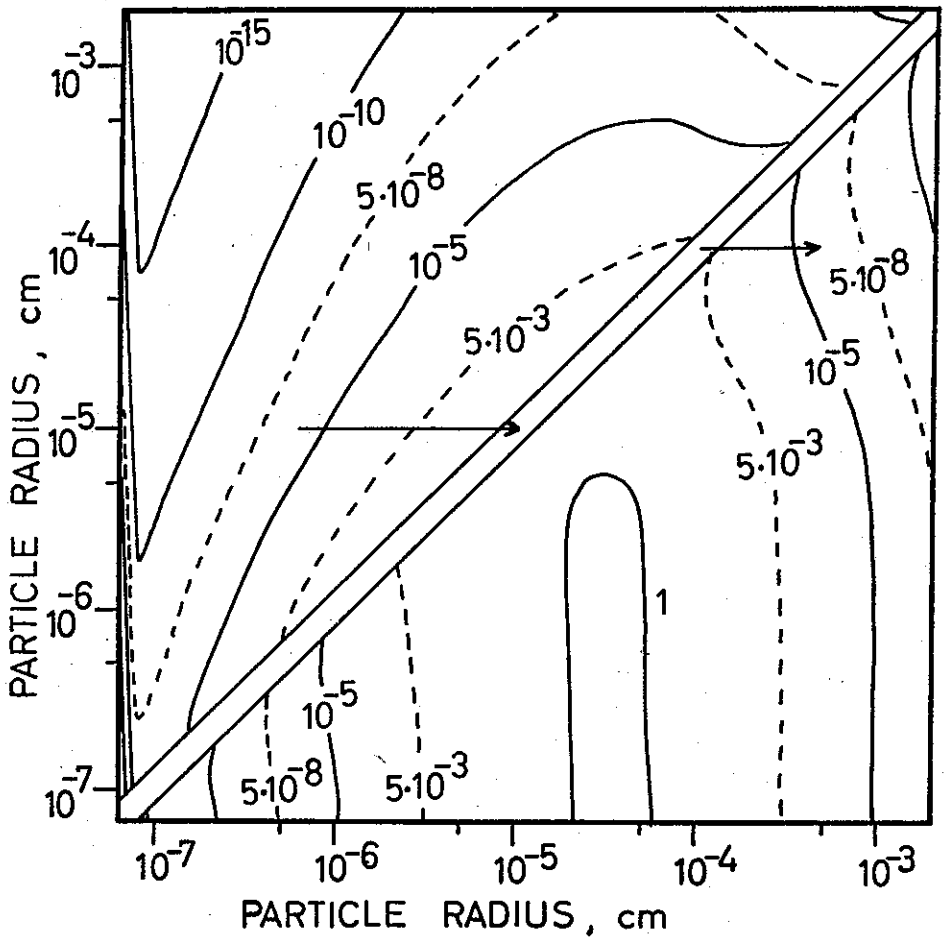

Fig. 4.12. *Coagulation mass transfer, dense aerosol.* Lower right: Fractional mass transfer from the ordinate to a decade in particle radius at abscissa values. Upper left: Fractional mass transfer to the ordinate from a decade in particle radius at abscissa values. Parameters for solid curve: small-particle supply 100 cm^{-3} a decade in particle radius at abscissa values. Parameters for solid curve: small-particle supply 100 $cm^{-3}s^{-1}$, other supply $10^{-11}gcm^{-3}s^{-1}$ with mode $10^{5}cm$ and $\sigma = 2.5$, removal coefficient 10^{-4} and exponent 1.75, air replacement time 3 hrs.

The upper left-hand parts of Figures 4.10—4.12 shows the origin of the mass entering a certain size region. The abscissase express supply sizes, while the ordinate (or the diagonal) expresses the size of the recipient. Secondary maxima correspond to the peaks in the size distribution. However, since integration horizontally should result in 1, and the numbers shown are low, it is obvious that most mass is drawn from sizes less displaced from the recipient size than the computation interval.

Weighted masswise the long jumps in particle size do not amount to much. The main contributing size has more than half the volume of the recipient size. Only close to the very lower end of the size distribution does a certain size region draw and important amount of mass below its immediate size environment, but here, of course, possible jumps are limited because of the minimum size.

When few small particles are present, the mass transfer is somewhat adjusted.

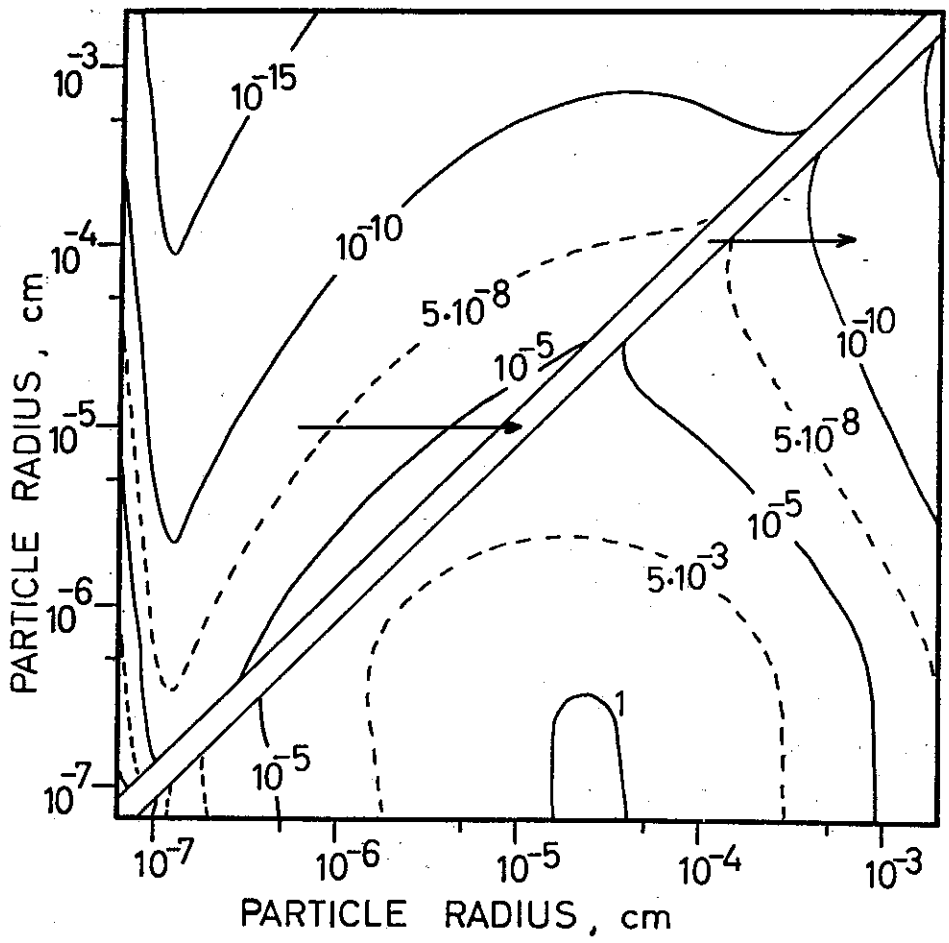

4.13.

Fig. 4.13. and 4.14. *Coagulation mass transfer, effect of small particles.* Lower right: Fractional mass transfer from the ordinate to a decade in particle radius at abscissa values. Upper left: Fractional mass transfer to the ordinate from a decade in particle radius at abscissa values. Parameters for the aerosol for Fig. 4.13: small-particle supply 0.1 $cm^{-3}s^{-1}$, other supply $10^{-15}gcm^{-3}s^{-1}$ with mode 10^{-5} cm and $\sigma = 2.5$, removal coefficient 10^{-4} and exponent 1.75, air replacement time 3 hrs. Except for no supply of small particles, Figure 4.14. is based on the same parameters.

Figures 4.13 and 4.14 are based on otherwise equal conditions, but 0.1 small particles are supplied per cm^3 per second to the aerosol on which Figure 4.13 is based, while this supply is lacking in the case of Figure 4.14.

It is obvious that the immediate effects of the small-particle peak is removed by the change, but this is not the most interesting conclusion to be drawn from the comparison. The lower right-hand part of the diagram, showing the distribution of recipients, does not indicate much change in the region of small particles. For medium and large particles, however, the numbers are much higher all over the diagram. These particles are therefore apt to grow with larger increments than before, which is only natural since the small particles making small increments possible, are now scarce. The change does

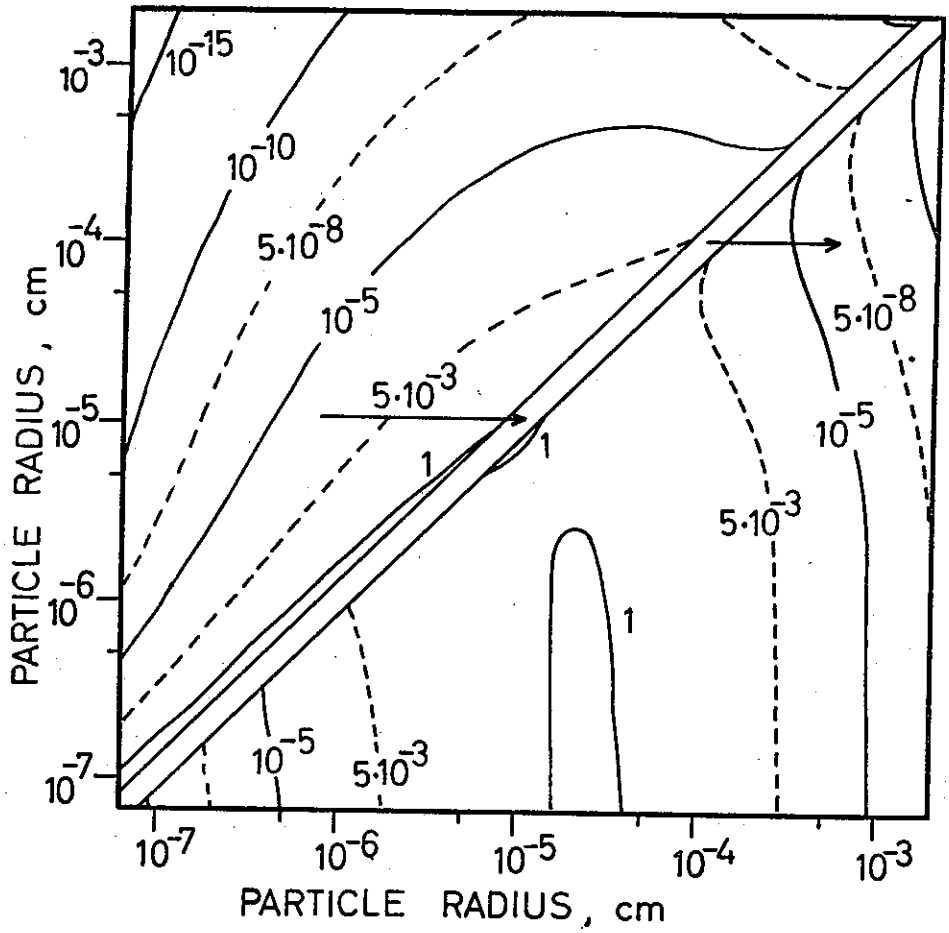

4.14.

not indicate a more rapid flow of mass. The relaxation time (see Figure 4.6) has increased over most of the size region, and this conteracts the larger increments for flow considerations.

The upper left-hand part of the diagram shows the origin of the particles entering a certain size. Apart from the change in the very left-hand part, all numbers have increased very much from Figure 4.13 to Figure 4.14. This emphasizes the fact that when small particles are scarce, source regions for mass are further removed from the recipient size than otherwise.

5. Conditions of formation versus size distribution. A multitude of parameters are involved in the generation of one particular aerosol. When all other conditions are fixed, the influence of one parameter may be studied by selective variation of that parameter. In general its influence is not independent of other conditions. In order to bring out the different aspects of this influence, the variation under different conditions has been studied.

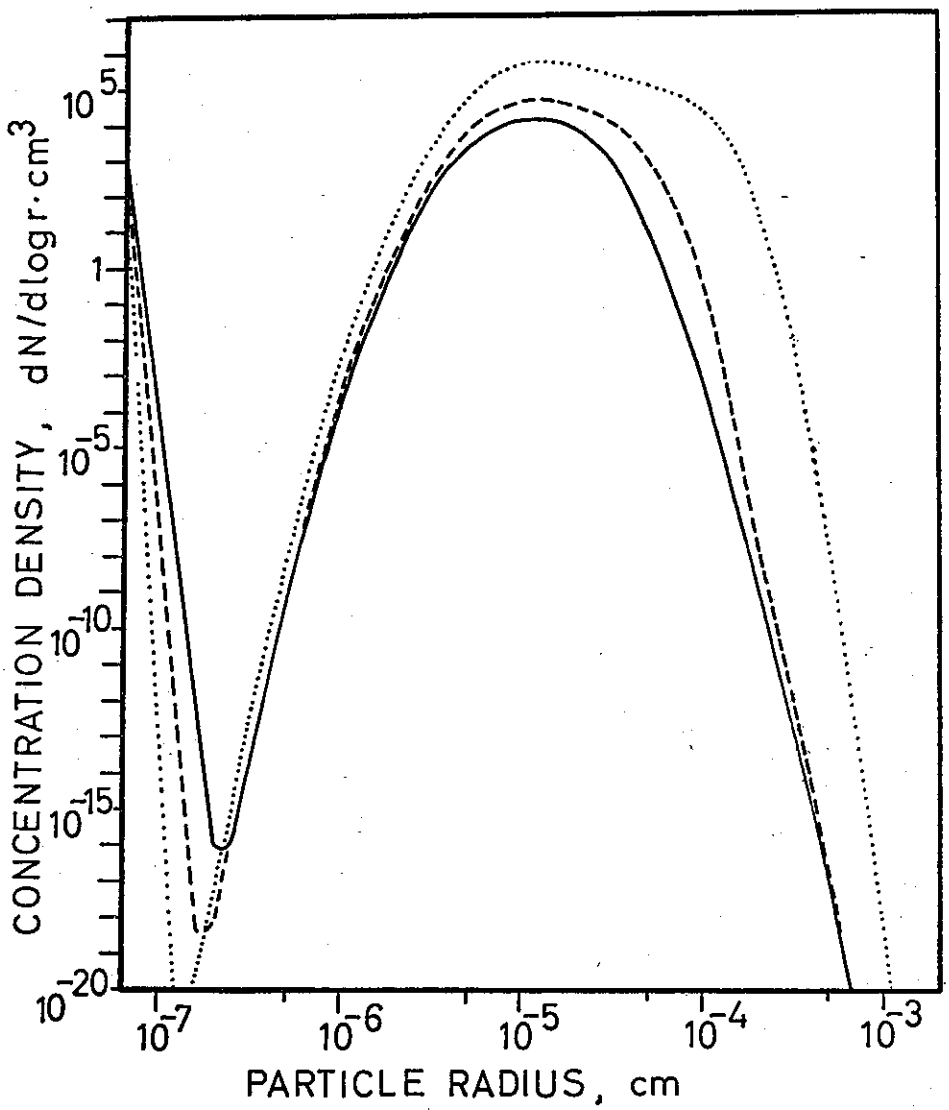

Fig. 5.1. *Aerosol size distribution for various mass supplies.* Parameters for solid curve: small-particle supply 100 $cm^{-3}s^{-1}$, other supply $10^{-15}gcm^{-3}s^{-1}$ with mode 10^{-5} cm and $\sigma = 1.5$, removal coefficient 10^{-5} and exponent 2, air replacement time 48 hrs. Except for mass supply $10^{-14}gcm^{-3}s^{-1}$ for the broken curve and 10^{-12} for the dotted curve, parameters remain unchanged.

5.1 Change in mass supply. Figures 5.1—5.3 illustrate the changes in aerosol size distribution when the mass supply is varied, and Figures 5.4—5.6 illustrate the associated changes in aerosol mass density, particle concentration and mass turn-over time.

Increased mass supply leads to increased mass concentration in the steady-state from Figures 5.1—5.3.

The supply of particles to the very lower end of the distribution was kept constant while the rest of the supply was changed. This led to decreasing amounts of small particles in the aerosol when the mass supply increased. The reason for this is that the increased number of large particles leads to an increase in the rate of particles trans-

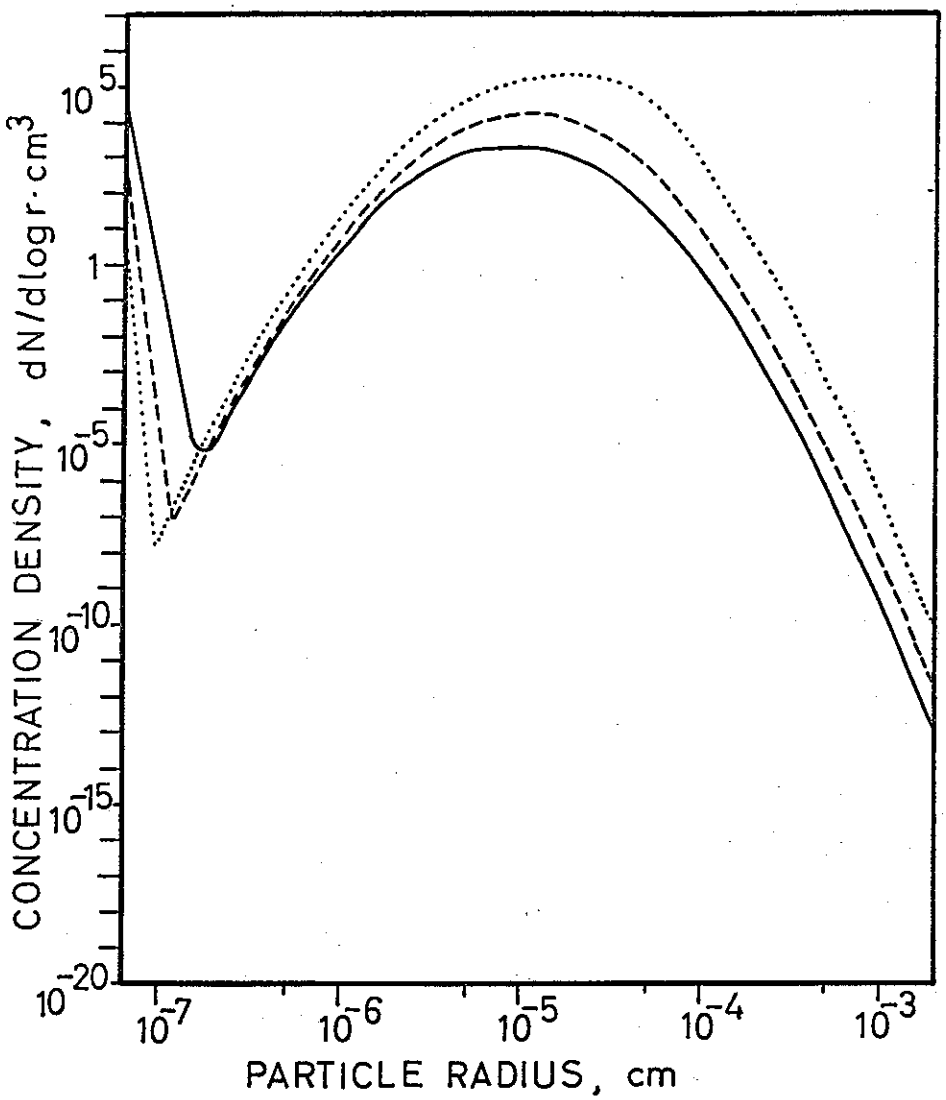

Fig. 5.2. *Aerosol size distribution for various mass supplies.* Parameters for solid curve: small-particle supply 100 $cm^{-3}s^{-1}$, other snpply $10^{-15}gcm^{-3}s^{-1}$ with mode 10^{-5} cm and $\sigma = 2$, removal coefficient 10^{-4} and exponent 2, air replacement time 24 hr<. Except for mass supply $10^{-14}gcm^{-3}s^{-1}$ for the broken curve and 10^{-12} for the dotted curve, parameters remain unchanged.

ferred from the small particle region by coagulation. In the steady-state this must be balanced by a lower concentration.

Change in mass supply may lead to a change from one to the other of the two main distribution forms outlined in chapter 4. In Figure 5.3 the lowest mass supply has led to such an accumulation of small particles that they dominate the distribution. It can be seen from Figure 5.5 that this aerosol has a particle concentration of more than 300,000 per cm^3, while the mass shown in Figure 5.4 is less than $5 \cdot 10^{-12}$ g/cm^3.

When the supply of larger particles is increased, the small particle accumulation in the aerosol rapidly decreases at the same time as the mass increases. The bulk of the particles is then found to be of medium and large sizes.

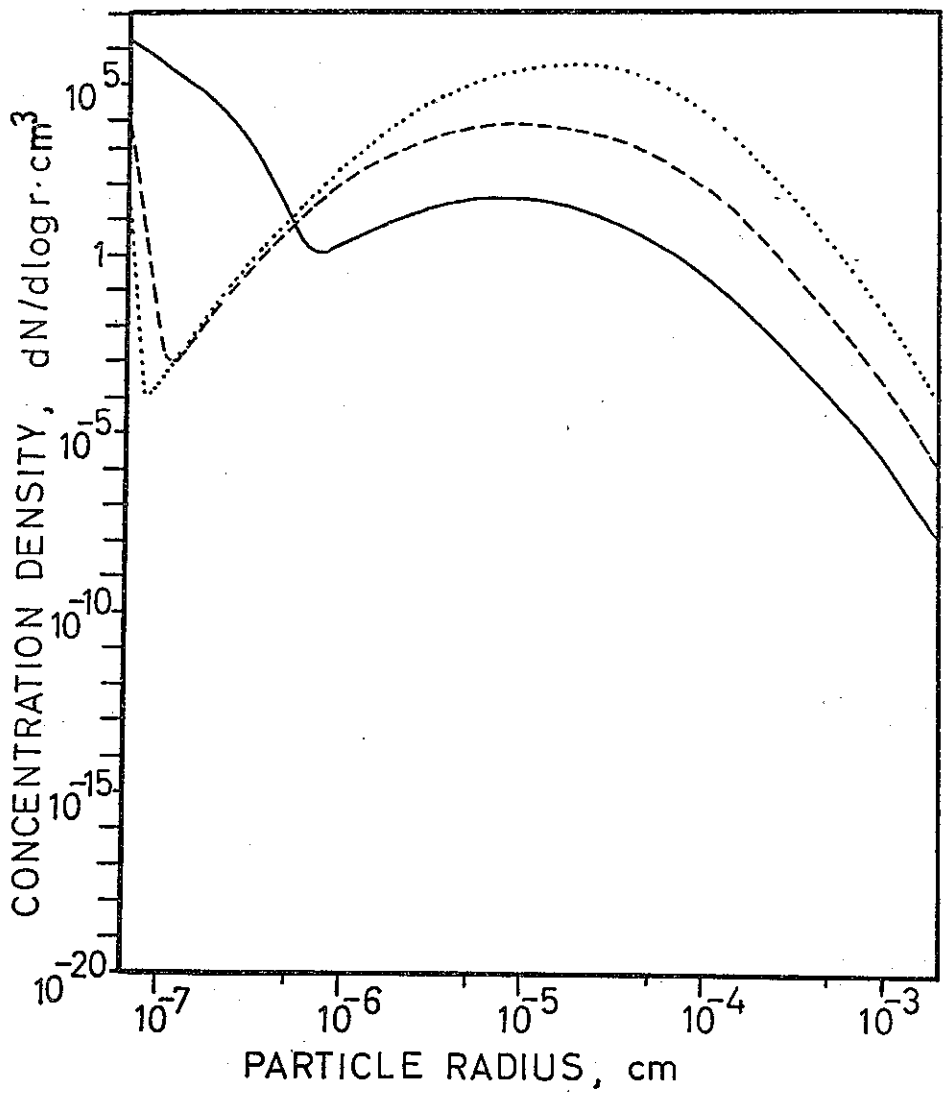

Fig. 5.3. *Aerosol size distribution for various mass supplies.* Parameters for solid curve: small-particle supply 100 $cm^{-3}s^{-1}$, other supply $10^{-15}gcm^{-3}s^{-1}$ with mode 10^{-5} cm and $\sigma = 2.5$, removal coefficient 10^{-4} and exponent 1.75, air replacement time 3 hrs. Except for mass supply $10^{-13}gcm^{-3}s^{-1}$ for the broken curve and 10^{-11} for the dotted curve, parameters remain unchanged.

For high rate of mass supply, the mass turn-over time decreases with increasing supply. For lower rates the effect is very small. It is the availability of the mass for removal, which is reflected here. A general trend in Figures 5.1—5.3 is a shift in mode towards larger sizes when the aerosol becomes denser. Large particles are more easily removed than small particles, and the higher up in the size distribution the bulk of the particles is found, the higher is the fraction of mass removed per time unit.

The number of particles per cm^3 shown in Figure 5.5 reflects the balance between the accumulation of particles in the lower and medium/upper end of the size region. When supply is low, the medium size mode is weakly developed, and the rate of transfer from the lower end is low. It is thus possible to build up a certain concentration here.

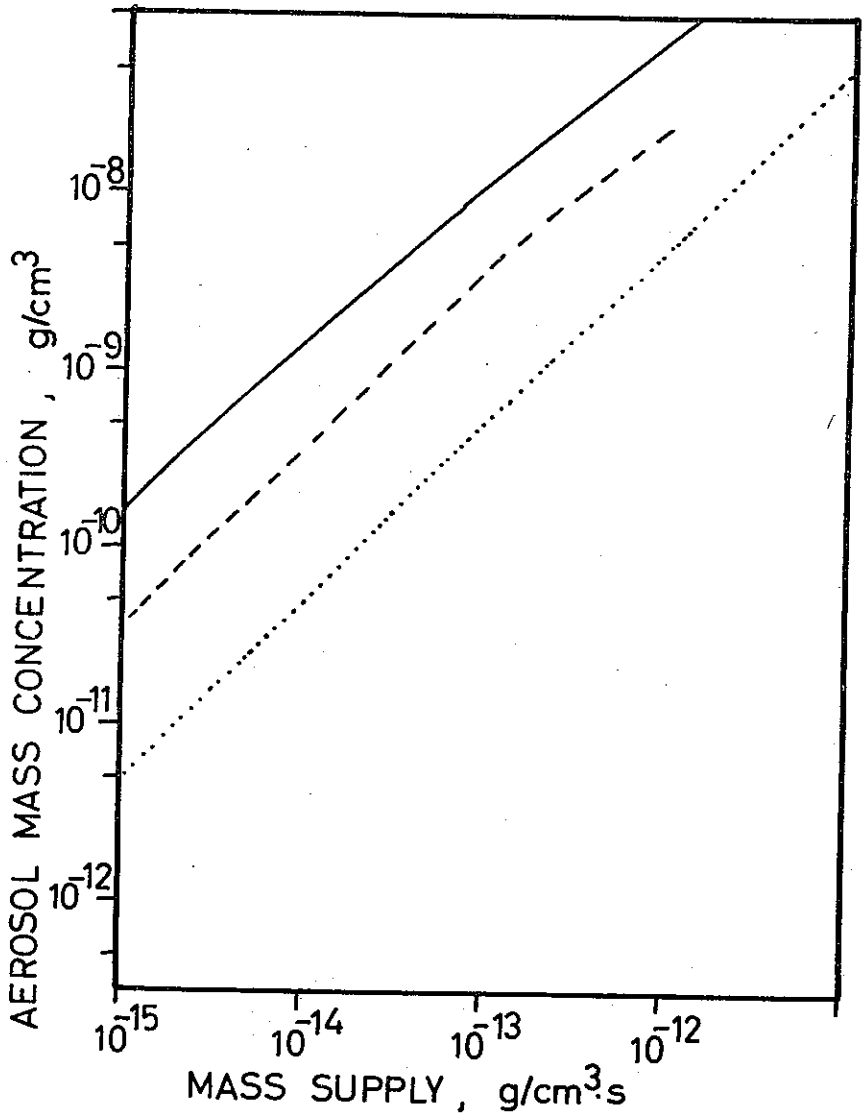

Fig. 5.4. *Aerosol mass for various mass supplies.* Solid curve refers to distributions from figure 5.1, broken curve to 5.2 and dotted curve to 5.3.

For the rates of small-size particle supply used in the computation, the steady state allows for a very high concentration.

When the mass supply is increased, the medium size mode in the aerosol becomes better developed, and transfer from the small-particle region is facilitated. Number-wise the decrease of small particles is more rapid than the build-up of larger particles, and total particle concentration decreases. However, after a certain stage of development of the medium mode is reached, so few particles are present in the lower size region that further reduction cannot compensate the increase in the medium mode. Total concentration will then climb with increasing mass supply.

For otherwise fixed conditions a minimum particle number will thus occur at a certain rate of supply. The actual minimum number, and its position on the mass supply scale, is much dependent on the rate of small-particle supply. The fairly high number

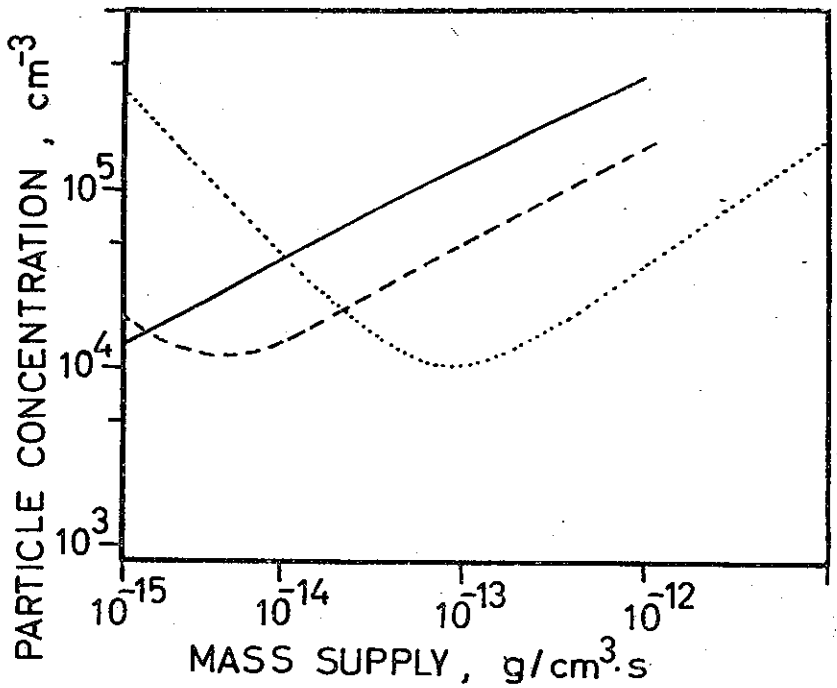

Fig. 5.5. *Aerosol particle concentration for various mass supplies.* Solid curve refers to distributions from fig. 5.1, broken curve to 5.2 and dotted curve to 5.3.

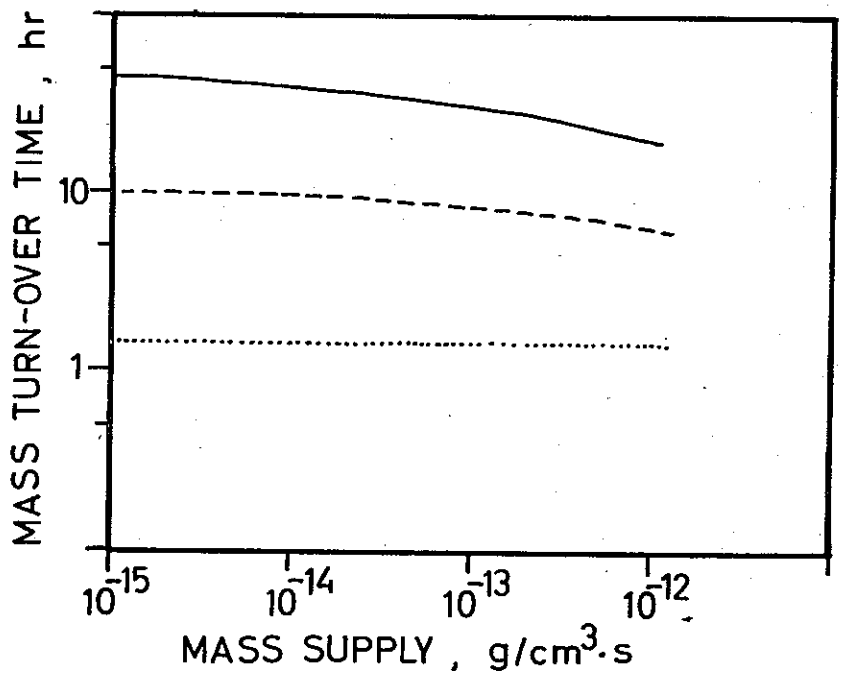

Fig. 5.6. *Mass turn-over time for various mass supplies.* Solid curve refers to distributions from fig. 5.1., broken curve to 5.2. and dotted curve to 5.3.

10,000, which appears on Figure 5.5, refers to a small-particle supply of 100 per cm^3 per second. If no small particles were supplied, the particle number for a mass supply of 10^{-15} $g/cm^3 \cdot s$ and the conditions on which Figure 5.3 is based, would be only 56.

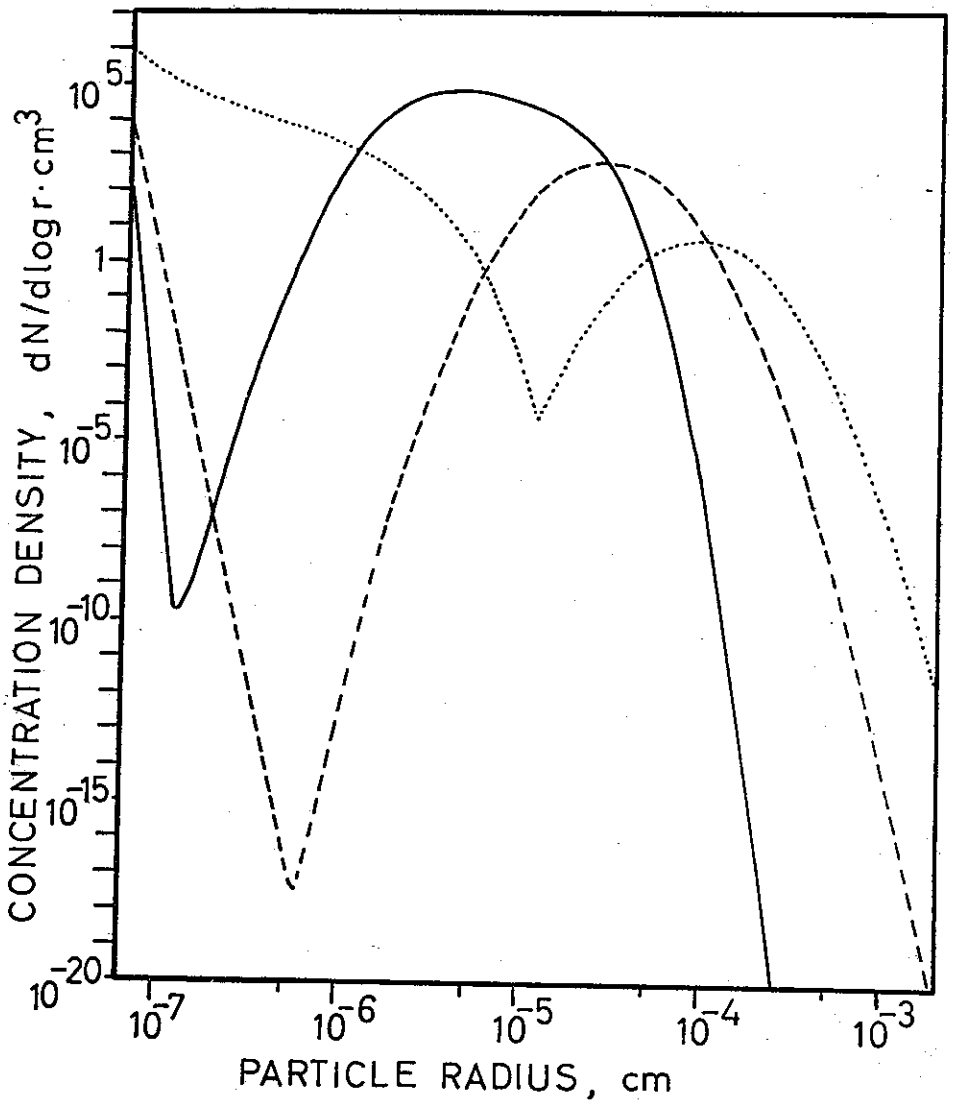

Fig. 5.7. *Aerosol size distribution for various supply modes.* Parameters for solid curve: small-particle supply 100 $cm^{-3}s^{-1}$, other supply $10^{-15}gcm^{-3}s^{-1}$ with mode $3.16 \cdot 10^{-6}$cm and $\sigma = 1.5$, removal coefficient 10^{-5} and exponent 2, air replacement time 48 hrs. Except for a shift in supply mode to $3.16 \cdot 10^{-5}$ cm for the broken curve and 10^{-4} for the dotted curve, parameters remain unchanged.

5.2 Change in size of supply mode. Figures 5.7—5.9 illustrate the changes in aerosol size distribution when mode of supply is varied, and Figures 5.10—5.12 show the associated changes in aerosol mass density, particle concentration, and mass turnover time.

Figures 5.7—5.9 illustrate that the mode of supply is reflected in the aerosol distribution, but not necessarily as the main feature.

When the supply mode is at a very small size, the aerosol mode is often shifted upwards together with a spread of the high concentration numbers towards somewhat larger sizes.

When the supply mode is placed at increasingly larger sizes, the strength of the aerosol mode is diminished and the mode may for extreme conditions be shifted downwards.

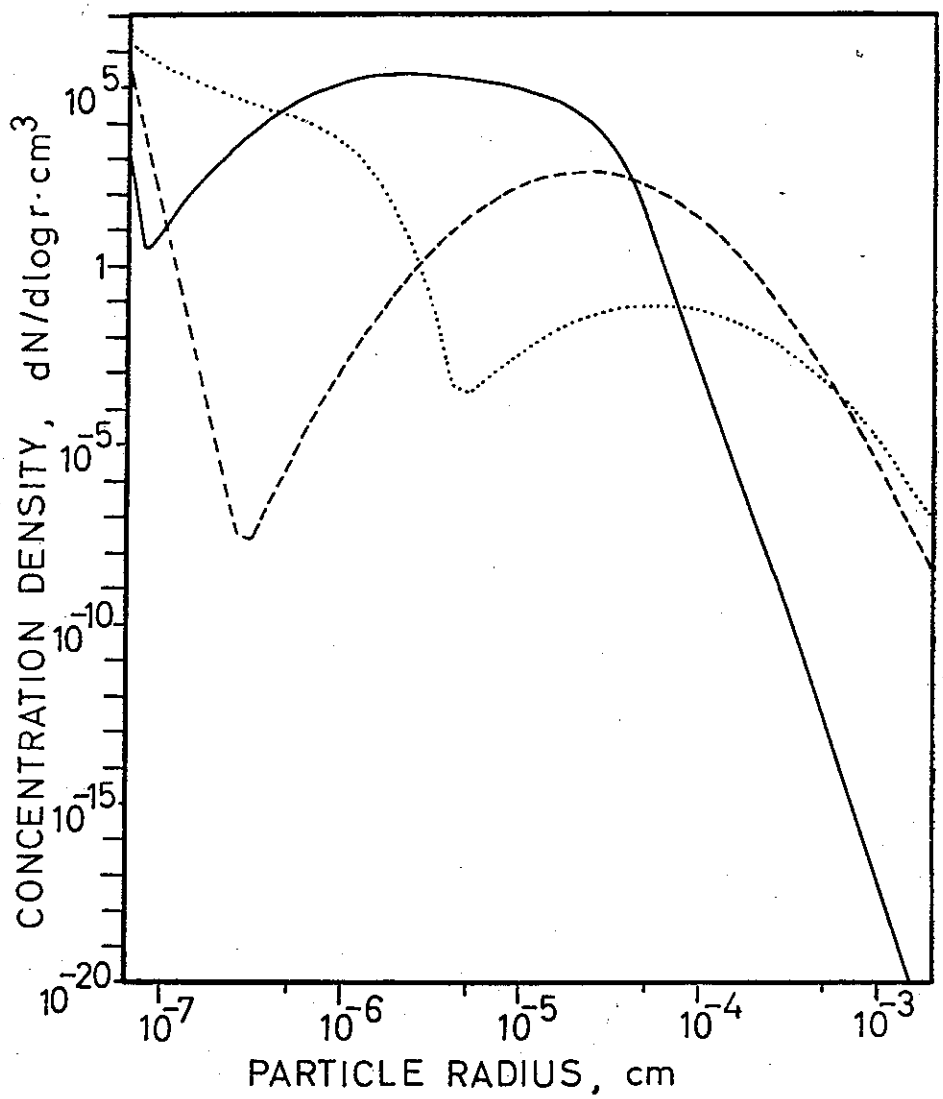

Fig. 5.8. *Aerosol size distribution for various supply modes.* Parameters for solid curve: small-particle supply 100 $cm^{-3}s^{-1}$, other supply $10^{-14}gcm^{-3}s^{-1}$ with mode 10^{-6} cm and $\sigma = 2$, removal coefficient 10^{-4} and exponent 2, air replacement time 24 hrs. Except for a shift in supply mode to $3.16 \cdot 10^{-5}$ cm for the broken curve and 10^{-4} for the dotted curve, parameters remain unchanged.

A combination of causes is at work: Increased mode leads to lower supply number and thus to less coagulation influence, while rate of removal increases.

Figure 5.10 indicates that the aerosol mass in general decreases with increasing particle size in the mode. With fixed rate of mass supply, the mass turn-over time in Figure 5.12 shows the same effect. As a result of low aerosol mass an accumulation of small particles occurs. This is evident in Figures 5.7—5.9.

When the supply mode is at a very large size, the aerosol size distribution may become one where the bulk of the particles is small, and the aerosol mass low, even though the supply distribution has a strong mode at higher sizes. This is illustrated by the distributions shown.

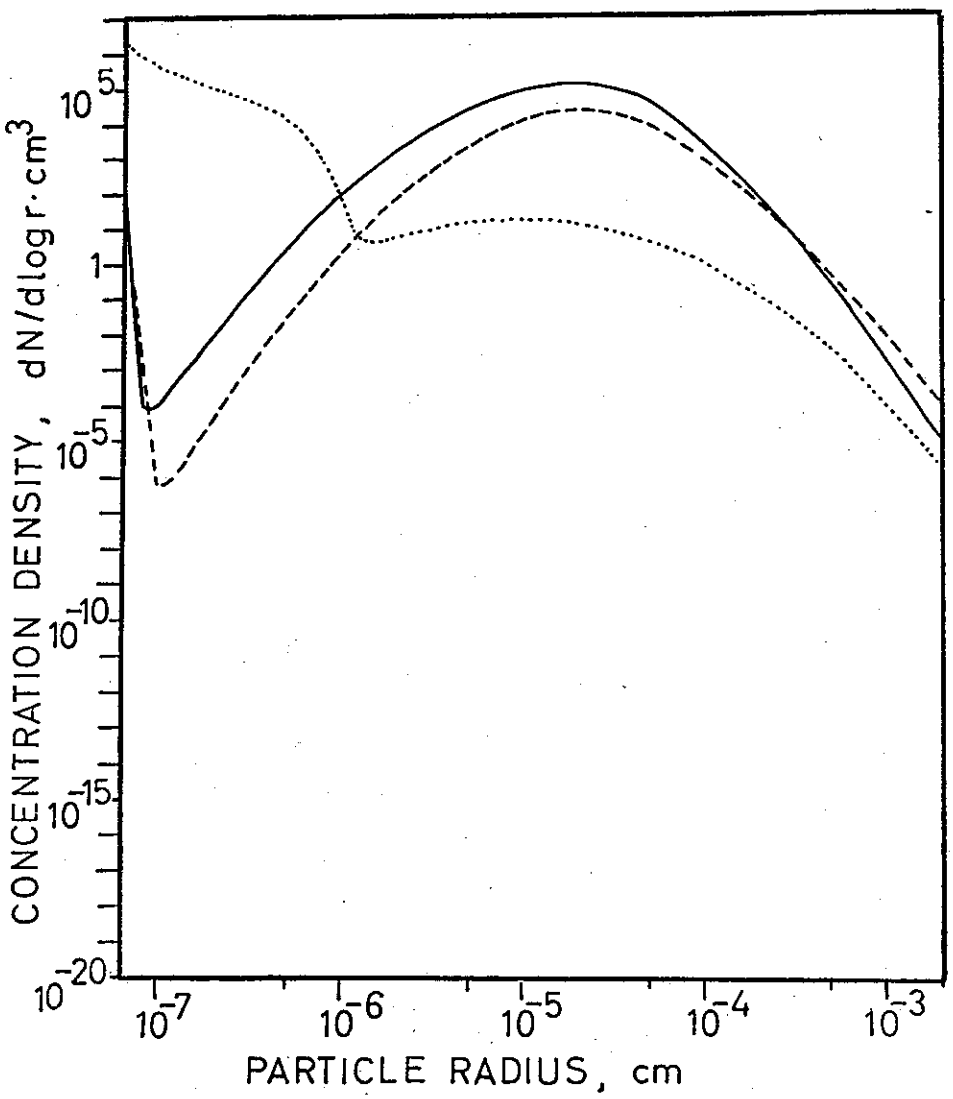

Fig. 5.9. *Aerosol size distribution for various supply modes.* Parameters for solid curve: small-particle supply 100 $cm^{-3}s^{-1}$, other supply $10^{-12}gcm^{-3}s^{-1}$ with mode 10^{-5} cm and $\sigma = 2.5$, removal coefficient 10^{-4} and exponent 1.75, air replacement time 96 hrs. Except for a shift in supply mode to $2.37 \cdot 10^{-5}$ cm for the broken curve and $3.16 \cdot 10^{-5}$ for the dotted curve, parameters remain unchanged.

The change may sometimes be rather abrupt, as indicated in Figures 5.9—5.12. For a supply mode size at $2.37 \cdot 10^{-5}$ cm the aerosol distribution has a definite medium size mode with mass of more than $4 \cdot 10^{-9}$ g/cm³, particle concentration 16,400 per cm³ and a mass turn-over time 1.1 hours. For a supply mode at $2.74 \cdot 10^{-5}$ cm the aerosol mass is 10^{-11} g/cm³, particle concentration more than 300,000 per cm³ and mass turn-over time 9 seconds.

When the supply mode is at small sizes, the aerosol particle concentration becomes high because these particles are not easily removed. For a medium supply size, a medium size aerosol mode is well developed, and the particle concentration decreases because few small particles can exist in the aerosol. For supply particles of greater sizes

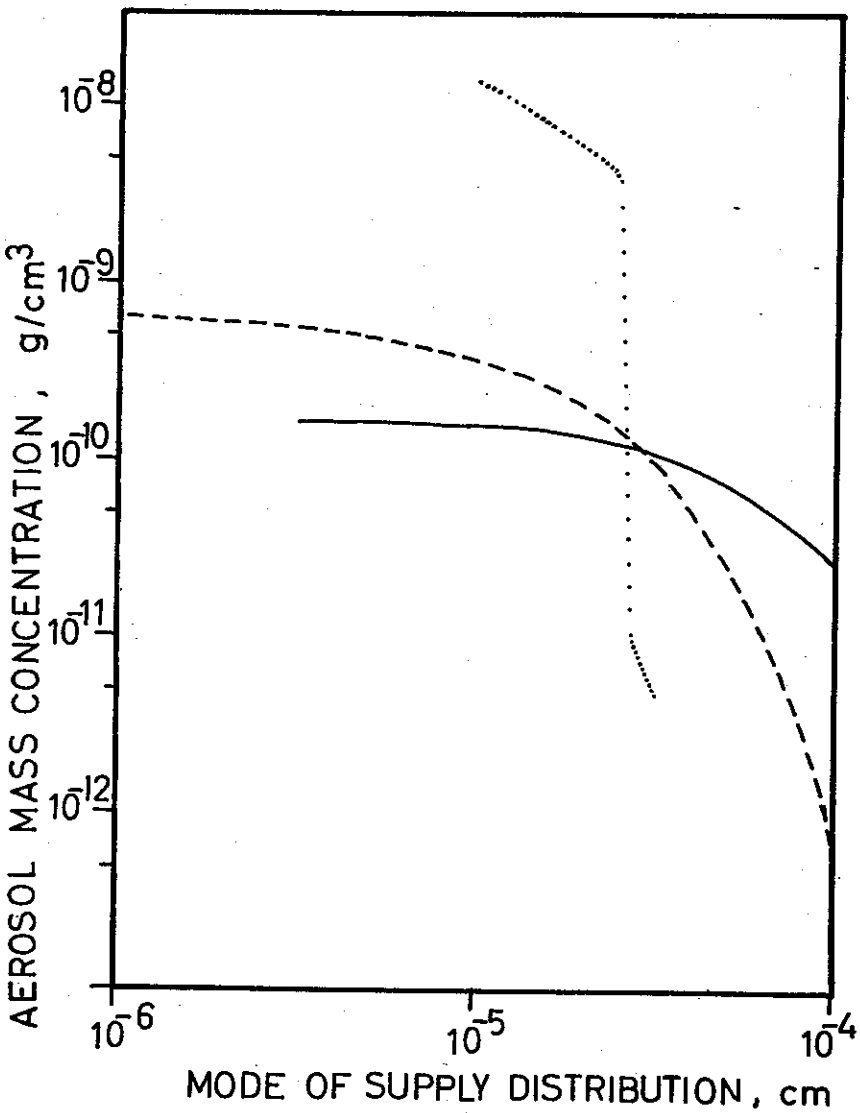

Fig. 5.10. *Aerosol mass for various supply modes.* Solid curve refers to distributions from Fig. 5.7., broken to 5.8. and dotted to 5.9.

a medium/large particle mode in the aerosol will not develop due to rapid removal. Small particles are therefore accumulated, and in spite of reduced mass the particle concentration is raised with further increase of the supply mode size.

The position of and the concentration at the minimum, together with the rise for large supply particles are all dependent on the supply of small particles. Figure 5.11 should only be regarded as typical in a qualitative sense.

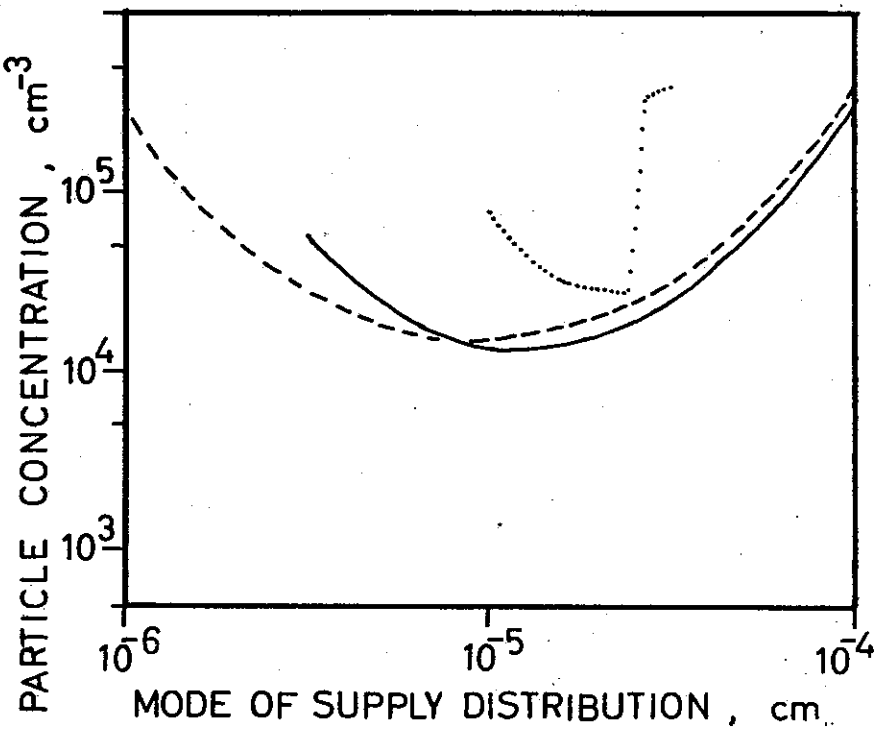

Fig. 5.11. *Aerosol particle concentration for various supply modes.* Solid curve refers to distributions from Fig. 5.7., broken curve to 5.8. and dotted curve to 5.9.

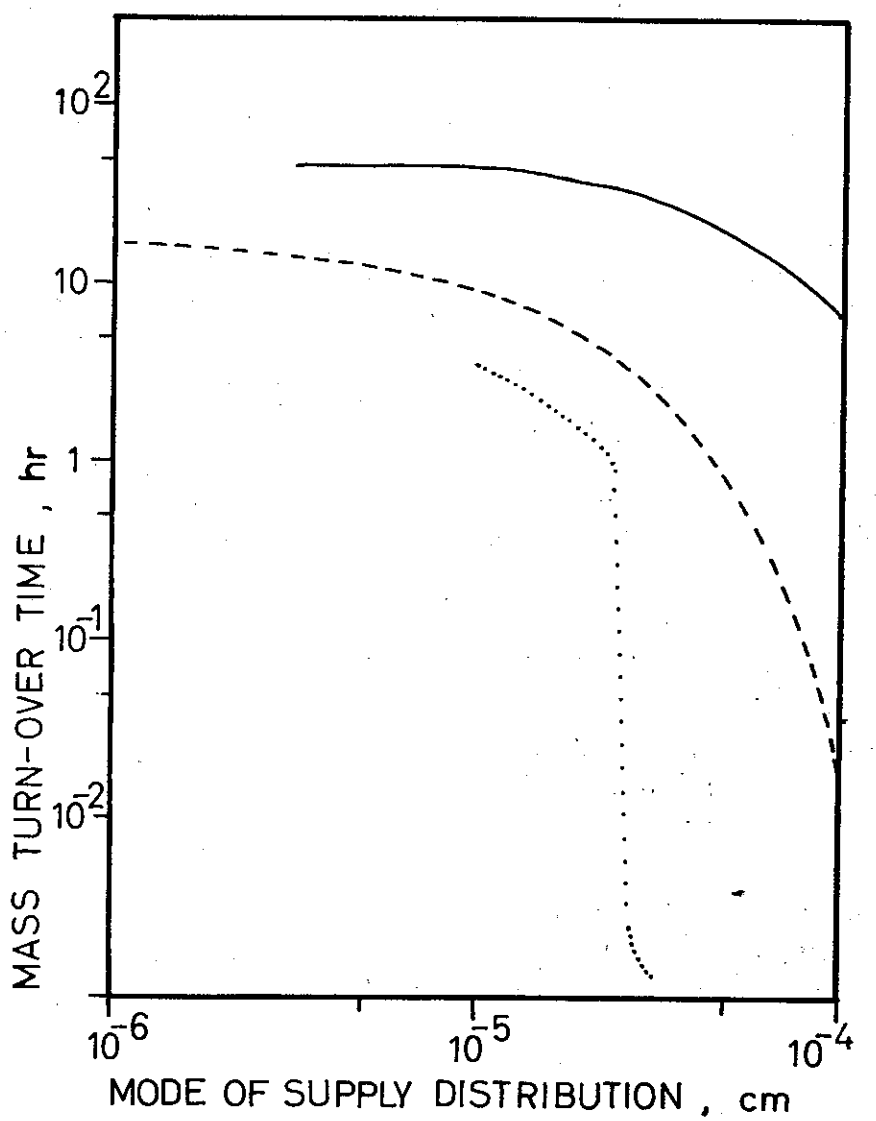

Fig. 5.12. *Mass turn-over time for various supply modes.* Solid curve refers to distributions from Fig. 5.7., broken curve to 5.8. and dotted curve to 5.9.

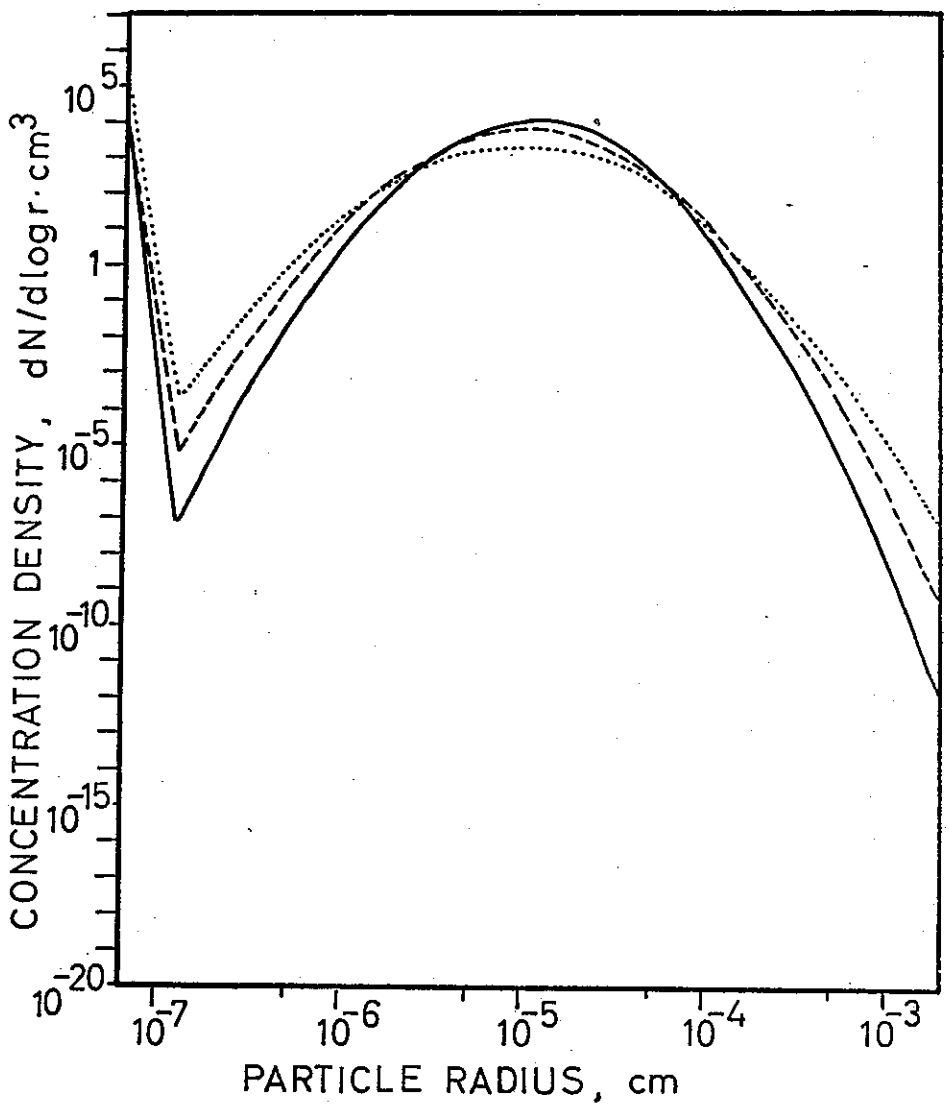

Fig. 5.13. *Aerosol size distribution for various supply spreads.* Parameters for solid curve: small-particle supply 100 $cm^{-3}s^{-1}$, other supply $10^{-14}gcm^{-3}s^{-1}$ with mode 10^{-5} cm and $\sigma = 2$, removal coefficient 10^{-4} and exponent 2, air replacement time 24 hrs. Except for increase of σ to 2.2 for the broken curve and to 2.5 for the dotted curve, parameters remain unchanged.

5.3 Change in size spread of supply particles. Figures 5.13—5.15 illustrate the changes in aerosol size distribution when the supply particles have a more or less narrow size distribution, and Figures 5.16—5.18 show the associated changes in aerosol mass density, particle concentration and mass turn-over time.

It is apparent that the supply spread is reflected in the aerosol, although some distortion occurs. For conditions leading to a pronounced aerosol mode at medium particle sizes (this is the case for Figure 5.13) the correspondence is particularly good. For larger supply spreads, an increased part of the mass is associated with particles in a region more easily removed, leading to the shorter mass turn-over time evident in Figure 5.18. It is seen from Figure 5.16 that it also leads to decreased mass in the

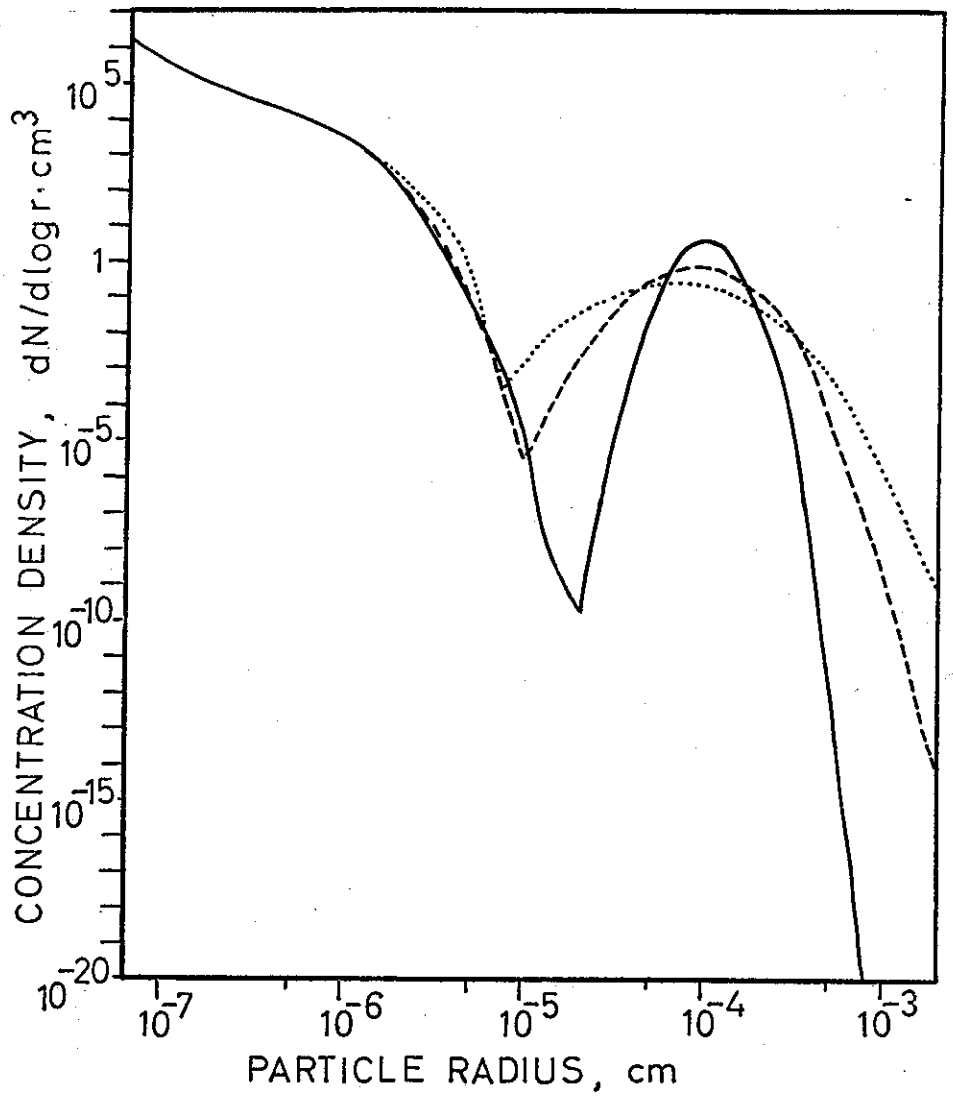

Fig. 5.14. *Aerosol size distribution for various supply spreads.* Parameters for solid curve: small-particle 100 $cm^{-3}s^{-1}$, other supply $10^{-15}gcm^{-3}s^{-1}$ with mode 10^{-4} cm and $\sigma = 1.25$, removal coefficient 10^{-4} and exponent 2, air replacement time 24 hrs. Except for increase of σ to 1.5 for the broken curve and to 1.75 for the dotted curve, parameters remain unchanged.

aerosol. This further renders possible the accumulation of small particles, which is seen in Figure 5.13.

The conditions on which Figure 5.14 are based have produced an aerosol distribution with the bulk of the particles in the small size region and with a low mass concentration. Mass decreases with increase in supply-particle spread also under these circumstances. An associated increase of small particles is evident in the aerosol size distribution.

In Figure 5.15, a change in type of distribution occurs due to the change in spread. In principle, the same type of change takes place as earlier, but the change is radical. Mass drops from $3 \cdot 10^{-9}$ to $4 \cdot 10^{-12}$ g/cm³, and simultaneously mass turn-over time drops from 50 minutes to 4 seconds.

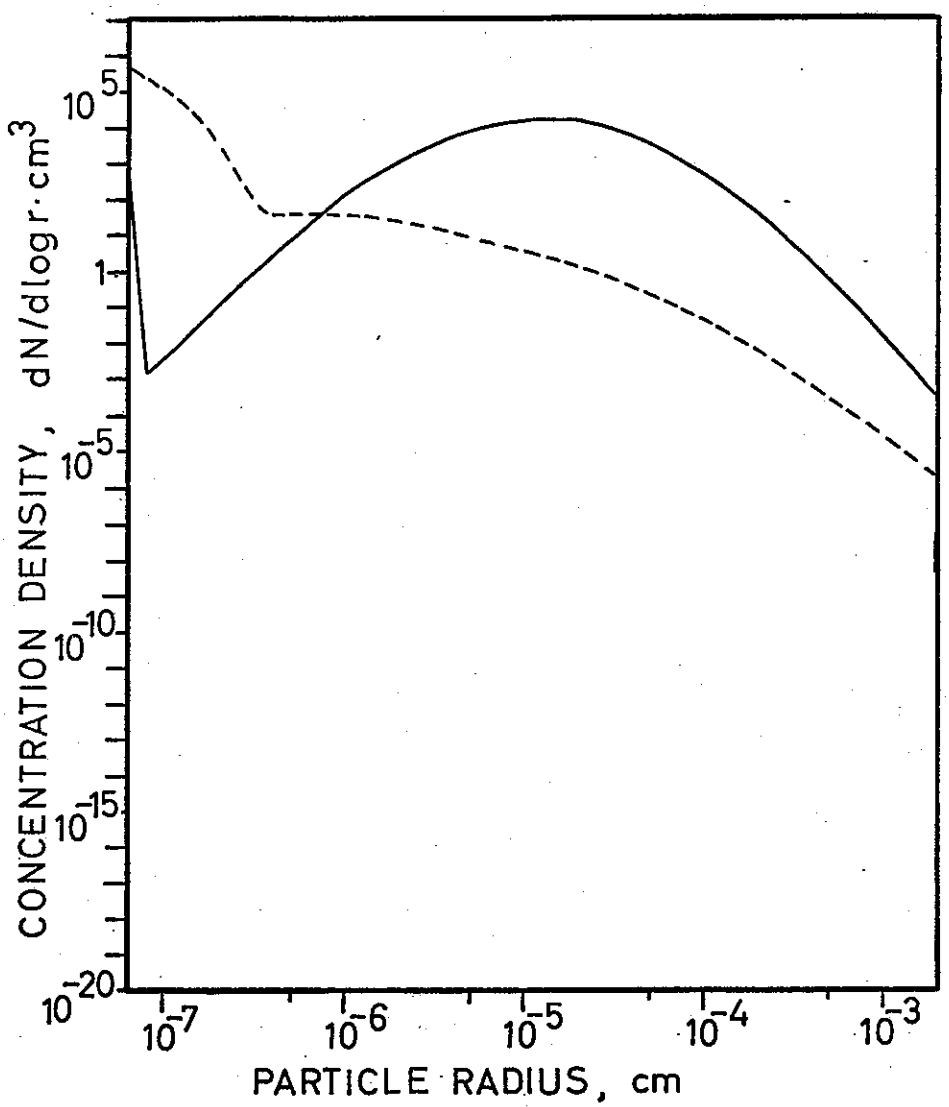

Fig. 5.15. *Aerosol size distribution for various supply spreads.* Parameters for solid curve: small-particle supply 10 $cm^{-3}s^{-1}$, other supply $10^{-12}gcm^{-3}s^{-1}$ with mode 10^{-5} cm and $\sigma = 3$, removal coefficient 10^{-4} and exponent 1.75, air replacement time 12 hrs. Except for increase of σ to 3.5 for the broken curve, parameters remain unchanged.

The aerosol particle concentrations in Figure 5.17 reflect the degree of balance between small and large particles. For conditions leading to a medium size aerosol mode, the particle concentration has a minimum for a certain spread. For a spread less than this, the higher concentrations are caused by medium/large particles. For larger spreads the reason is increased amount of small particles.

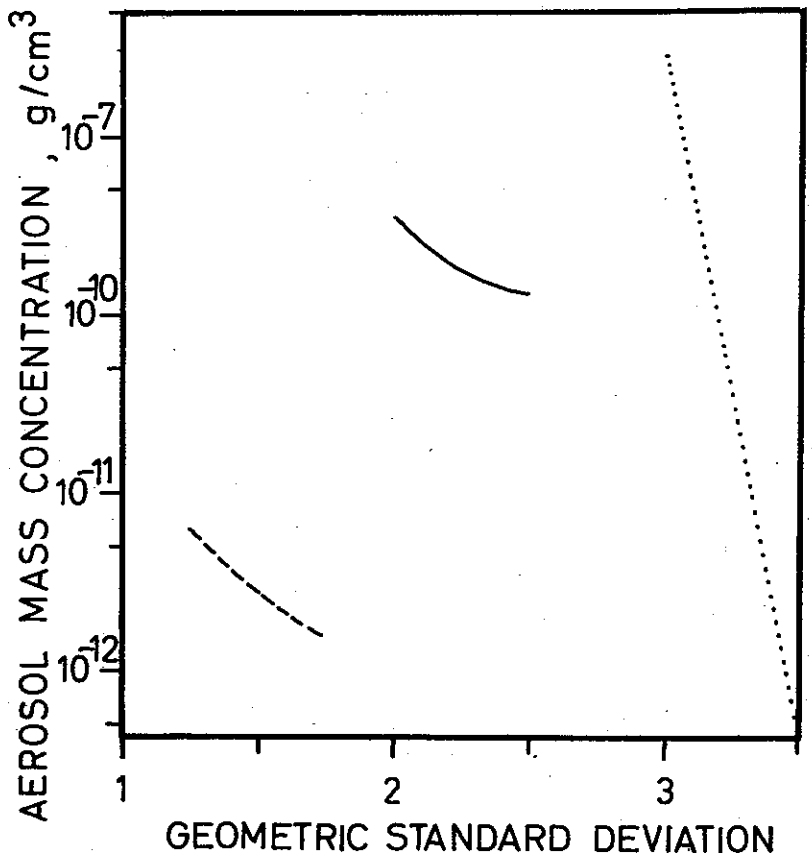

Fig. 5.16. *Aerosol mass for various supply spreads.* Solid curve refers to Fig. 5.13., broken curve to 5.14. and dotted curve to 5.15.

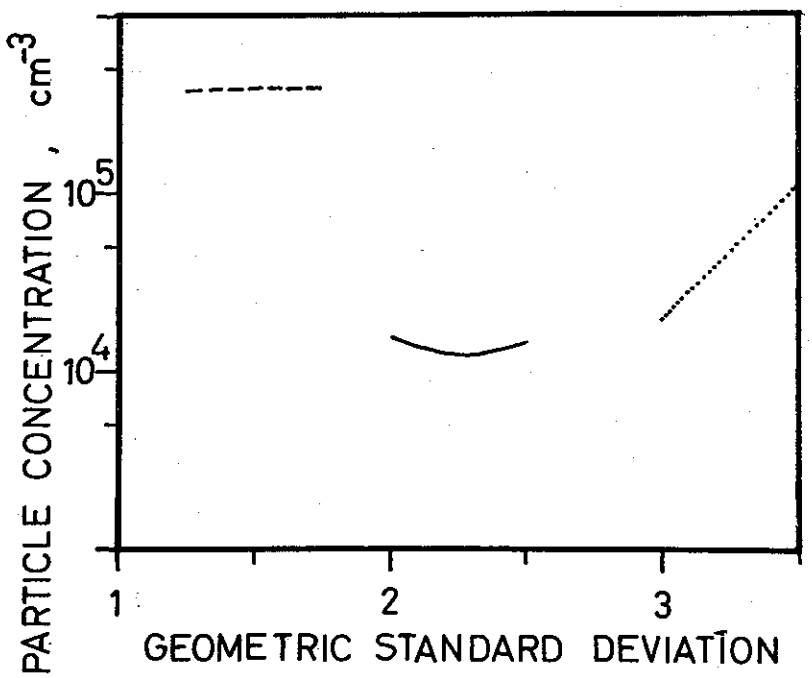

Fig. 5.17. *Aerosol particle concentration for various supply spreads.* Solid curve refers to Fig. 5.13., broken curve to 5.14. and dotted curve to 5.15.

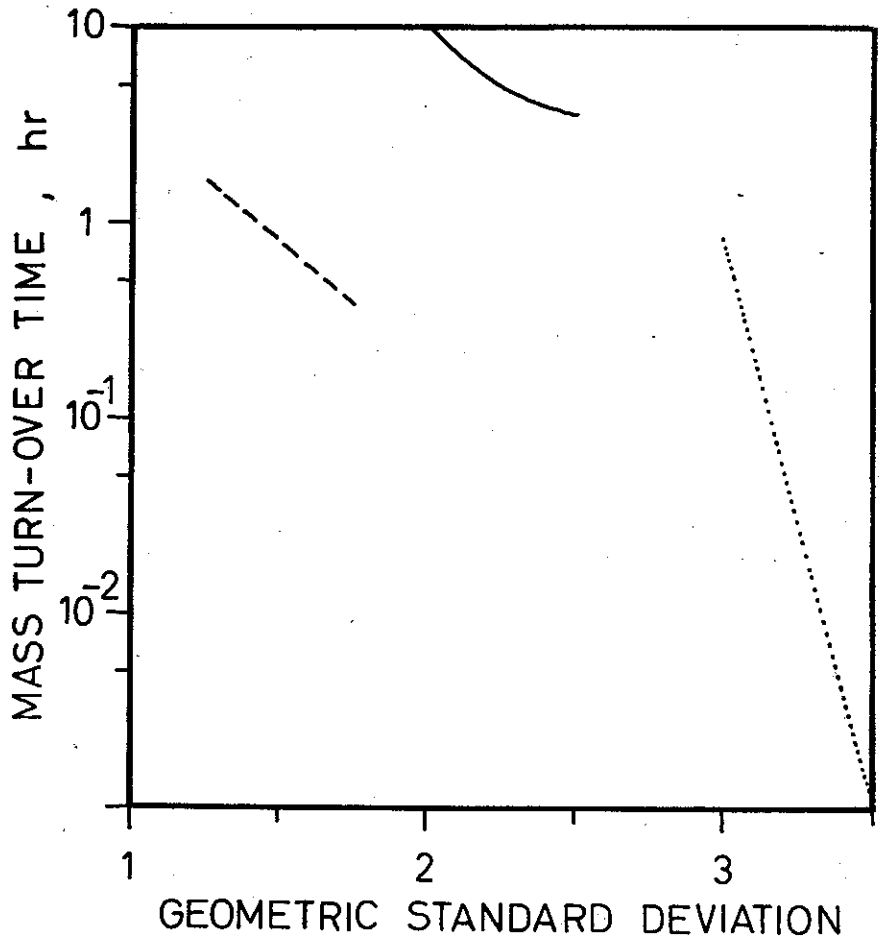

Fig. 5.18. *Mass turn-over time for various supply spreads.* Solid curve refers to Fig. 5.13., broken curve to 5.14 and dotted curve to 5.15.

5.4 Change in rate of small-particle supply. Figures 5.19 and 5.20 illustrate the changes in aerosol size distribution, when change occurs in the supply of particles at the lower end of the size distribution. Associated changes in particle concentration are shown in Figure 5.21. Since the aerosol mass and the mass turn-over time only show insignificant changes, diagrams are not presented.

An increase in small-particle supply increases the concentration of particles in the lower size region of the aerosol, but it does not noticeably affect the medium and upper size region. The increased amounts of small particles weigh little in the mass account and consequently do not affect the mass turn-over time. But the particle concentration may increase considerably.

A completely different situation is created if the small-particle supply is the main supply to the aerosol. Figure 5.22 illustrates the situation when only small particles are supplied. Only the lower size region is then filled up by particles in the aerosol.

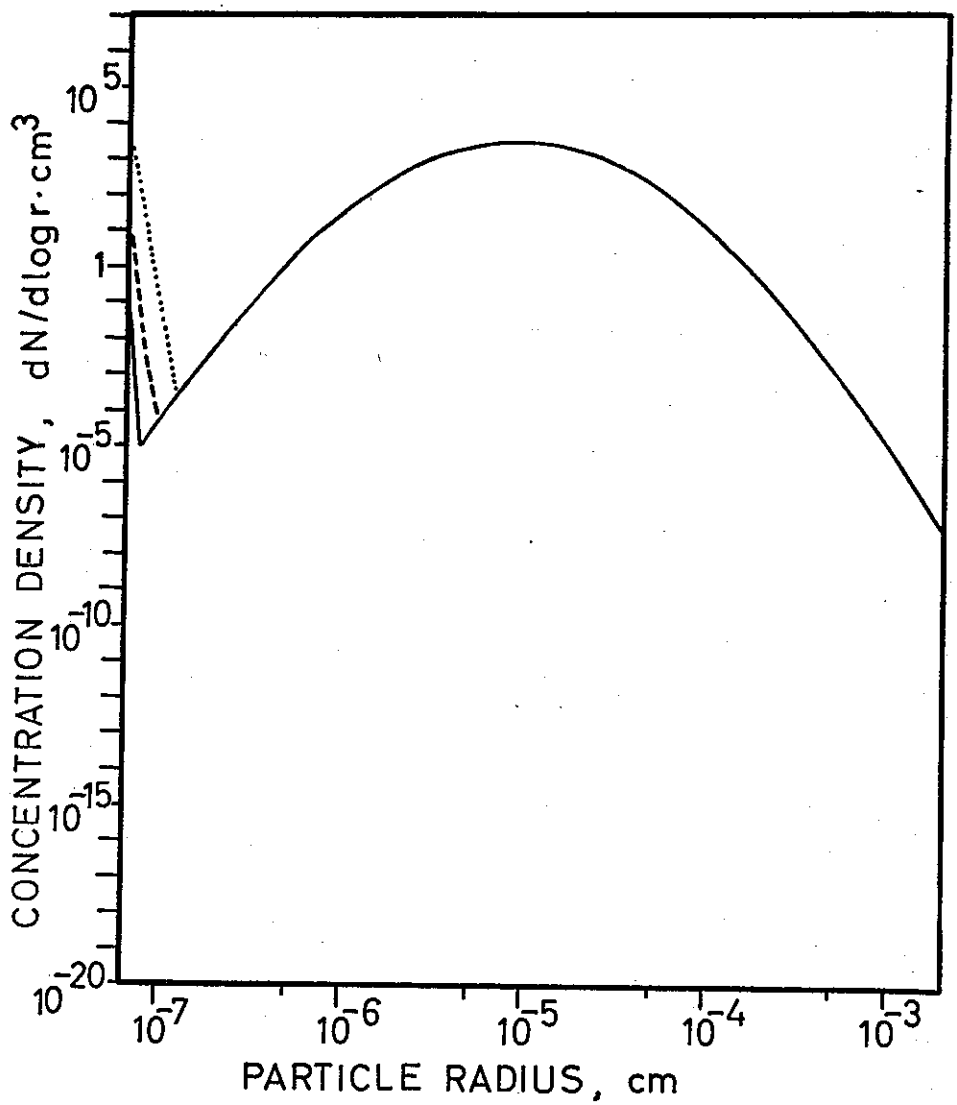

Fig. 5.19. *Aerosol size distribution for various small-particle supplies.* Parameters for solid curve: small-particle supply 0.01 $cm^{-3}s^{-1}$, other supply $10^{-14}gcm^{-3}s^{-1}$ with mode 10^{-5} cm and $\sigma = 2.5$, removal coefficient 10^{-4} and exponent 2, air replacement time 24 hrs. Except for increase in small-particle supply to 1 $cm^{-3}s^{-1}$ for the broken curve and to 100 for the dotted curve, parameters remain unchanged.

When the supply is small, say less than 0.1 particles per cm^3 per second, a peak appears at the supply size, and the peak gradually becomes broader as the supply increases. For greater supply a secondary mode appears between 10^{-6} and 10^{-5} cm radius, and a minimum between the lower peak and this mode. The radical change in the distribution is probably due to the variable coagulation coefficient. It can be seen from Figure 2.3 that maximum values occur in this size region.

The aerosol mass increases rapidly with the supply. This is shown in Figure 5.23. The particle concentration shown in Figure 5.21 also increases with particle supply.

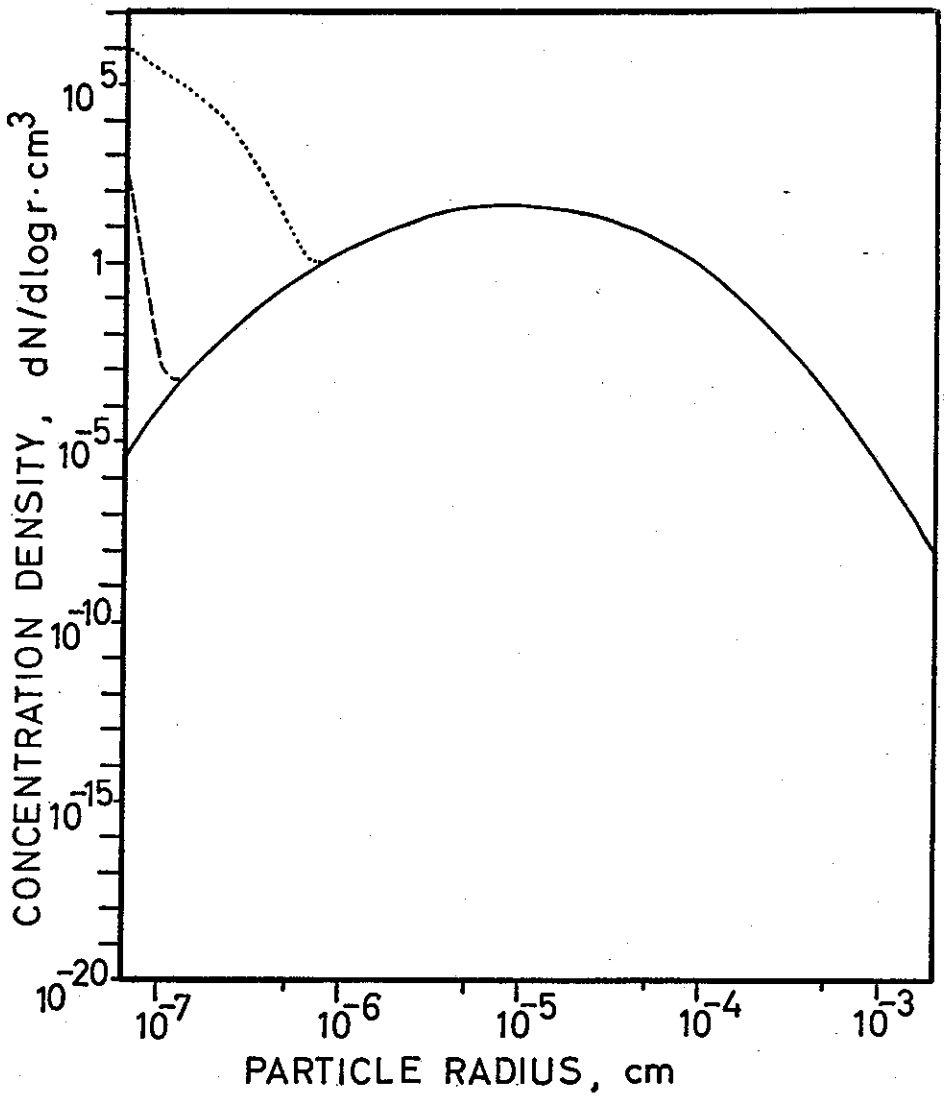

Fig. 5.20. *Aerosol size distribution for various small-particle supplies.* Parameters for solid curve: small-particle supply 0 $cm^{-3}s^{-1}$, other supply $10^{-15}gcm^{-3}s^{-1}$ with mode 10^{-5} cm and $\sigma = 2.5$, removal coefficient 10^{-4} and exponent 1.75, air replacement time 3 hrs. Except for increase in small-particle supply to 0.1 $cm^{-3}s^{-1}$ for the broken curve and to 100 for the dotted curve, parameters remain unchanged.

Fig. 5.21. *Aerosol particle concentration for various small-particle supplies.* Solid curve refers to Fig. 5.19, broken curve to 5.20 and dotted curve to 5.22.

Fig. 5.22. *Aerosol size distribution for various small-particle supplies.* Parameters for solid curve: small-particle supply 0.001 $cm^{-3}s^{-1}$, no other supply, removal coefficient 10^{-6} and exponent 1.75, air exchange time 5000 hrs. Except for increase in small-particle supply to 0.1 $cm^{-3}s^{-1}$ for the broken curve and to 10 for the dotted curve, parameters remain unchanged.

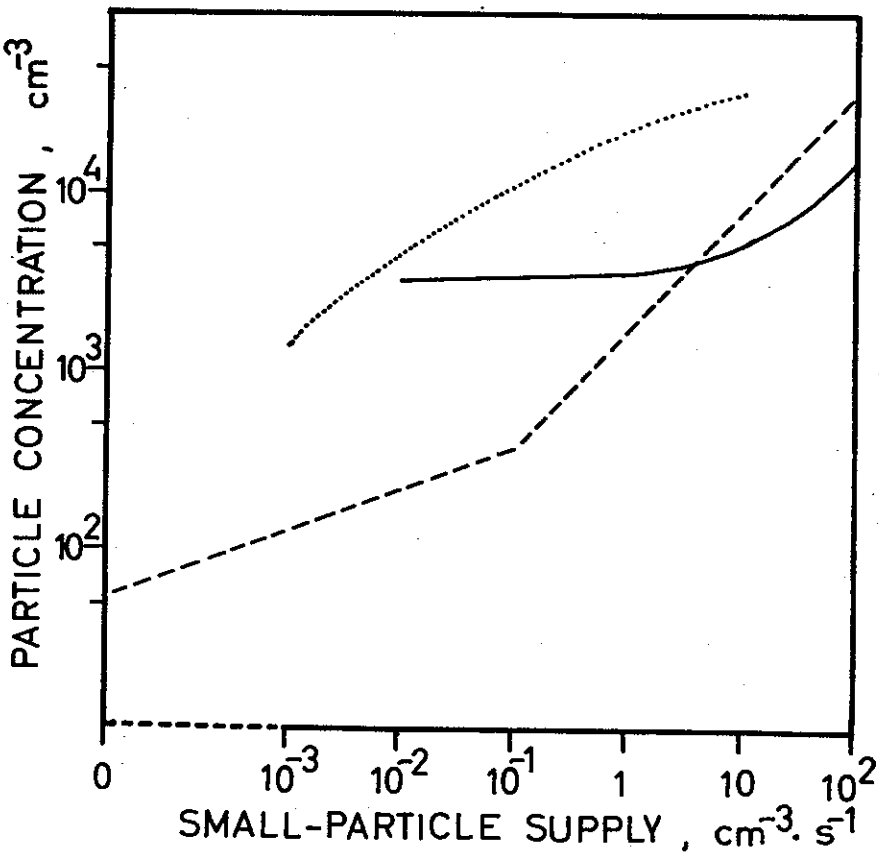
PARTICLE CONCENTRATION , cm^{-3}
10^4
10^3
10^2
0
10^{-3}
10^{-2}
10^{-1}
1
10
10^2
SMALL-PARTICLE SUPPLY , cm^{-3}. s^{-1}

5.21.

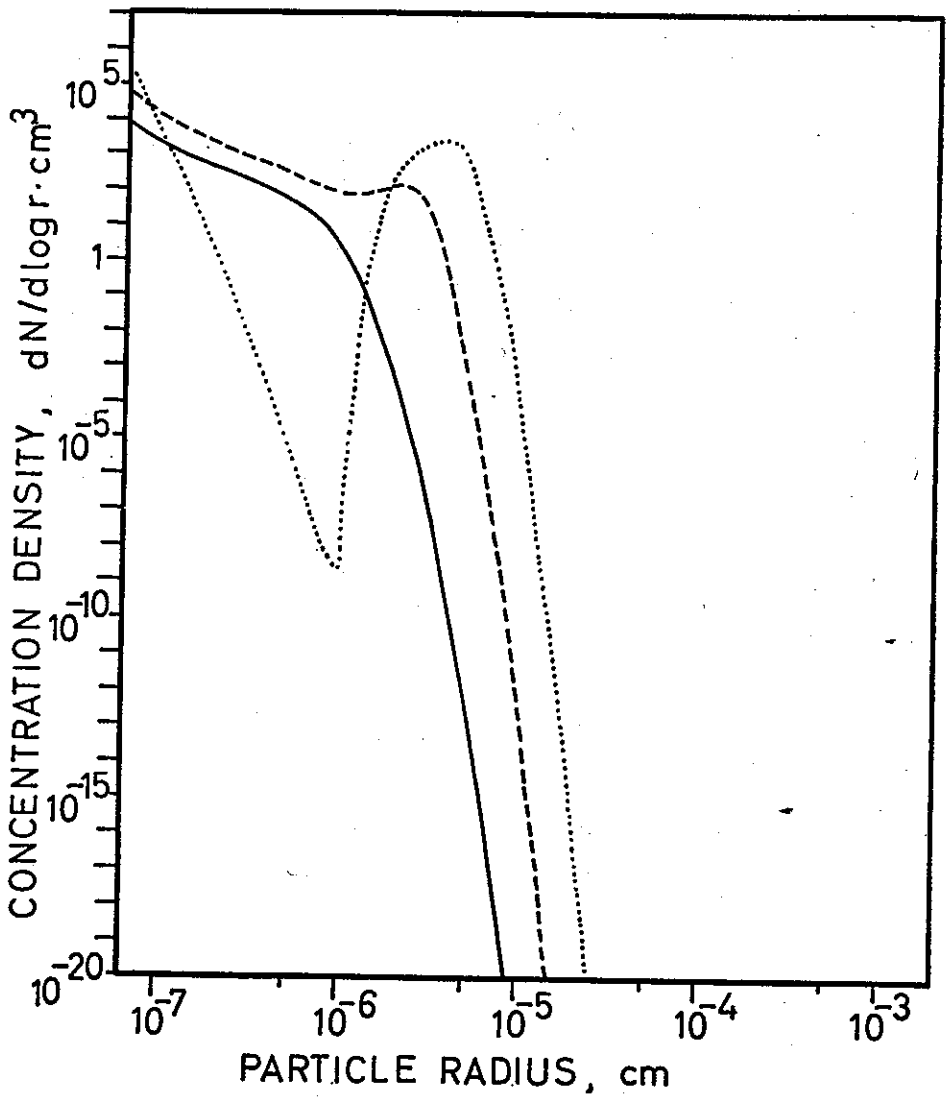
CONCENTRATION DENSITY, dN/dlogr·cm^3
10^5
1
10^{-5}
10^{-10}
10^{-15}
10^{-20}
10^{-7}
10^{-6}
10^{-5}
10^{-4}
10^{-3}
PARTICLE RADIUS, cm

5.22.

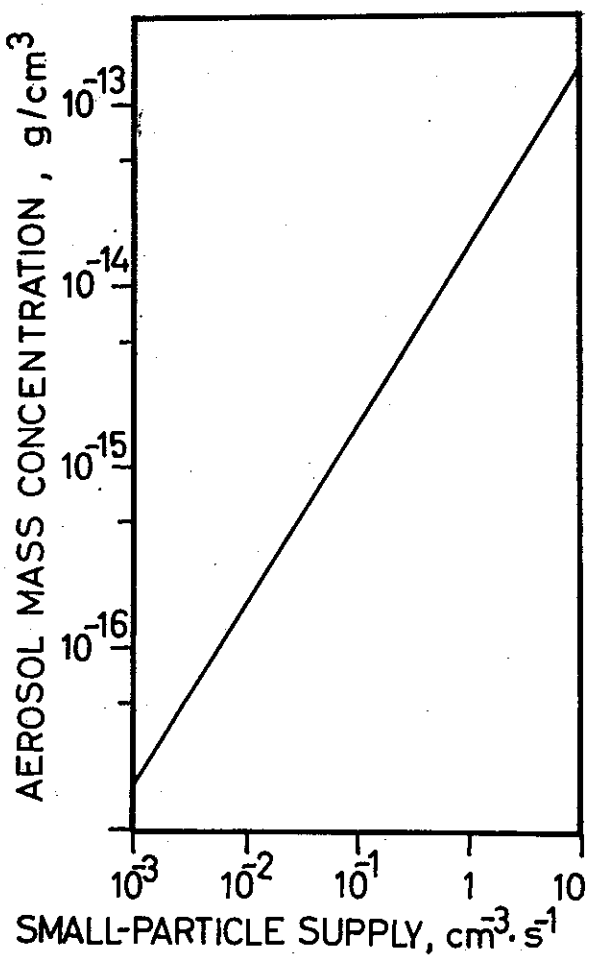

Fig. 5.23. *Aerosol mass for various small-particle supplies.* The curve refers to the distributions in Fig. 5.22.

Mass turn-over time, however, is only slightly affected under the conditions studied. It decreases about 7 per cent when particle supply increases from 10^{-3} to 10 per cm^3 per second.

5.5 Change in aerosol dilution. Figures 5.24—5.27 illustrate the change in aerosol size distribution when the degree of dilution is varied, and Figures 5.28—5.30 show the associated changes in aerosol mass density, particle concentration and mass turn-over time.

The first-order effect of dilution is a decrease in concentration, and this is indeed the trend observed for the main modes in Figures 5.24 to 5.27. The reduction in aerosol mass, which is evident from Figure 5.28, leads to the secondary effect of accumulation of small particles, and this effect is strong enough to increase the small-particle concentration with increasing dilution. As a result the total particle concentration may have a minimum value for a certain rate of dilution, which can be noticed in Figure 5.29. Mass turn-over times in Figure 5.30 show a general decrease with increasing dilution.

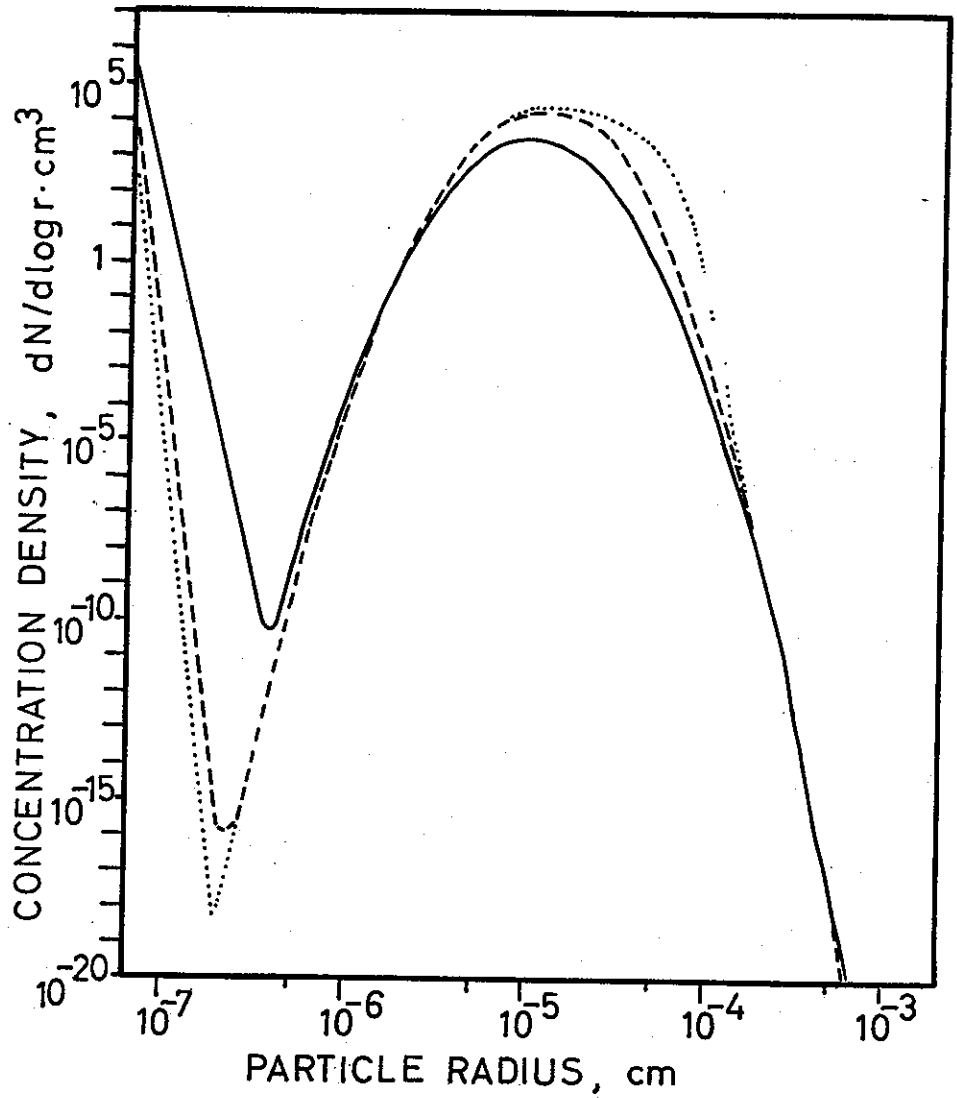

Fig. 5.24. *Aerosol size distribution for various degrees for dilution.* Parameters for solid curve: small-particle supply 100 $cm^{-3}s^{-1}$, other supply $10^{-15}gcm^{-3}s^{-1}$ with mode 10^{-5} cm and $\sigma = 1.5$, removal coefficient 10^{-5} and exponent 2, air replacement time 3 hrs. Except for increase in air replacement time to 48 hrs. for the broken curve and to 5000 hrs. for the dotted curve, parameters remain unchanged.

Figure 5.27 is based on conditions leading to most of the mass being accumulated on small particles. The dilution effect is noticeable over most of the distribution. But coagulation conditions are not changed appreciably, and only at the very lower end of the size region does a small increase in particle concentration take place with increased dilution.

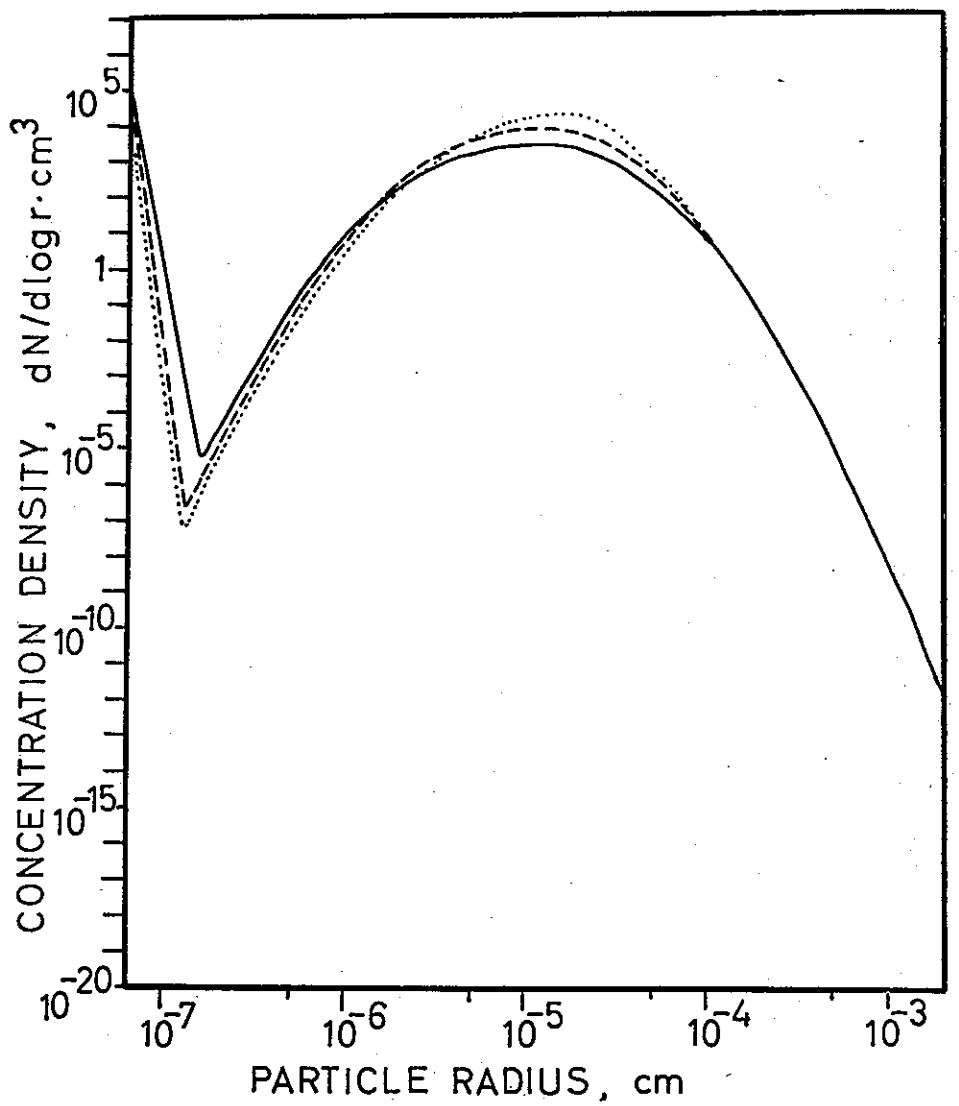

Fig. 5.25. *Aerosol size distribution for various degrees of dilution.* Parameters for solid curve: small-particle supply 100 $cm^{-3}s^{-1}$, other supply $10^{-14}gcm^{-3}s^{-1}$ with mode 10^{-5} cm and $\sigma = 2$, removal coefficient 10^{-4} and exponent 2, air replacement time 3 hrs. Except for increase in air replacement time to 12 hrs. for the broken curve and to 48 hrs. for the dotted curve, parameters remain unchanged.

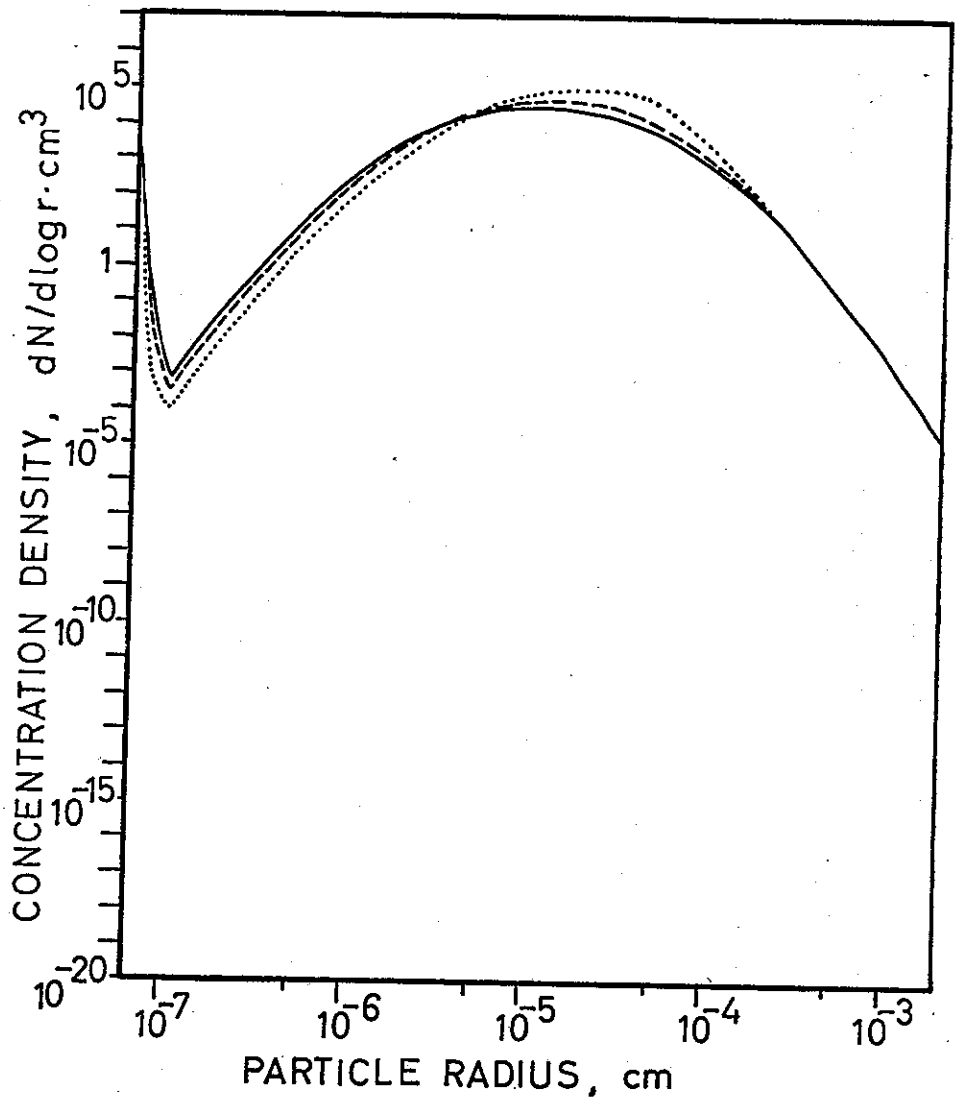

Fig. 5.26. *Aerosol size distribution for various degrees of dilution.* Parameters for solid curve: small-particle supply 100 $cm^{-3}s^{-1}$, other supply $10^{-12}gcm^{-3}s^{-1}$ with mode 10^{-5} cm and $\sigma = 2.5$, removal coefficient 10^{-4} and exponent 1.75, air replacement time 1.5 hrs. Except for increase in air replacement time to 3 hrs. for the broken curve and to 96 hrs. for the dotted curve, parameters remain unchanged.

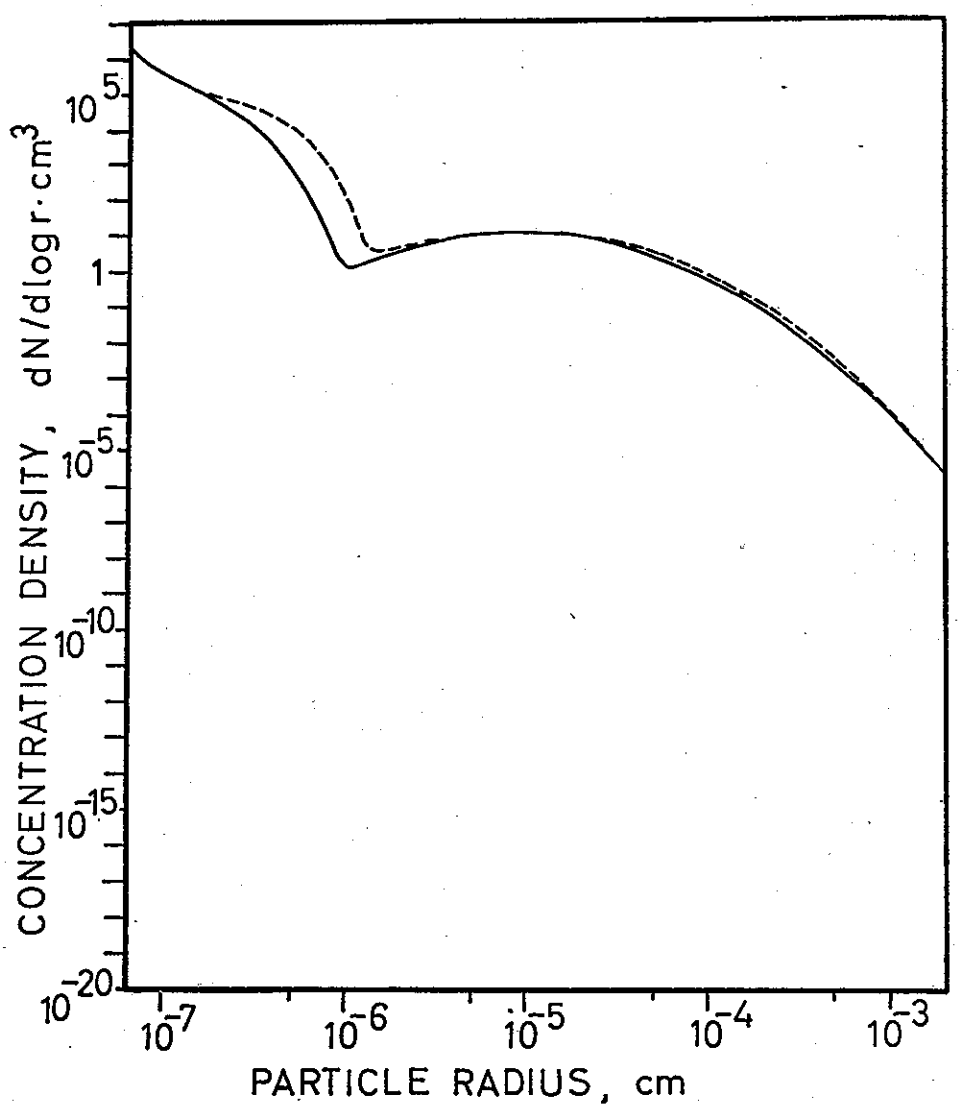

Fig. 5.27. *Aerosol size distribution for various degrees of dilution.* Parameters for solid curve: small-particle supply 100 $cm^{-3}s^{-1}$, other supply $10^{-12}gcm^{-3}s^{-1}$ with mode $3.16 \cdot 10^{-5}$ cm and $\sigma = 2.5$, removal coefficient 10^{-4} and exponent 1.75, air replacement time 6 hrs. Except for increase in air replacement time to 96 hrs. for the broken curve, parameters remain unchanged.

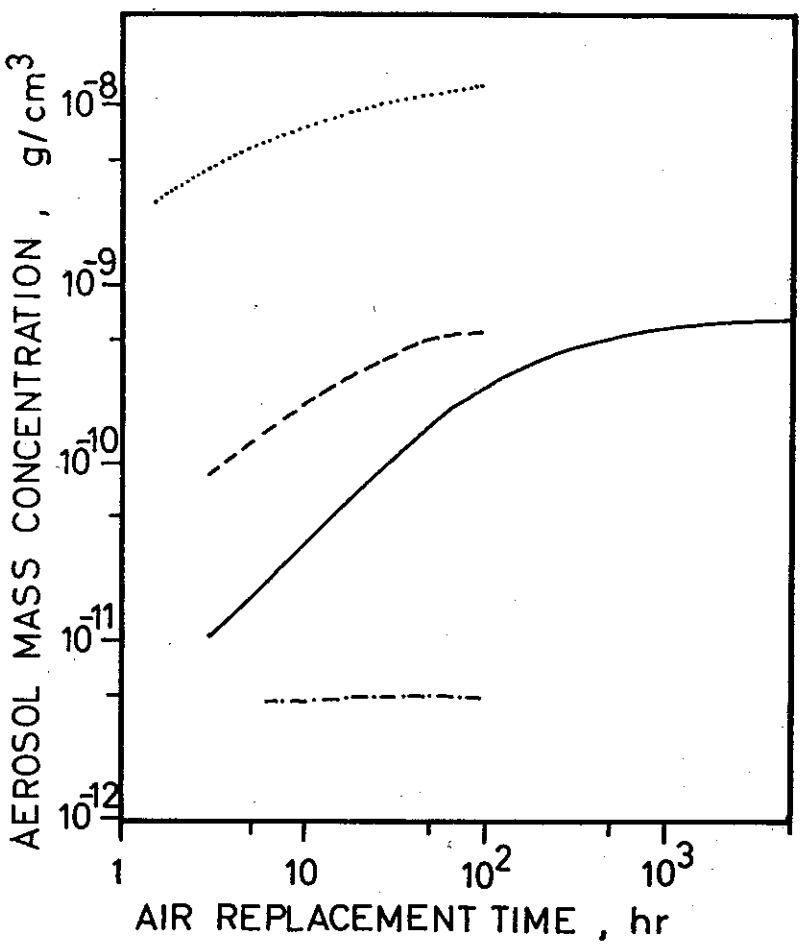

Fig. 5.28. *Aerosol mass for various air replacement times.* Solid curve refers to Fig. 5.24, broken curve to 5.25, dotted curve to 5.26 and broken/dotted curve to 5.27.

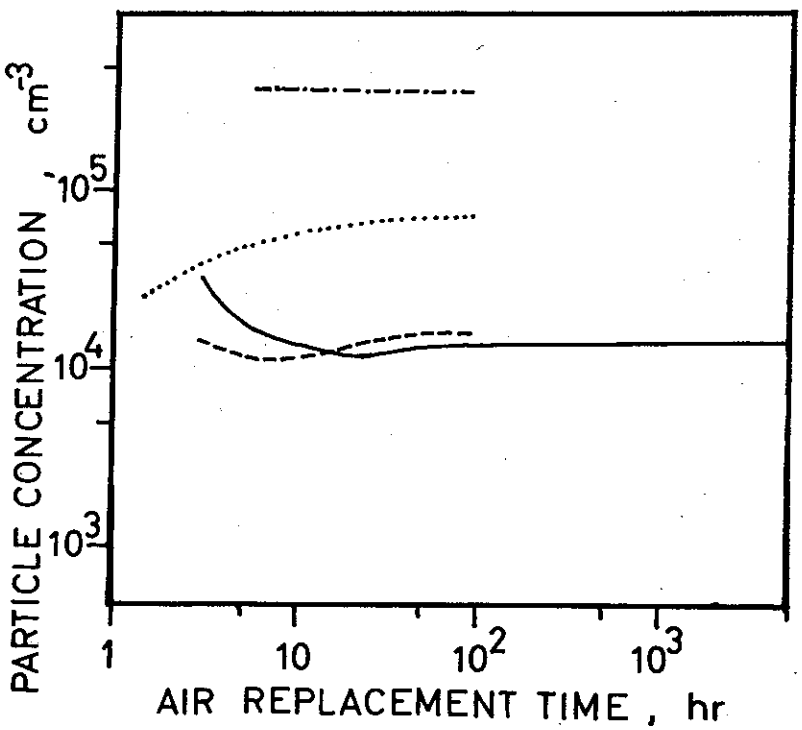

Fig. 5.29. *Aerosol particle concentration for various air replacement times.* Solid curve refers to Fig. 5.24., broken to 5.25, dotted to 5.26 and broken/dotted curve to 5.27.

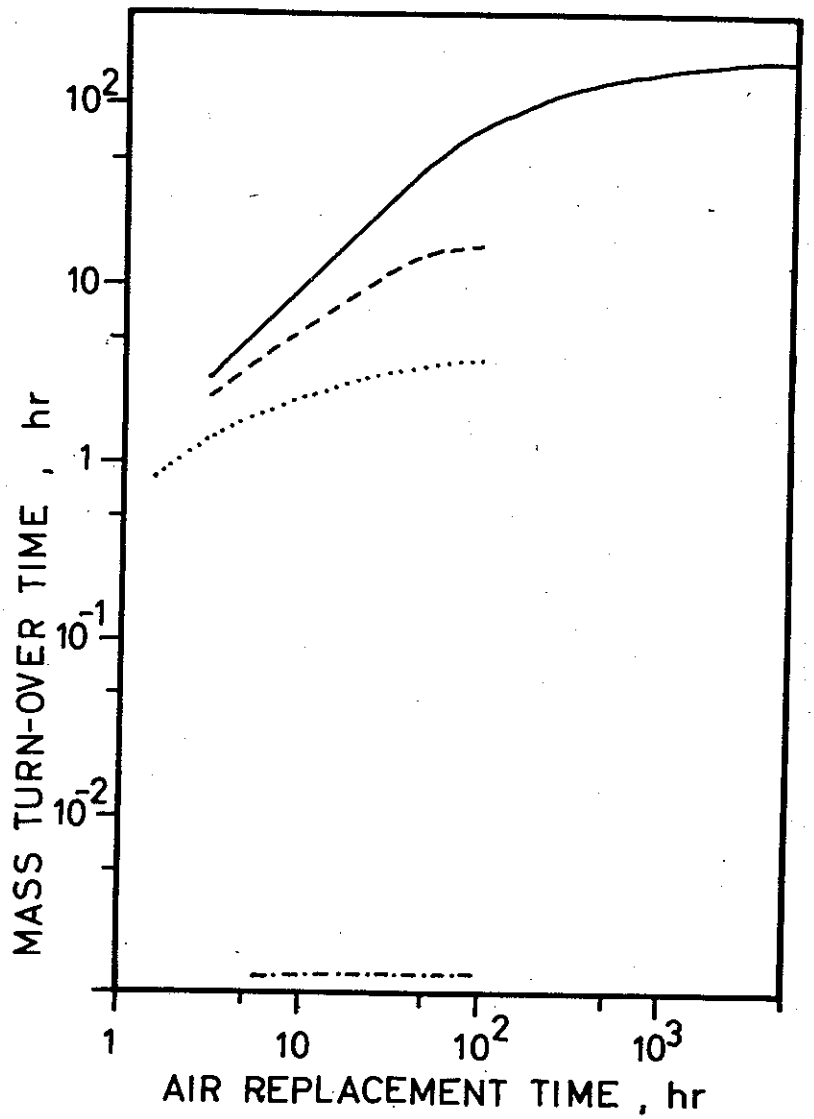

Fig. 5.30. *Mass turn-over time for various air replacement times.* Solid curve refers to Fig. 5.24., broken to 5.25, dotted to 5.26 and broken/dotted curve to 5.27.

5.6 Change in removal coefficient. Figures 5.31—5.34 illustrate the changes in aerosol size distribution when the removal coefficient is varied, and Figures 5.35—5.37 show the associated changes in aerosol mass density, particle concentration and mass turn-over time.

The primary effect of an increase in removal coefficient is a decrease in aerosol density, leading to a lower mass and a shorter mass turn-over time. The secondary effect of a build-up of small particles, because the amount of large particles decreases, is evident in all the Figures 5.30—5.34. The total particle concentration in Figure 5.36 reflects the balance, and particle concentration may decrease, pass a minimum value or increase, depending on the other conditions.

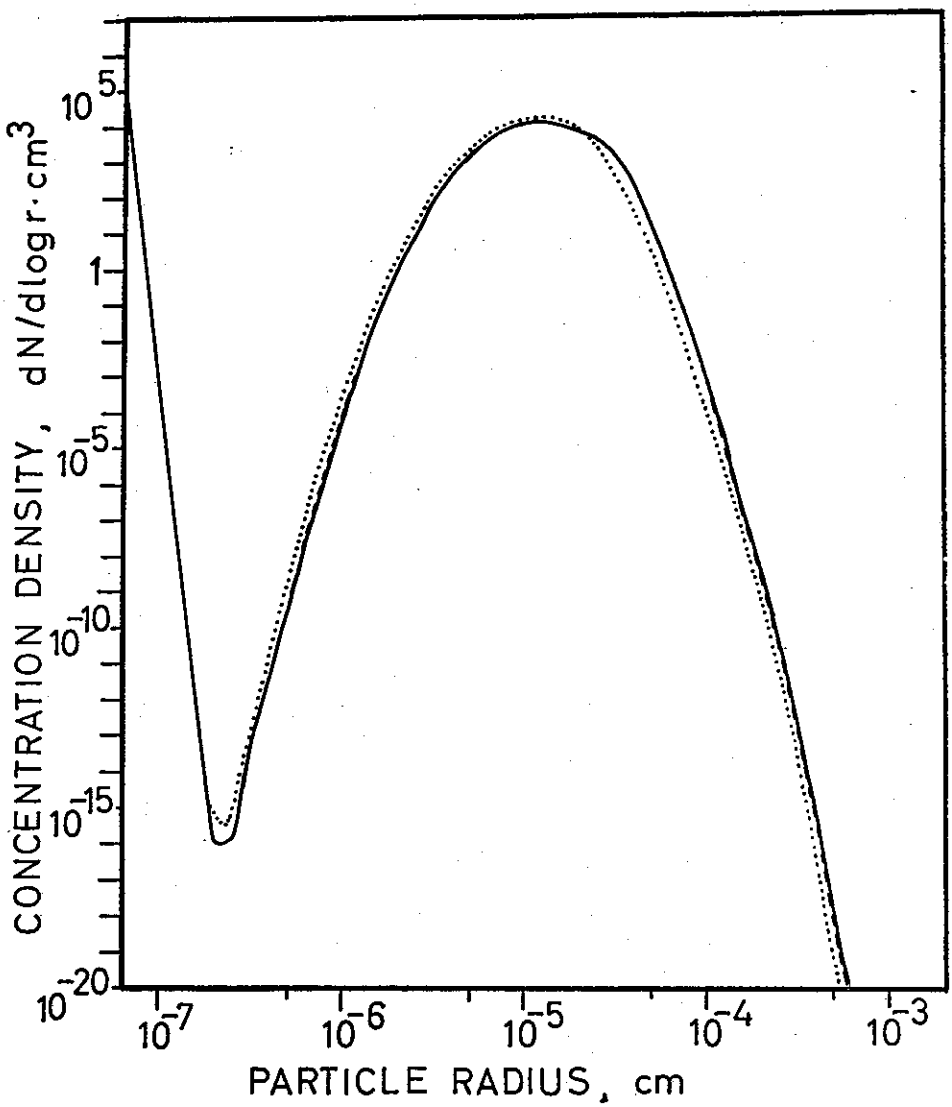

Fig. 5.31. *Aerosol size distribution for various removal coefficients.* Parameters for solid curve: small-particle supply 100 $cm^{-3}s^{-1}$, other supply $10^{-15}gcm^{-3}s^{-1}$ with mode 10^{-5} cm and $\sigma = 1.5$, removal coefficient 10^{-5} and exponent 2, air replacement time 96 hrs. Except for an increase in removal coefficient to $3.16 \cdot 10^{-5}$ for the broken curve and to 10^{-4} for the dotted curve, parameters remain unchanged.

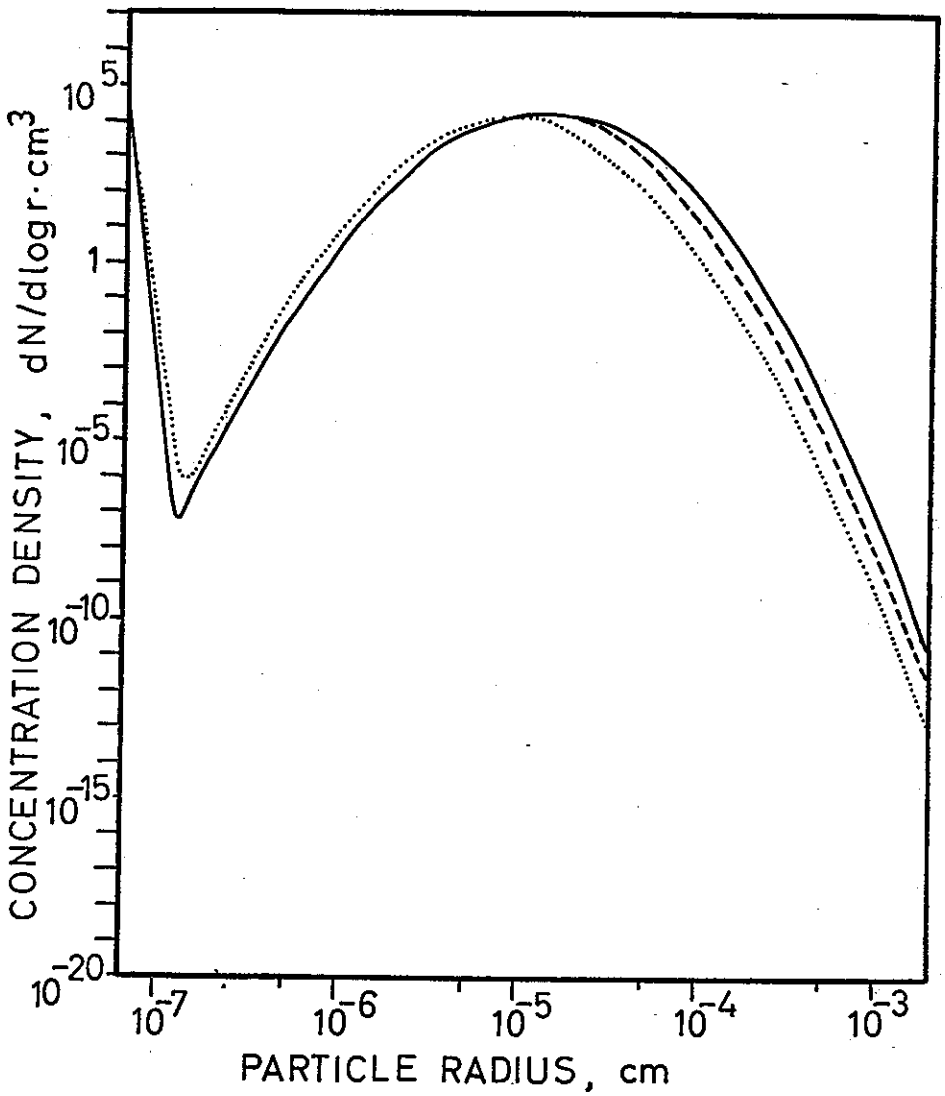

Fig. 5.32. *Aerosol size distribution for various removal coefficients.* Parameters for solid curve: small-particle supply 100 $cm^{-3}s^{-1}$, other supply $10^{-14}gcm^{-3}s^{-1}$ with mode 10^{-5} cm and $\sigma = 2$, removal coefficient 10^{-5} and exponent 2, air replacement time 24 hrs. Except for an increase in removal coefficient to 10^{-4} for the broken curve and to 10^{-3} for the dotted curve, parameters remain unchanged.

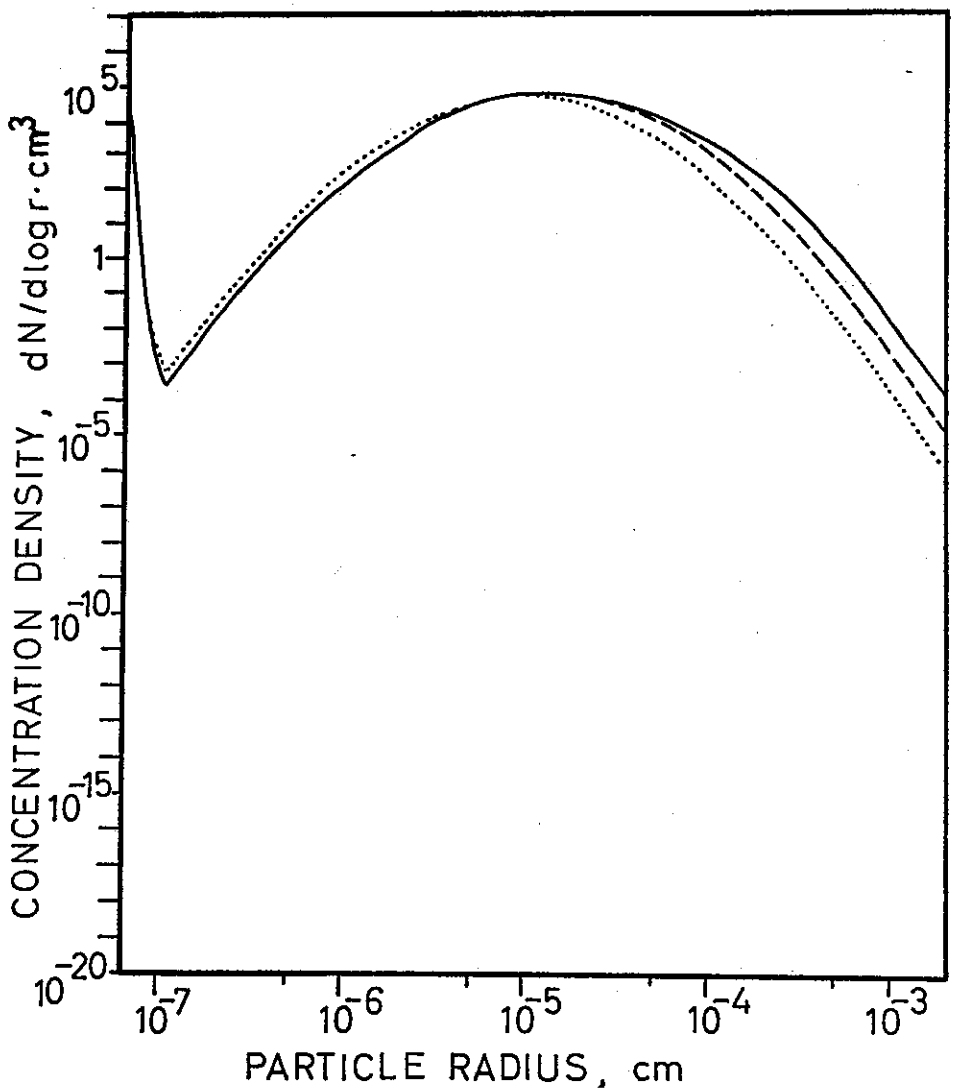

Fig. 5.33. *Aerosol size distribution for various removal coefficients.* Parameters for solid curve: small-particle supply 100 $cm^{-3}s^{-1}$, other supply $10^{-12}gcm^{-3}s^{-1}$ with mode $10^{-5}cm$ and $\sigma = 2.5$, removal coefficient 10^{-5} and exponent 1.75, air replacement time 3 hrs. Except for an increase in removal coefficient to 10^{-4} for the broken curve and to 10^{-3} for the dotted curve, parameters remain unchanged.

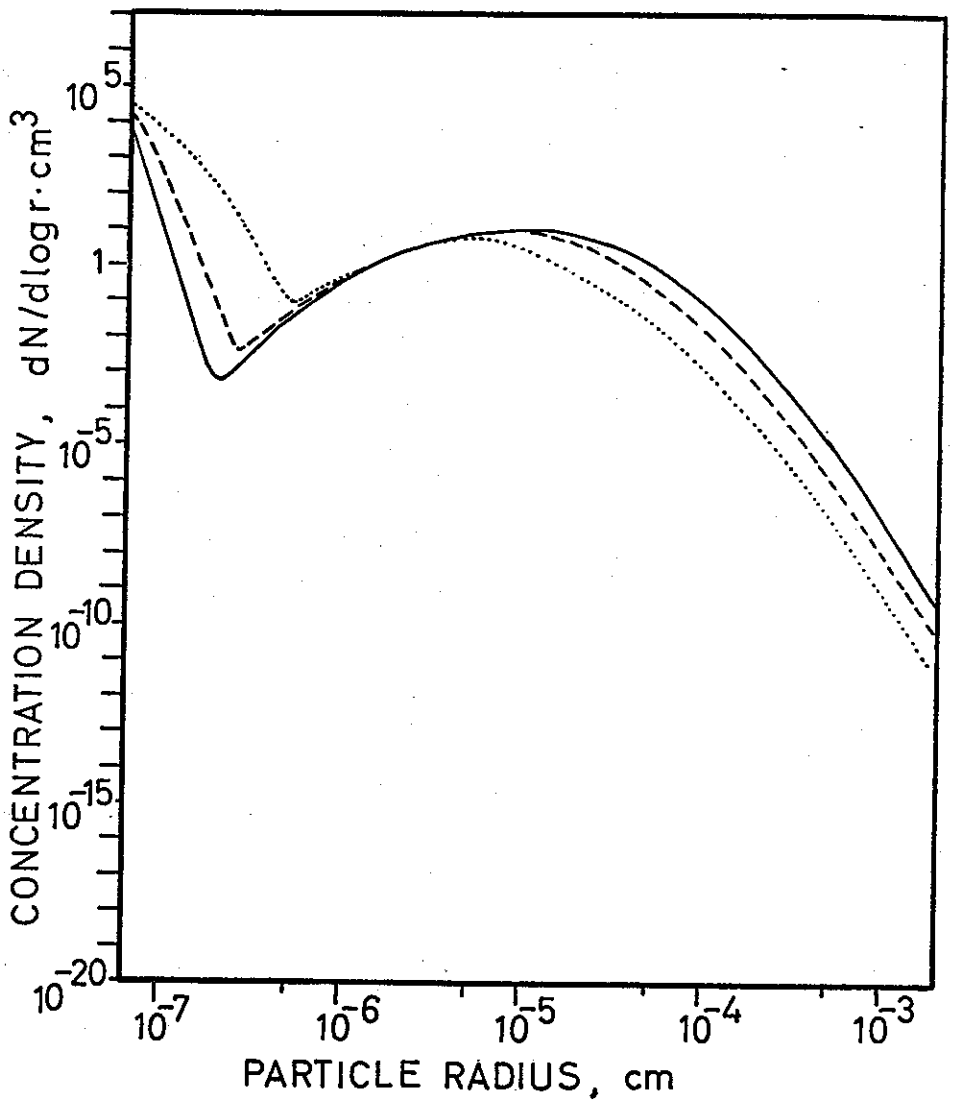

Fig. 5.34. *Aerosol size distribution for various removal coefficients.* Parameters for solid curve: small-particle supply 0.1 $cm^{-3}s^{-1}$, other supply $10^{-17}gcm^{-3}s^{-1}$ with mode 10^{-5} cm and $\sigma = 2.5$, removal coefficient 10^{-5} and exponent 2, air replacement time 96 hrs. Except for an increase in removal coefficient to 10^{-4} for the broken curve and to 10^{-3} for the dotted curve, parameters remain unchanged.

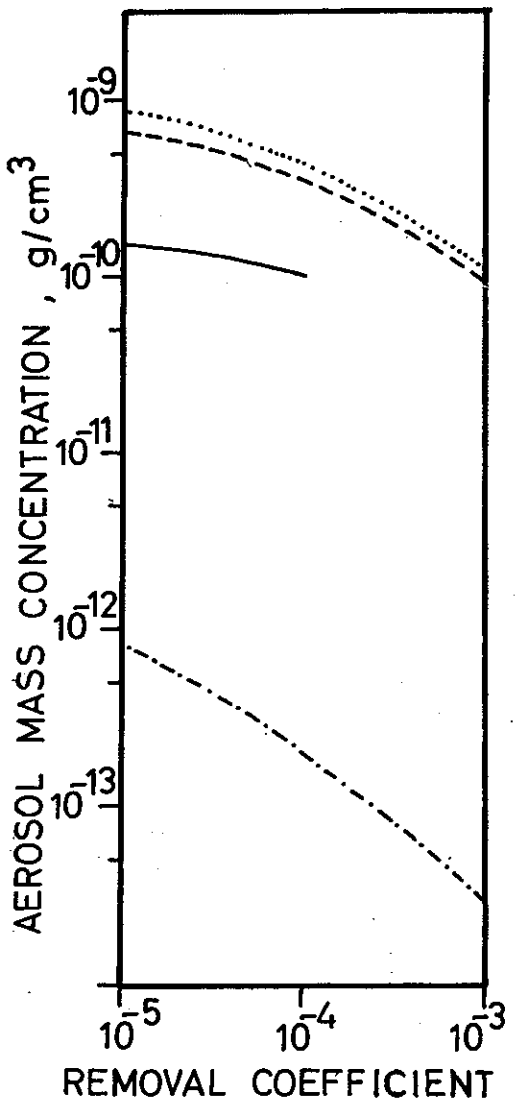

Fig. 5.35. *Aerosol mass for various removal coefficients.* Solid curve refers to Fig. 5.31, broken to 5.32, dotted curve to 5.33, broken/dotted curve to 5.34.

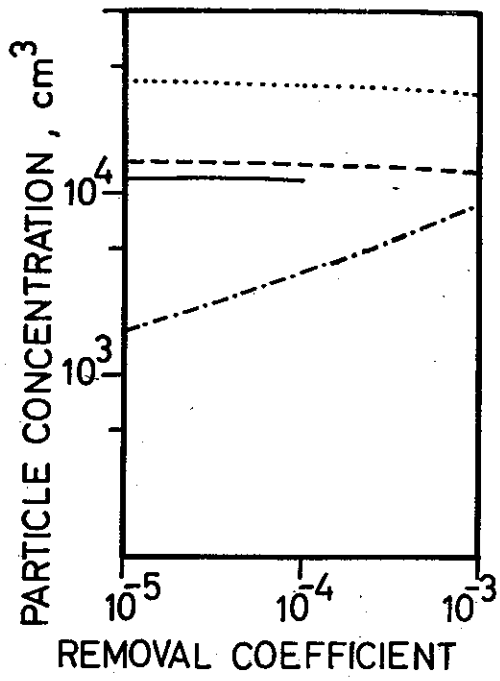

Fig. 5.36. *Aerosol particle concentration for various removal coefficients.* Solid curve refers to Fig. 5.31, broken to 5.32, dotted curve to 5.33, broken/dotted curve to 5.34.

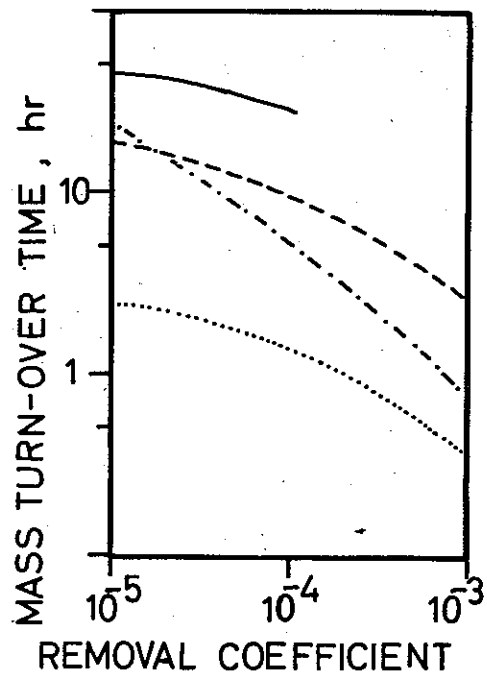

Fig. 5.37. *Mass turn-over time for various removal coefficients.* Solid curve refers to Fig. 5.31, broken to 5.32, dotted curve to 5.33, broken/dotted curve to 5.34.

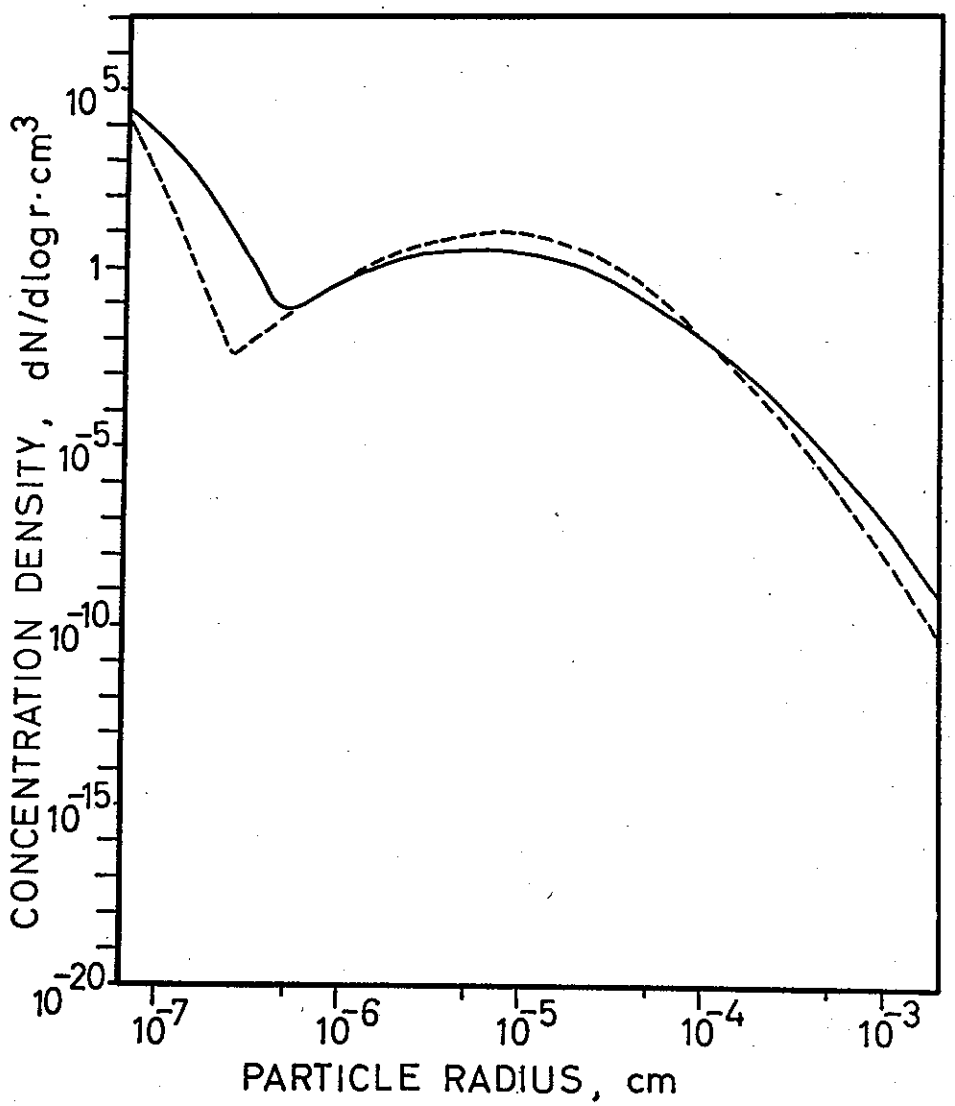

Fig. 5.38. *Aerosol size distribution for various removal exponents.* Parameters for solid curve: small-particle supply 0.1 $cm^{-3}s^{-1}$, other supply $10^{-17}gcm^{-3}s^{-1}$ with mode 10^{-5} cm and $c = 2.5$, removal coefficient 10^{-4} and exponent 1, air replacement time 96 hrs. Except for increase of the removal exponent to 2 for the broken curve, parameters remain unchanged.

5.7 Change in removal exponent. Figures 5.38 and 5.39 illustrate the change in aerosol size distribution when the removal exponent is varied, and Figures 5.40—5.42 show the associated changes in aerosol mass density, particle concentration and mass turn-over time.

According to formula (2.3) the primary effect of an increase in the removal exponent is stronger removal in the size range above 1μ radius and less beneath. For the distributions shown an increase in mass and mass turn-over time results, while particle concentration decreases or increases depending on the build-up of small particles.

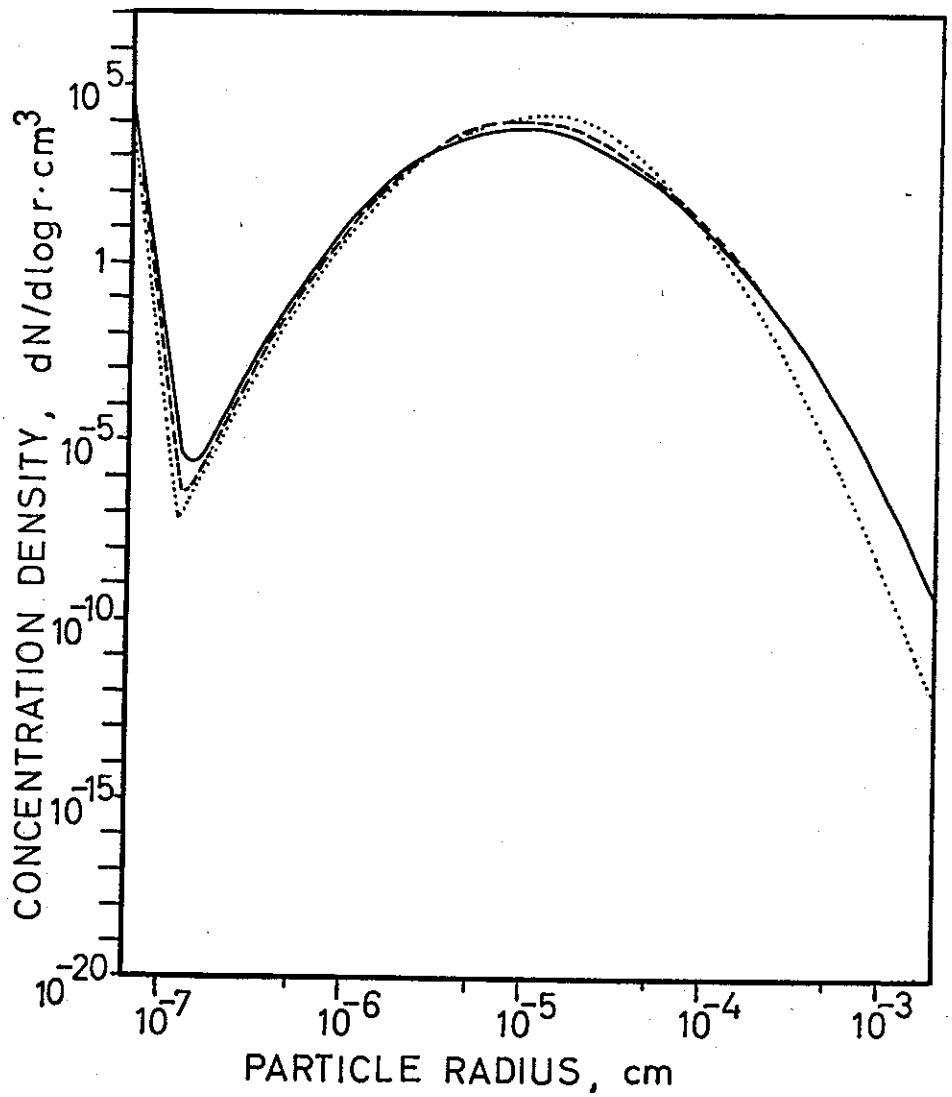

Fig. 5.39. *Aerosol size distribution for various removal exponents.* Parameters for solid curve: small-particle supply 100 $cm^{-3}s^{-1}$, other supply $10^{-14}gcm^{-3}s^{-1}$ with mode 10^{-5} cm and $\sigma = 2$, removal coefficient 10^{-4} and exponent 0.5, air replacement time 24 hrs. Except for increase of the removal exponent to 1 for the broken curve and to 2 for the dotted curve, parameters remain unchanged.

Since even the qualitative effect depends on which particle size is left unaffected (here 1μ radius), quantitative effects of change in removal exponent cannot be discussed without paying regard to this size.

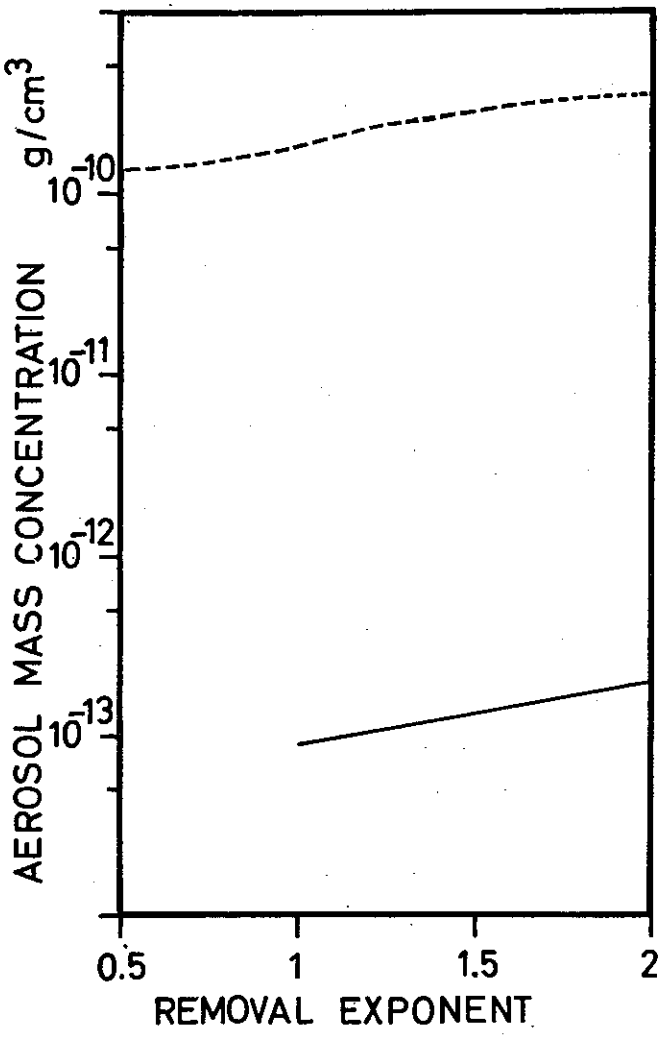

Fig. 5.40. *Aerosol mass for various removal exponents.* The solid curve refers to figure 5.38, and the broken curve to 5.39.

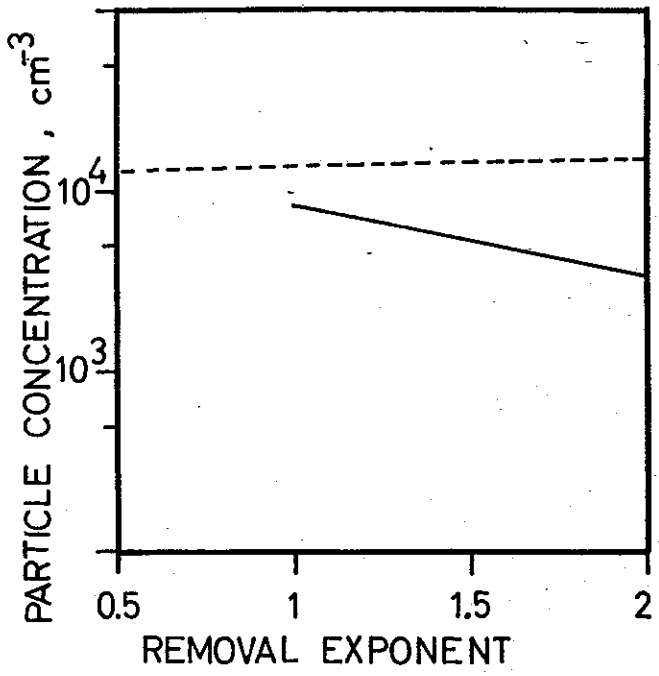

Fig. 5.41. *Aerosol particle concentration for various removal exponents.* The solid curve refers to Fig. 5.38 and the broken curve to 5.39.

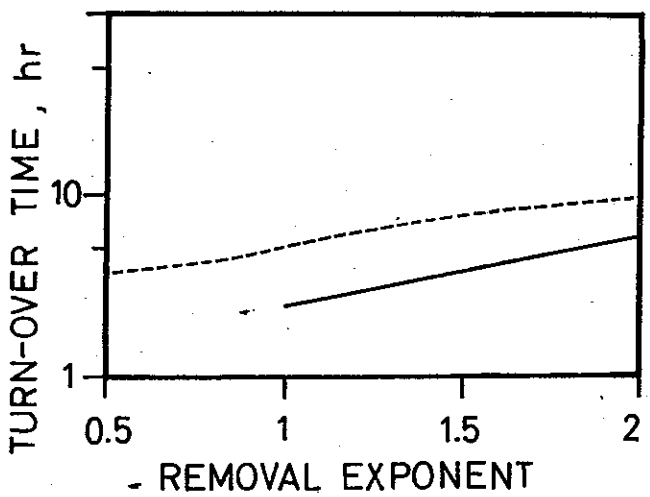

Fig. 5.42. *Mass turn-over time for various removal exponents.* The solid curve refers to Fig. 5.38 and the broken curve to 5.39.

5.8 Change in temperature and pressure. Temperature and pressure change the coagulation coefficient slightly, as indicated in Figures 2.4 and 2.5. The corresponding change in the steady-state aerosol distribution is very small.

When the temperature is decreased from 293 to 233 K, a slight decrease is caused in the coagulation. The result is more small particles and less medium/large ones, but the change is so small that it is hardly noticeable in the type of diagram used in this paper.

When the pressure is decreased from 1013 to 800 mb, a slight increase of coagulation takes place. The result is less small particles and more medium/large ones. The change is not large enough to be worth considering in this case either.

6. Natural radioactivity within the aerosol. Natural radioactivity caused by radon and thoron descendants is always present in the air, and its distribution on the particles may be an indication on the state of the aerosol.

Radon and thoron are radioactive gases formed by nuclear disintegration of solid elements in the soil. Part of the gases produced seeps out and mixes into the air layers close to the ground. Within an aerosol some supply of the radioactive gases is always present, but concentration varies widely depending on geology, state of the ground (wet, dry, snow-covered) and weather.

The descendants of radon and thoron are solid products. When the gases decay, the descendants are produced in atomic form, and they tend to deposit on solid substances quite rapidly. In an aerosol this means deposition on the particles, and the initial cumulative distribution should be expressed by

$$D_j = \frac{\int_{r_{min}}^{r_j} K_{1,i} \cdot n_i \cdot d\log r_i}{\int_{r_{min}}^{\infty} K_{1,i} \cdot n_i \cdot d\log r_i} \qquad (6.1)$$

where it is assumed that the size of the primary radioactive product is the lowest possible in the matrix in use, and that the mass added is insignificant.

The coagulation coefficient $K_{1,i}$ may be somewhat different for radioactive and non-radioactive elements, because a radioactive atom is an ion at the moment of birth, and electrical effects are not taken into account for coagulation. This is most serious for a dense aerosol, where the ions are not necessarily neutralized before the bulk of them are caught by particles. It is not taken into consideration during computation.

Equation (6.1) is often understood to represent the distribution of radioactivity within an aerosol, but objections should be raised to this: The equation has no margin for radioactive products not attached to particles, which may be important in less dense aerosols, and no attention has been paid to the internal flow of matter in the aerosol.

For steady state conditions the distribution of radioactivity may be computed more accurately, when the coagulation constant is known over the whole distribution.

Steady state implies that no change occurs in the rate of radon and thoron decay and that a steady-state aerosol is present. The absolute magnitude of the rate of supply is so variable in nature that only relative quantities are of interest. It will, however, be assumed that the concentration of radioactive particles is far less than the concentration of normal ones for any size present. This is normally the case in nature.

Since air from the outside is mixed into the aerosol in the model discussed, the radioactive conditions of the outside air must be taken into account. In the model it is assumed that the outside air does not contain any aerosol mass. This does not imply that no radioactivity is present. With radon or thoron gas present, but without aerosol particles, very small radioactive nuclei should build up towards a concentration in equilibrium with the gaseous precursors. The concentration would be too small for significant coagulation to take place, and no growth in particle size should occur.

With this picture in mind, two different radioactivity models have been developed. For the non-radioactive environment model it is assumed that the air mixed into the aerosol does not contain any radioactivity whatsoever. For the radioactive environment model it is assumed that the outside air has the same concentration of radioactive gases as the aerosol in equilibrium with decay products. These elements are associated with particles of the lowest size existing in the aerosol.

It is the shortlived descendants *RaA*, *RaB* and *RaC* with radioactive halflives of 3.05, 26.8 and 19.7 minutes which are of interest in the radium decay chain, and *ThA* with 0.158 seconds and *ThB* and *ThC* with 10.6 and 1.1 hours in the thorium decay chain. For convenience it will be assumed that R atoms of *RaA* or *ThA* are produced per second per cm^3 within the aerosol.

Let A, B and C be the concentration of radioactive descendants in the aerosol, and λ_A, λ_B and λ_C the corresponding decay constants. In analogy to particles

$$a_j = \left(\frac{dA}{d\log r}\right)_j \qquad b_j = \left(\frac{dB}{d\log r}\right)_j \qquad c_j = \left(\frac{dC}{d\log r}\right)_j$$

indicate the concentration attached to particles per logarithmic size unit. For conversion of supply concentration rate to concentration density rate the considerations in connection with equation (2.1) are valid.

The change in the concentration of a certain radioactive element is now determined by supply and removal of that particular element. For the non-radioactive environment model the changes at the very lowest end of the distribution are

$$\frac{da_1}{dt} = \frac{R}{\log r_1/r_2} - a_1 \cdot \left\{ \int_{r_{\min}}^{\infty} K_{1,i} \cdot n_i \cdot d\log r_i + \alpha \left(\frac{r_1}{r_p}\right)^2 + \gamma + \lambda_A \right\} \tag{6.2}$$

$$\frac{db_1}{dt} = \lambda_A \cdot a_1 - b_1 \cdot \left\{ \int_{r_{\min}}^{\infty} K_{1,i} \cdot n_i \cdot d\log r_i + \alpha \cdot \left(\frac{r_1}{r_p}\right)^2 + \gamma + \lambda_B \right\} \tag{6.3}$$

The expression for C is analogous to that for B.

$\log r_1/r_2$ is the logarithmic interval between radii for which accounts are kept. α and γ are the parameters defined for the aerosol calculation.

Steady state requirement leads to

$$a_1 = \frac{\frac{R}{\log r_1/r_2}}{\int_{r_{\min}}^{\infty} K_{1,i} \cdot n_i \cdot d\log r_i + \alpha \left(\frac{r_1}{r_p}\right)^g + \gamma + \lambda_A} \tag{6.4}$$

$$b_1 = \frac{\lambda_A \cdot a_1}{\int_{r_{\min}}^{\infty} K_{1,i} \cdot n_i \cdot d\log r_i + \alpha \left(\frac{r_1}{r_p}\right)^g + \gamma + \lambda_B} \tag{6.5}$$

$$c_1 = \frac{\lambda_B \cdot b_1}{\int_{r_{\min}}^{\infty} K_{1,i} \cdot n_i \cdot d\log r_i + \alpha \left(\frac{r_1}{r_p}\right)^g + \gamma + \lambda_C} \tag{6.6}$$

When radioactive environment is studied, the supply of radioactive nuclei in the equilibrium distribution from the environment must be taken into account. Let A, B and C be the concentration of the different nuclei in the environment. Under equilibrium conditions

$$R = \lambda_A \cdot A = \lambda_B \cdot B = \lambda_C \cdot C$$

giving $A = \frac{R}{\lambda_A}$, $B = \frac{R}{\lambda_B}$ and $C = \frac{R}{\lambda_C}$

A fraction γ of this mixture is added to the aerosol per second, therefore

$$\frac{da_1}{dt} = \frac{R}{\log r_1/r_2} + \frac{\gamma \cdot R}{\lambda_A \cdot \log r_1/r_2} - a_i \left\{ \int_{r_{\min}}^{\infty} K_{1,i} \cdot n_i \cdot d\log r_i + \alpha \left(\frac{r_1}{r_p}\right)^g + \gamma + \lambda_A \right\} \tag{6.7}$$

$$\frac{db_1}{dt} = \lambda_A \cdot a_1 + \frac{\gamma \cdot R}{\lambda_B \cdot \log r_1/r_2} - b_1 \cdot \left\{ \int_{r_{\min}}^{\infty} K_{1,i} \cdot n_i \cdot d\log r_i + \alpha \left(\frac{r_1}{r_p}\right)^g + \gamma + \lambda_B \right\} \tag{6.8}$$

where again the expression for C is analogous to that for B.

Steady state gives

$$a_1 = \frac{\frac{R}{\log r_1/r_2} + \frac{\gamma \cdot R}{\lambda_A \cdot \log r_1/r_2}}{\int_{r_{\min}}^{\infty} K_{1,i} \cdot n_i \cdot d\log r_i + \alpha \left(\frac{r_1}{r_p}\right)^g + \gamma + \lambda_A} \tag{6.9}$$

$$b_1 = \frac{\lambda_A \cdot a_1 + \dfrac{\gamma \cdot R}{\lambda_B \cdot \log r_1/r_2}}{\int_{r_{min}}^{\infty} K_{1,i} \cdot n_i \cdot d\log r_i + \alpha \left(\frac{r_1}{r_p}\right)^g + \gamma + \lambda_B} \tag{6.10}$$

$$c_1 = \frac{\lambda_B \cdot b_1 + \dfrac{\gamma \cdot R}{\lambda_C \cdot \log r_1/r_2}}{\int_{r_{min}}^{\infty} K_{1,i} \cdot n_i \cdot d\log r_i + \alpha \left(\frac{r_1}{r_p}\right)^g + \gamma + \lambda_C} \tag{6.11}$$

For any other size than the lowest one, the expressions for the two models are identical, since no radioactivity enters directly from the environment.

$$\frac{da_j}{dt} = \int_{r_{min}}^{r_j \cdot 2^{-1/3}} K_{i,k} \cdot (a_i \cdot n_k + a_k \cdot n_i) \cdot \left(\frac{r_j}{r_k}\right)^3 \cdot d\log r_i$$

$$- a_j \cdot \left\{ \int_{r_{min}}^{\infty} K_{j,i} \cdot n_i \cdot d\log r_i + \alpha \left(\frac{r_j}{r_p}\right)^g + \gamma + \lambda_A \right\} \tag{6.12}$$

$$\frac{db_j}{dt} = \lambda_A \cdot a_j + \int_{r_{min}}^{r_j \cdot 2^{-1/3}} K_{i,k} \cdot (b_i \cdot n_k + b_k \cdot n_i) \cdot \left(\frac{r_j}{r_k}\right)^3 \cdot d\log r_i$$

$$- b_j \cdot \left\{ \int_{r_{min}}^{\infty} K_{j,i} \cdot n_i \cdot d\log r_i + \alpha \left(\frac{r_j}{r_p}\right)^g + \gamma + \lambda_B \right. \tag{6.13}$$

where size k is defined by $v_i + v_k = v_j$.

The expression for c_j is analogous to that for b_j.

For the purpose of computation the terms containing a, b and c for the intermediate size k may be split through linear interpolation on the $\log r$-scale, giving terms referring to the sizes for which accounts are kept:

$$K_{i,k} \cdot a_k = K_{i,j-1} \cdot a_{j-1} + \frac{\log \dfrac{r_k}{r_j - 1}}{\log \dfrac{r_j}{r_{j-1}}} \cdot (K_{i,j} \cdot a_j - K_{i,j-1} \cdot a_{j-1})$$

$$= K_{i,j-1} \cdot a_{j-1} \cdot \frac{\log \dfrac{r_k}{r_{j-1}}}{\log \dfrac{r_j}{r_{j-1}}} + K_{i,j} \cdot a_j \cdot \frac{\log \dfrac{r_k}{r_{j-1}}}{\log \dfrac{r_j}{r_{j-1}}}$$

Applying this procedure, explicit expressions for the steady states are found

$$a_j = \frac{\int_{r_{min}}^{r_j \cdot 2^{-1/3}} \left[K_{i,k} \cdot a_i \cdot n_k + K_{i,j-1} \cdot a_{j-1} \cdot n_i \cdot \frac{\log \frac{r_j}{r_k}}{\log \frac{r_j}{r_{j-1}}} \right] \cdot \left(\frac{r_j}{r_k} \right)^3 \cdot d\log r_i}{\int_{r_{min}}^{\infty} K_{i,j} \cdot n_i \cdot d\log r_i - \int_{r_{min}}^{r_j \cdot 2^{-1/3}} K_{i,j} \cdot n_i \cdot \frac{\log \frac{r_k}{r_{j-1}}}{\log \frac{r_j}{r_{j-1}}} \cdot \left(\frac{r_j}{r_k} \right)^3 \cdot d\log r_i + \alpha \left(\frac{r_j}{r_p} \right)^g + \gamma + \lambda_A} \tag{6.14}$$

$$b_j = \frac{\int_{r_{min}}^{r_j \cdot 2^{-1/3}} \left[K_{i,k} \cdot b_i \cdot n_k + K_{i,j-1} \cdot b_{j-1} \cdot n_i \cdot \frac{\log \frac{r_j}{r_k}}{\log \frac{r_j}{r_{j-1}}} \right] \cdot \left(\frac{r_j}{r_k} \right)^3 \cdot d\log r_i + \lambda_A \cdot a_j}{\int_{r_{min}}^{\infty} K_{i,j} \cdot n_i \cdot d\log r_i - \int_{r_{min}}^{r_j \cdot 2^{-1/3}} K_{i,j} \cdot n_i \cdot \frac{\log \frac{r_k}{r_{j-1}}}{\log \frac{r_j}{r_{j-1}}} \cdot \left(\frac{r_j}{r_k} \right)^3 \cdot d\log r_i + \alpha \left(\frac{r_j}{r_p} \right)^g + \gamma + \lambda_B} \tag{6.15}$$

$$c_j = \frac{\int_{r_{min}}^{r_j \cdot 2^{-1/3}} \left[K_{i,k} \cdot c_i \cdot n_k + K_{i,j-1} \cdot c_{j-1} \cdot n_i \cdot \frac{\log \frac{r_j}{r_k}}{\log \frac{r_j}{r_{j-1}}} \right] \cdot \left(\frac{r_j}{r_k} \right)^3 \cdot d\log r_i + \lambda_B \cdot b_j}{\int_{r_{min}}^{\infty} K_{i,j} \cdot n_i \cdot d\log r_i - \int_{r_{min}}^{r_j \cdot 2^{-1/3}} K_{i,j} \cdot n_j \cdot \frac{\log \frac{r_k}{r_{j-1}}}{\log \frac{r_j}{r_{j-1}}} \cdot \left(\frac{r_j}{r_k} \right)^3 d\log r_i + \alpha \left(\frac{r_j}{r_p} \right)^g + \gamma + \lambda_C} \tag{6.16}$$

These formulas only require

a) the numbers for the radioactivity earlier in the decay chain
b) the numbers for lower sizes than the one under consideration.

Starting with element a and the smallest particle size, accounts for the whole radioactivity distribution can be computed successively.

The cumulative distribution of radioactivity on the different particle sizes can now be expressed as

$$R_j = \frac{\int_{r_{min}}^{r_j} (\lambda_A \cdot a_i + \lambda_B \cdot b_i + \lambda_C \cdot c_i) \cdot d\log r}{\lambda_A \cdot A + \lambda_B \cdot B + \lambda_C \cdot C} \tag{6.17}$$

which may be compared with earlier estimates based on equation (6.1).

From an accuracy point of view an uncertain aspect in the procedure is the need for interpolation between the matrix numbers in order to bring out the numbers used. Similar doubts may be voiced for the computation of the aerosol particle distribution. For steady-state radioactivity the accuracy of the computation may be tested by examining the degree of radioactive equilibrium. In a steady state where no radioactivity is lost, the radioactivity of *RaA*, *RaB*, and *RaC* must each be equal to the rate R of *RaA* supply.

For type 2 aerosols with a mass turnover time long compared to the radioactivity half-lives, the requirement is fulfilled at least up to 3 digits.

The steady-state aerosol was more difficult to reach for type 1 distributions. Radioactivity distributions were thus often based on a cruder aerosol approximation, and it was not unusual that the computations resulted in slightly more radioactivity than equilibrium conditions would allow. For type 1 distributions equilibrium should be expected, and results are applied with caution.

Lack of radioactive equilibrium has earlier been used (2, 4) for estimating the age of the aerosol. Steady state conditions are then assumed, and with an aerosol turnover time T, a fraction $\lambda = 1/T$ disappears per time unit. When no radioactivity is introduced from the environment, the concentrations are then determined by

$$\frac{dB}{dt} = \lambda_A \cdot A - B \cdot (\lambda_B + \lambda)$$

$$\frac{dC}{dt} = \lambda_B \cdot B - C \cdot (\lambda_C + \lambda)$$

leading to the two expressions for T in steady state.

$$T_{B/A} = \frac{B}{\lambda_A \cdot A - \lambda_B \cdot B} \qquad (6.18)$$

$$T_{C/A} = \frac{C}{\lambda_B \cdot B - \lambda_C \cdot C}$$

If two ratios are considered simultaneously, the effect of dilution may be eliminated even for a radioactive environment

$$\frac{dB}{dt} = \lambda_A \cdot A + \gamma \cdot \frac{R}{\lambda_B} - (\lambda_B + \lambda) \cdot B \qquad (6.19)$$

$$\frac{dB}{dt} = \lambda_B \cdot B + \gamma \cdot \frac{R}{\lambda_C} - (\lambda_C - \lambda) \cdot C$$

For steady state conditions T is found

$$T = \frac{\lambda_B \cdot B - \lambda_C \cdot C}{\lambda_B(\lambda_A \cdot A - \lambda_B \cdot B) - \lambda_C(\lambda_B \cdot B - \lambda_C \cdot C)} \qquad (6.20)$$

It should be noticed that the equation is valid also for non-radioactive environment, since the earlier expressions are re-established by setting $\gamma = 0$. For measurement purposes equation (6.20) has the drawback of requiring high accuracy in determination of the radioactivity of the individual elements. It is therefore not readily applicable.

7. Distribution of aerosol radioactivity.

7.1 General features. If no radioactivity is present in the environment of the aerosol, long radioactivity turn-over times are necessary for radioactive equilibrium to exist in the aerosol. Turn-over time must, of course, in this connection be compared to radioactive lifetimes in the decay chain. When the turn-over time is short, radon descendants up to *RaC*, with a mean lifetime for the chain of some 70 minutes, should show a distribution closer to equilibrium than thoron descendants with 16.5 hours.

If dilution is small, aerosols with type 1 distribution in general have a very long radioactive turn-over time, regardless of their mass turn-over time. They will in general show radioactive equilibrium.

For aerosols of type 2 distribution the connection between mass turn-over times and radioactive equilibrium conditions, measured in terms of the fraction of equilibrium activity exhibited by *RaC* and *ThC*, is shown in Figure 7.1. The change in mass turn-

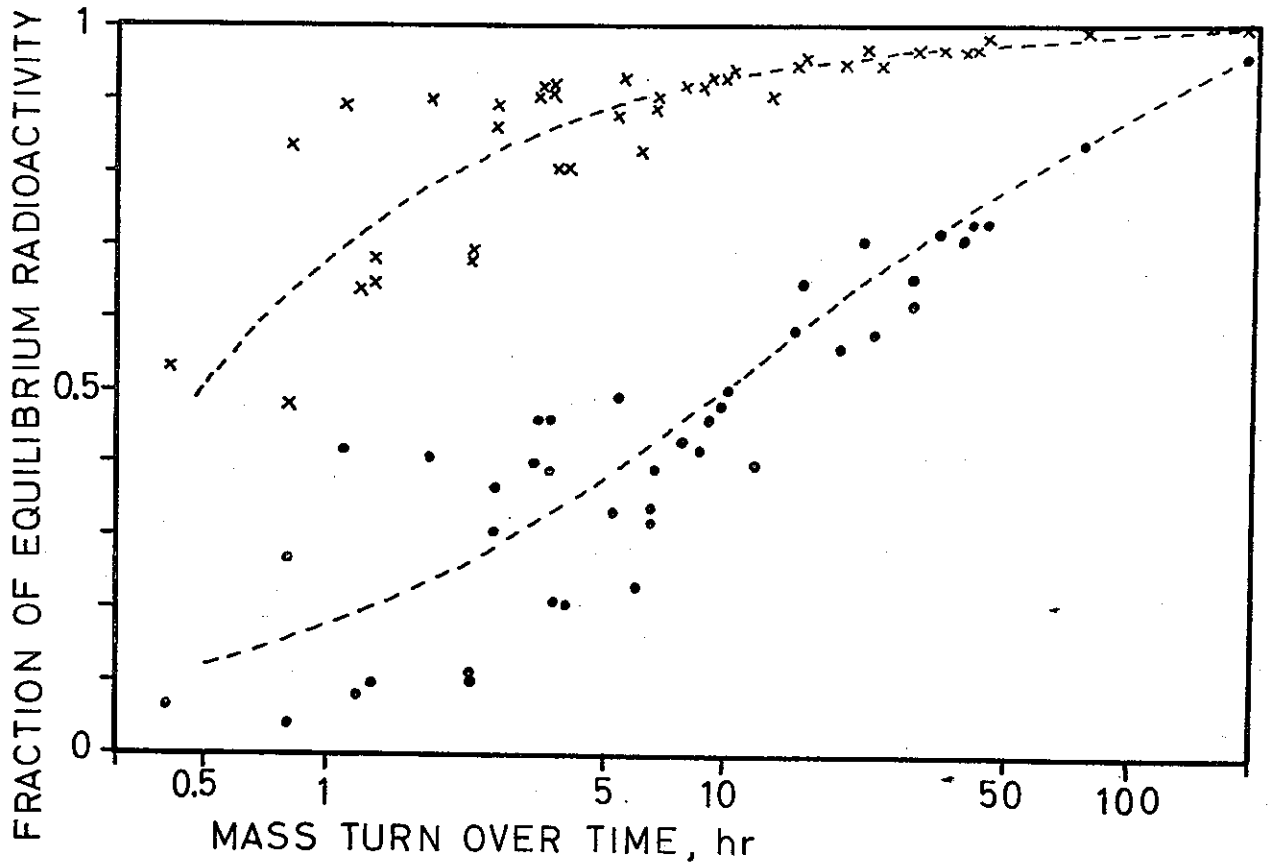

Fig. 7.1. *RaC and ThC radioactivity in relation to mass turn-over times.* Crosses refer to RaC and dots to ThC.

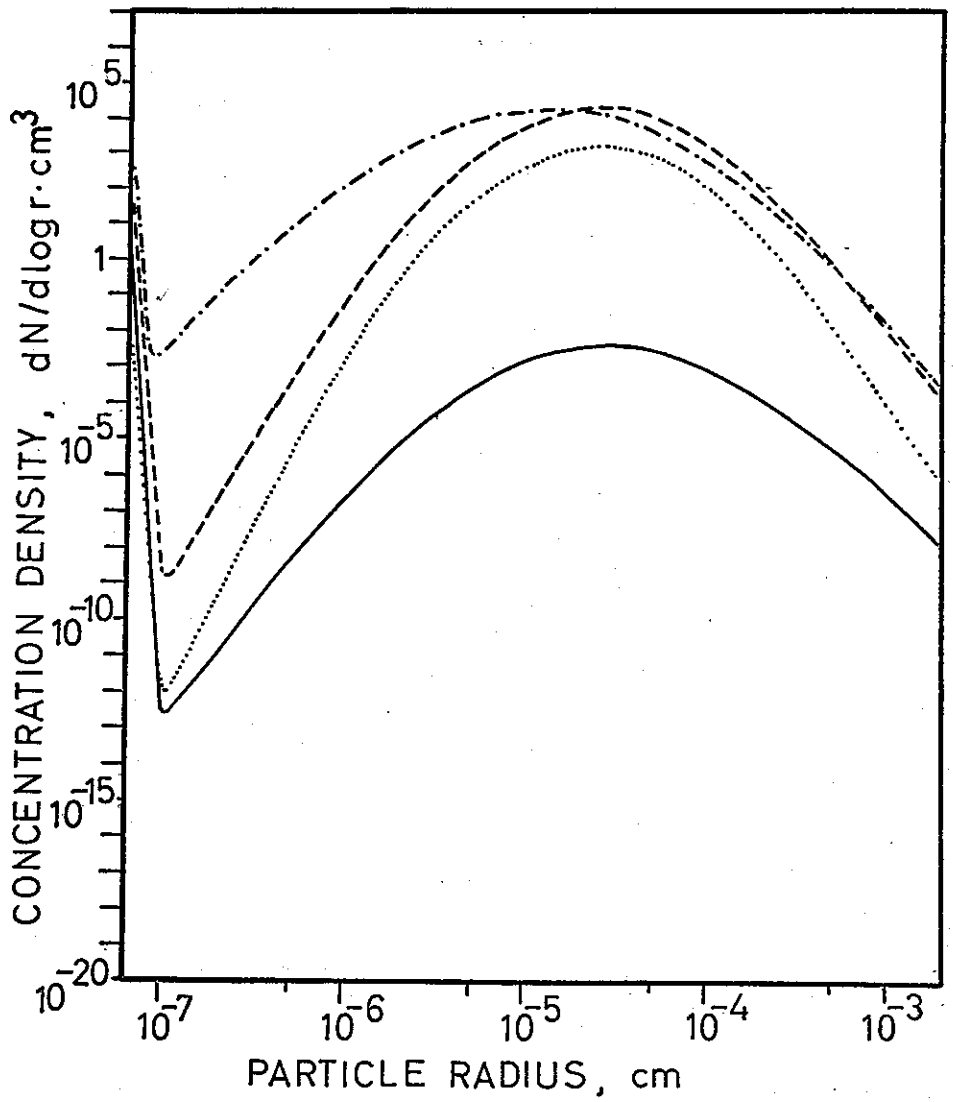

Fig. 7.2. *Size distribution for Tn descendants in an aerosol with non-radioactive environment.* Parameters for the aerosol: small-particle supply 10 $cm^{-3}s^{-1}$, other supply $10^{-12}gcm^{-3}s^{-1}$ with mode 10^{-5} cm and $\sigma = 3$, removal coefficient 10^{-4} and exponent 1.75, air replacement time 12 hrs. ThA distribution is shown by the solid curve, ThB by the broken and ThC by the dotted, mass by the broken and dotted. Distributions are normalized to disintegration of 1 Tn nucleus per cm^3 per second.

over time is brought about in various ways, and for this reason some spread is found within the diagram. Radioactivity turn-over times may be longer than mass turn-over times, but cannot possibly be shorter. The spread is therefore great for short mass turn-over times. For longer ones, the radioactivity is bound to be close to equilibrium, and the spread decreases.

The diagram clearly shows that *RaC* is closer to equilibrium than *ThC*. If the other isotopes are examined in the same way, the products early in the decay chain prove to be closer to equilibrium than those late in the chain. *ThA*, with less than a second lifetime, is hardly ever off equilibrium in an aerosol.

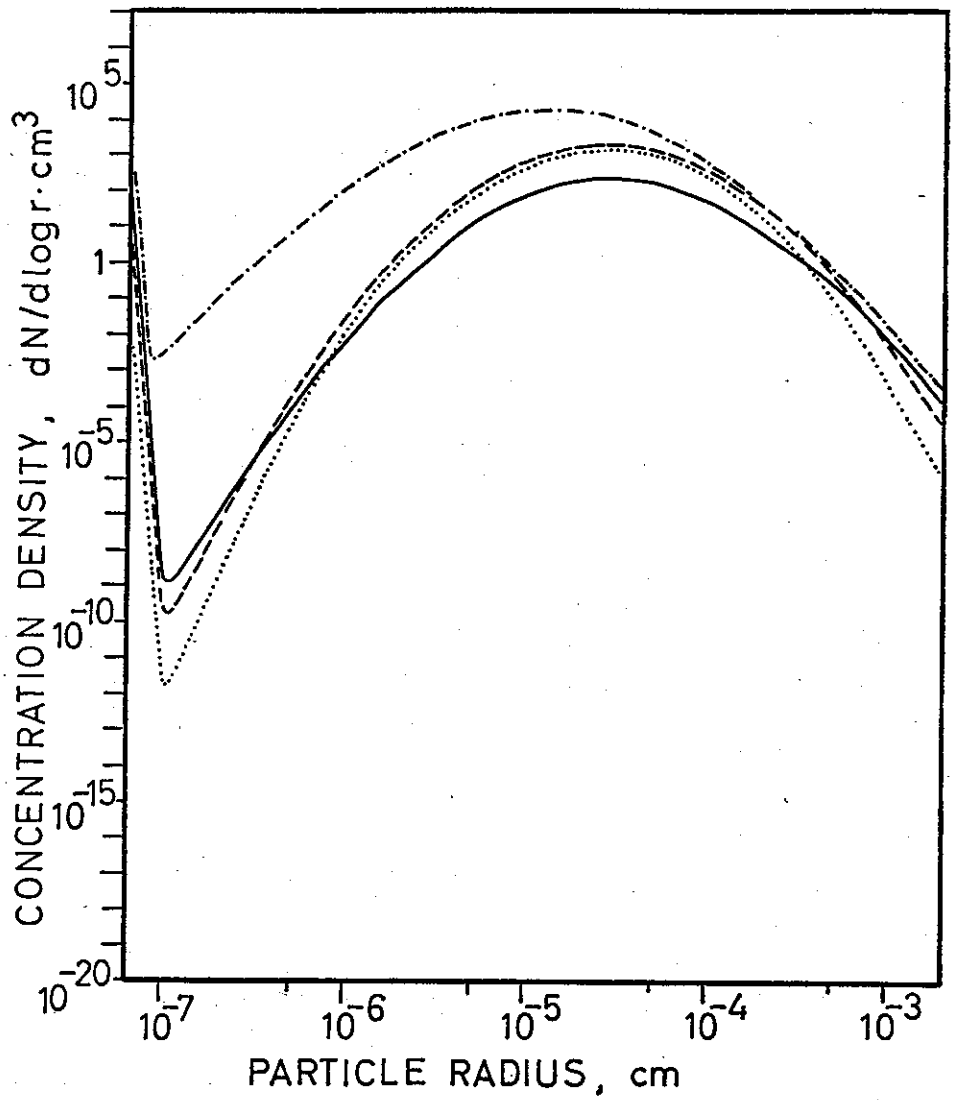

Fig. 7.3. *Size distribution for Rn descendants in an aerosol with non-radioactive environment.* The aerosol is the same as that in Fig. 7.2. The solid curve shows RaA, the broken RaB and the dotted RaC, mass by the broken and dotted. Normalized to disintegration of 1 Rn nucleus per cm^3 per second.

An example of the distribution of individual radioactive elements is shown in Figures 7.2 and 7.3. A few typical features of the distribution should be noticed.

a) The peaks at the lower end of the size range indicate that a certain fraction of every element is present as non-attached atoms. This fraction is highest for the elements first in the decay chain, and may for the short-lived *ThA* be quite dominant.
b) The modes in the distributions of radioactive elements are displaced towards larger aerosol size compared to the mode in the aerosol size distribution itself.
c) The positions of the individual modes are normally different. Long aerosol residence time as a particulate element will shift the distribution towards larger sizes because of the coagulation effect, but an opposite shift may occur because more removal takes place, particularly at the upper end.

The shifts between individual distributions have the consequence that ratios between radioactive elements change from one particle size region to another. When samples are taken of atmospheric radioactivity, sampling procedures are sometimes used, which enrich the sample in small particles (e.g. electrostatic or diffusion samples), large particles (e.g. impactors or centripeters) or particles from other size regions (e.g. some filters or rainwater). In such cases one should avoid drawing conclusions which tacitly imply that the sample taken is representative for the aerosol. A measured lack of radioactive equilibrium may just as well be caused by the sampling method as by the condition of the aerosol.

The type of model chosen for aerosol exchange with the pure environmental air is also important when actual measurements are to be interpreted.

Dense aerosol layers are usually found over cities. Since exchange of air with the environment takes place, the composition of the air within the aerosol must to some degree reflect the composition of the air in the environment. Normal meteorological conditions require production within the city to be very much higher than outside in order to establish a marked difference in the radon content of the air. Radon has after all a mean radioactive lifetime of 5.4 days, long compared to local exchange processes.

The non-radioactive environment model can therefore seldom be applied with a reasonable expectation of success. However, due to very low radon production over the sea, the right conditions may exist within coastal cities, when the wind is blowing from the sea.

For inland locations it is hardly possible to establish a situation with very much less radon in the environmental air than in the aerosol. It is true that in a city larger stone surfaces may be exposed than in the open country, with higher radon production as a result, but it is difficult to imagine a production which is higher by more than a small factor.

Thoron has a mean radioactive life-time of only 77 seconds and should for any reasonable meteorological conditions have an air concentration in agreement with local production. In the decay chain, however, the descendants have combined lifetimes of 16.5 hours. For *ThB* and *ThC* at inland locations, it is difficult to avoid the air concentration becoming more smoothed out geographically than the aerosol itself.

For inland locations, and for coastal locations, when the wind is blowing offshore, no particular reason exists for assuming radon or thoron concentrations within the aerosol to be higher or lower than those outside. A better model should thus be to assume that the radon and thoron content in the aerosol is equal to that in the pure air outside it.

Since removal should be slow when no particles are present, descendants in the pure air are assumed to be present with a concentration corresponding to radioactive equilibrium, and particle size as small as possible. This corresponds to the radioactive environment model described in chapter 6.

The type of radioactivity model is especially important when ratios between elements are determined and used as measures for aerosol age. Deductions based on a model different from that offered by nature may be preposterous.

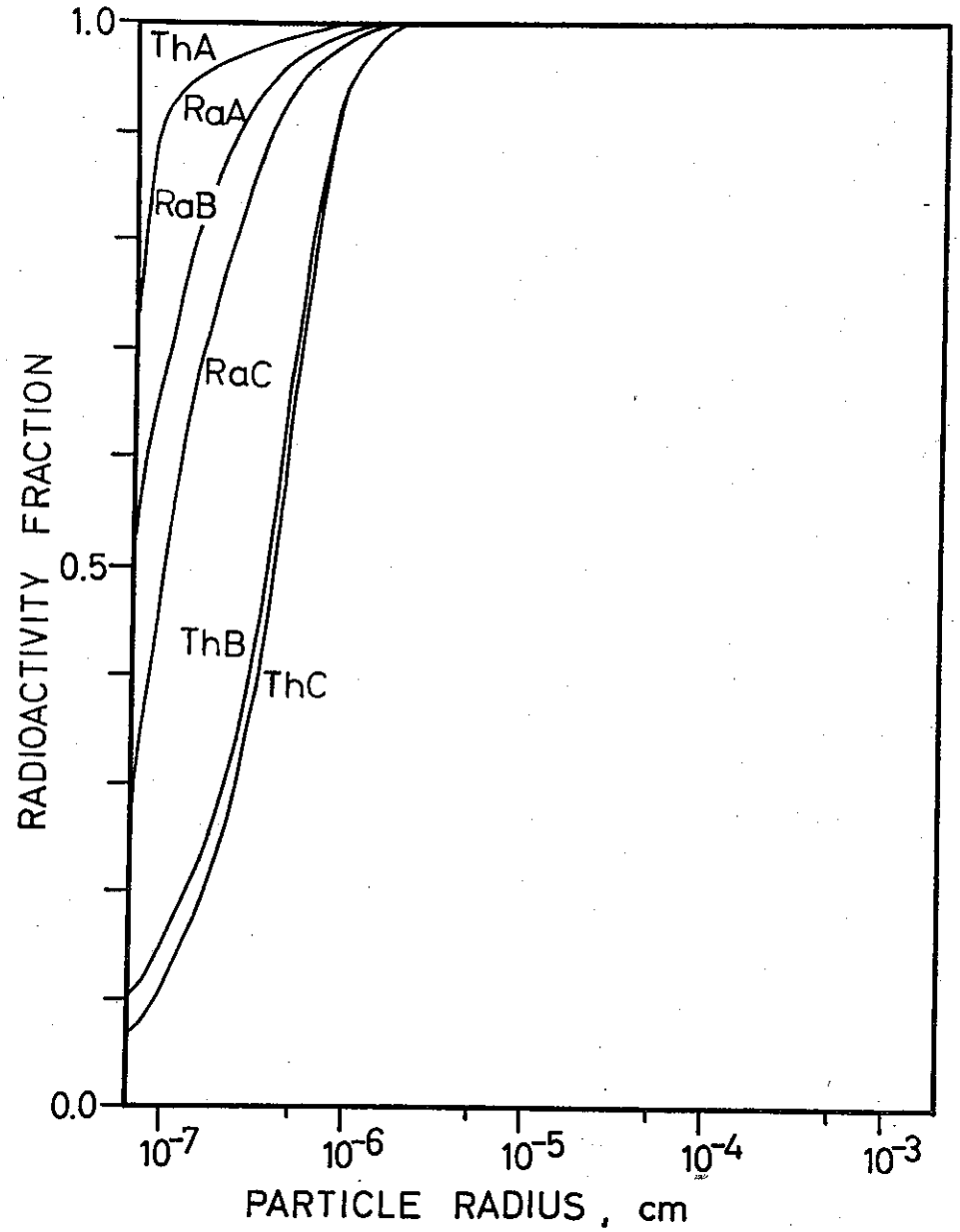

Fig. 7.4. *Normalized cumulative radioactivity distributions — Radiactive environment.* Parameters for the aerosol: small-particle supply 100 $cm^{-3}s^{-1}$, other supply $10^{-14}gcm^{-3}s^{-1}$ with mode 10^{-4} cm and $\sigma = 2$, removal coefficient 10^{-4} and exponent 1.8, air replacement time 24 hrs.

7.2 Radioactivity in a thin aerosol. When the aerosol mass concentration is very low, the deposition of primary radioactive elements on particles takes a long time. The steady-state radioactivity distribution is therefore one with an appreciable part of the radiactivity not attached to particles. Cumulative radiactivity distributions for three aerosols are presented in Figures 7.4—7.6.

The fraction of non-attached elements decreases from *ThA* through *RaA*, *RaB*, *RaC*, *ThB* to *ThC*, i.e. in the order of increasing life-time as particulate elements. *ThA* has only attached itself to other particles to an insignificant degree, having only a frac-

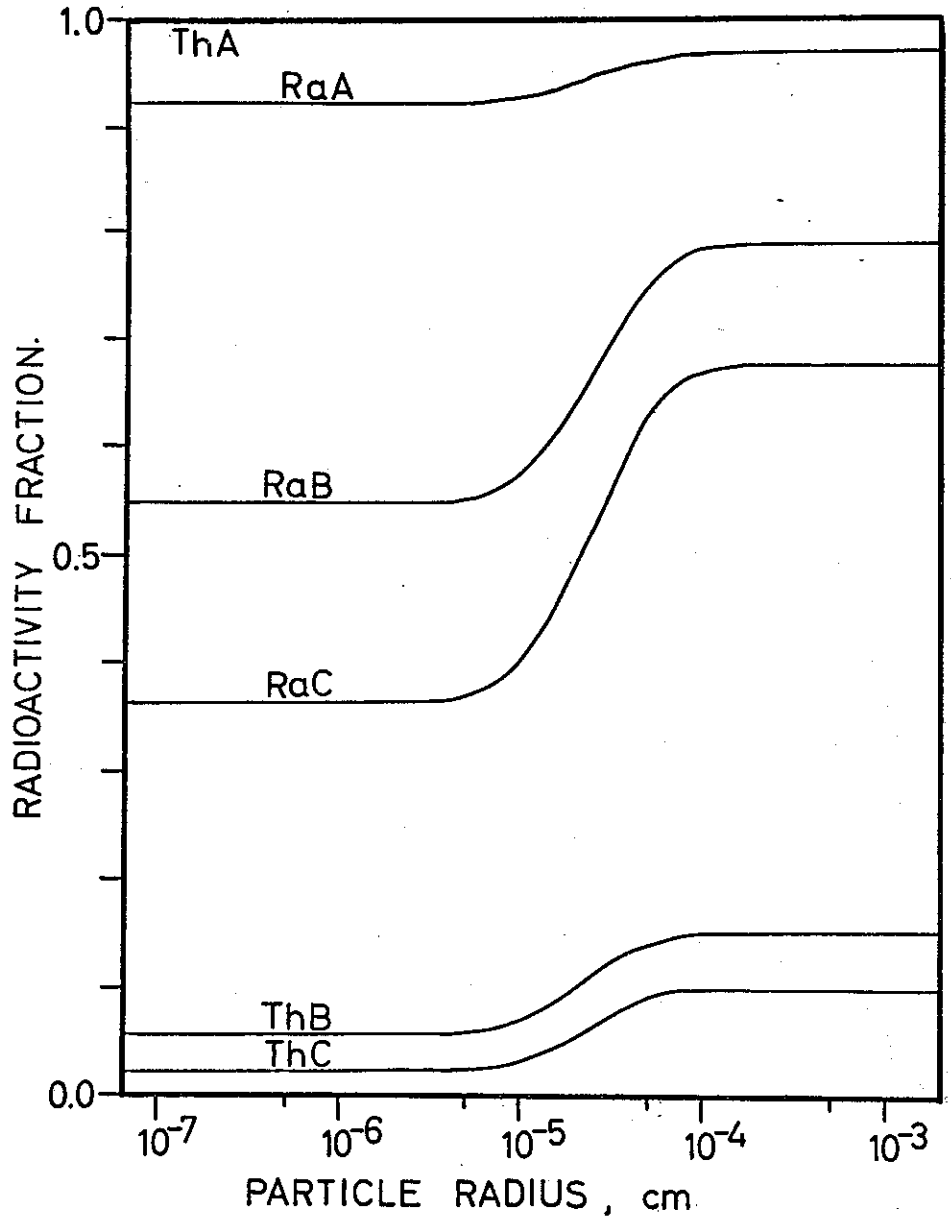

Fig. 7.5. *Normalized cumulative radiactivity distributions — Non-radioactive environment.* Parameters for the aerosol: small-particle supply 0 $cm^{-3}s^{-1}$, other supply $10^{-15}gcm^{-3}s^{-1}$ with mode 10^{-5} cm and $\sigma = 2.5$, removal coefficient 10^{-4} and exponent 1.75, air replacement time 3 hrs.

tion of a second to do so. *ThB* and *ThC* have ample time, but removal processes may reduce the amount of those elements below equilibrium. Since the bulk of the particles is very small, dilution is the only effective removal process. Lack of equilibrium will therefore only show up to a noticeable degree in an aerosol in exchange with non-radioactive air in the environment. This is the case in Figure 7.5.

The distribution of accumulated radioactivity of the first three elements of the decay chain is shown in Figures 7.7—7.9, together with cumulative mass distribution and deposition distribution of non-attached elements. The latter is often referred to as the

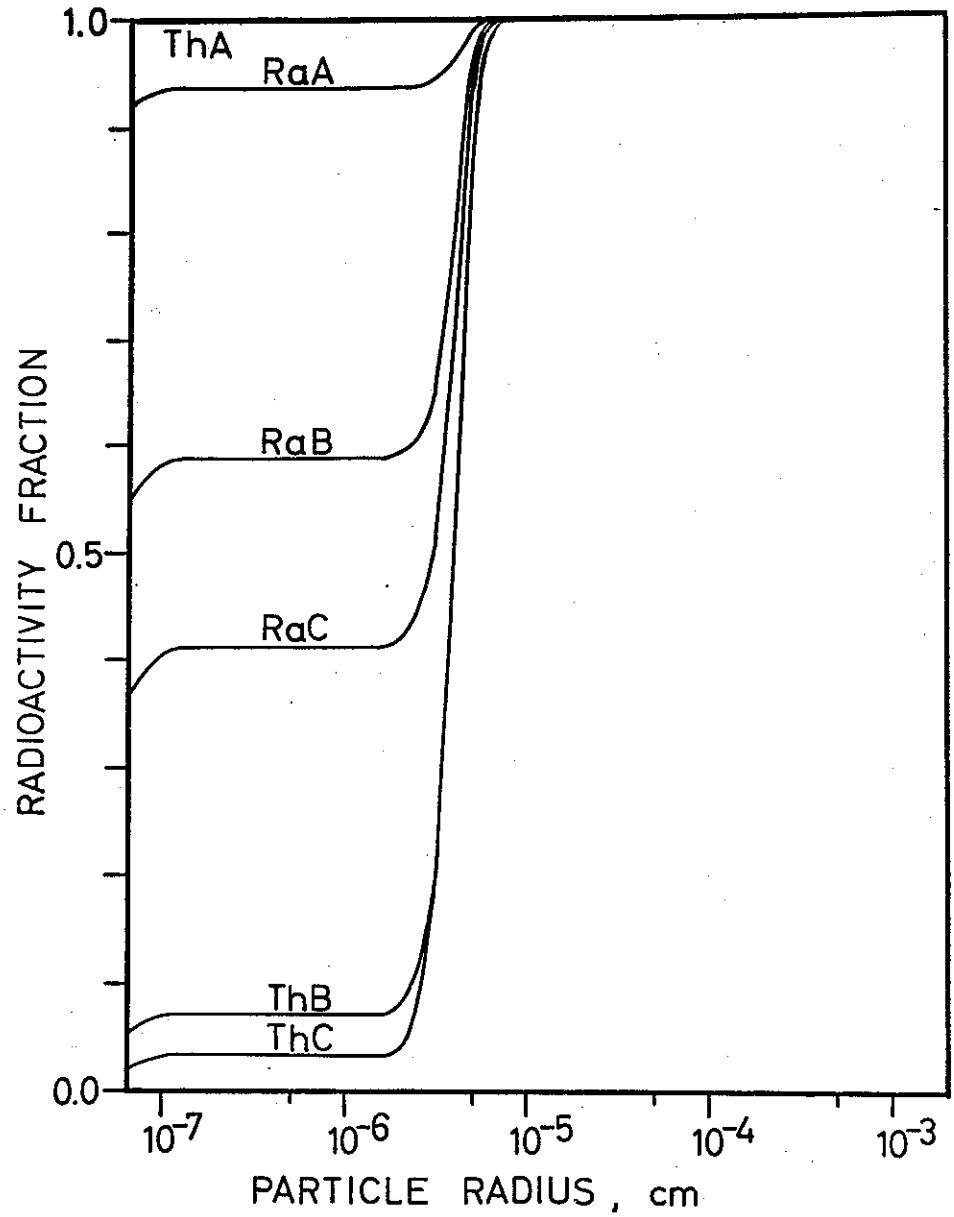

Fig. 7.6. *Normalized cumulative radioactivity distributions — Non-radioactive environment.* Parameters for the aerosol: small-particle supply 10 $cm^{-3}s^{-1}$, no other supply, removal coefficient 10^{-6} and exponent 1.75, air replacement time 5000 hrs.

theoretical radioactivity distribution. However, due to non-attached radioactive elements and coagulation, the deposition distribution seldom agrees with the radioactivity distribution.

Steady-state distributions reflect

a) time available for deposition, limited by removal or dilution,

b) radioactive life-times of the elements

c) radioactivity conditions in the environmental air.

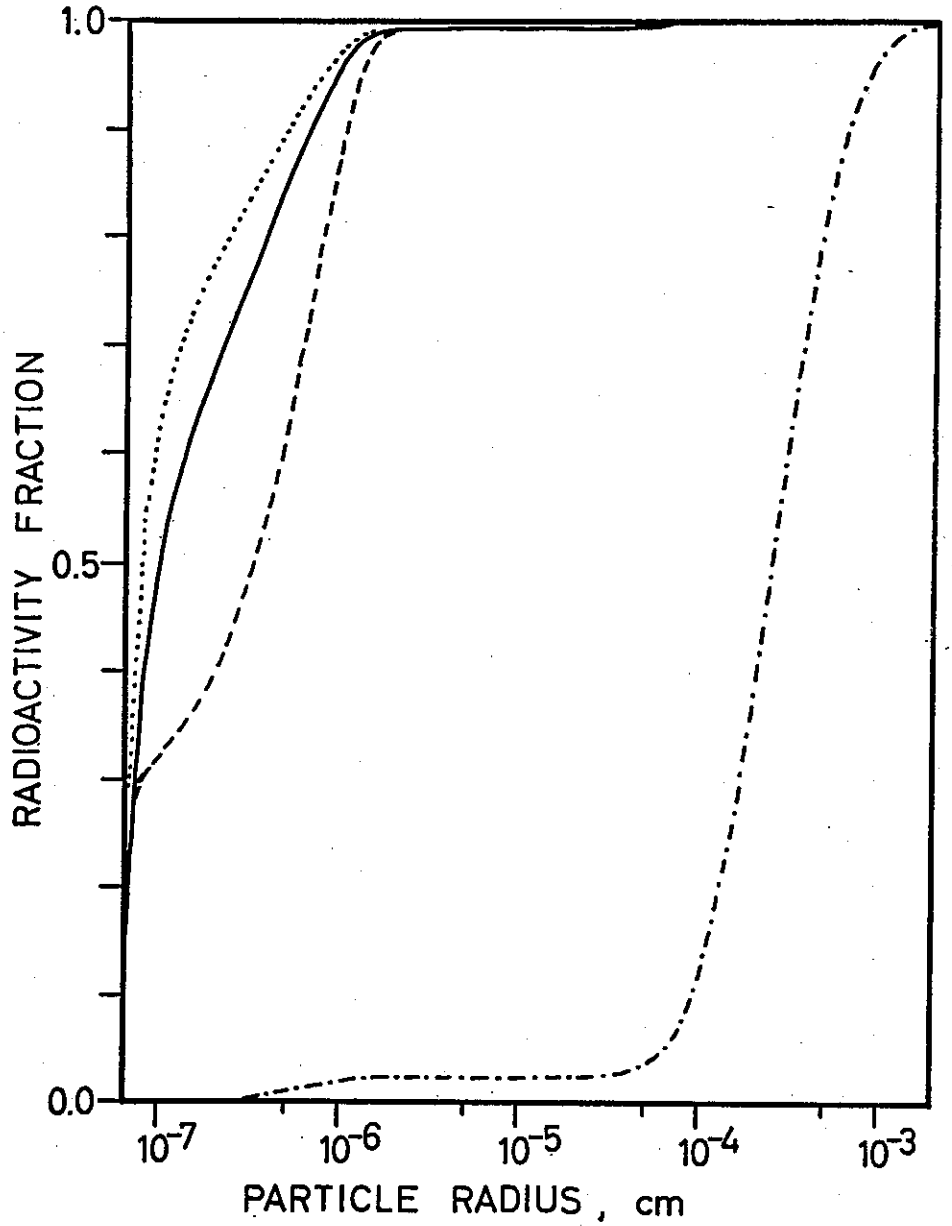

Fig. 7.7. *Cumulative distributions, fraction of individual total.* The aerosol and the environment are the same as in Fig. 7.4. Solid curve indicates deposition distribution for free nuclei, broken curve steady-state distribution for radioactivity from Tn descendants, dotted for Rn descendants. Broken/dotted curve shows aerosol mass distribution.

In a low-mass aerosol the bulk of the particles tends to have small sizes, and direct removal of mass tends to be slow. Time available for deposition is therefore in all essentials limited by the dilution only. If dilution is slow, radon descendants are normally associated with smaller particles than thoron descendants.

The reason is the lower total radioactive life in the former chain. If the typical time before deposition is between 70 minutes and 16.5 hours, and if this time really is available, most of the radon chain elements up to *RaC* disintegrate as non-attached

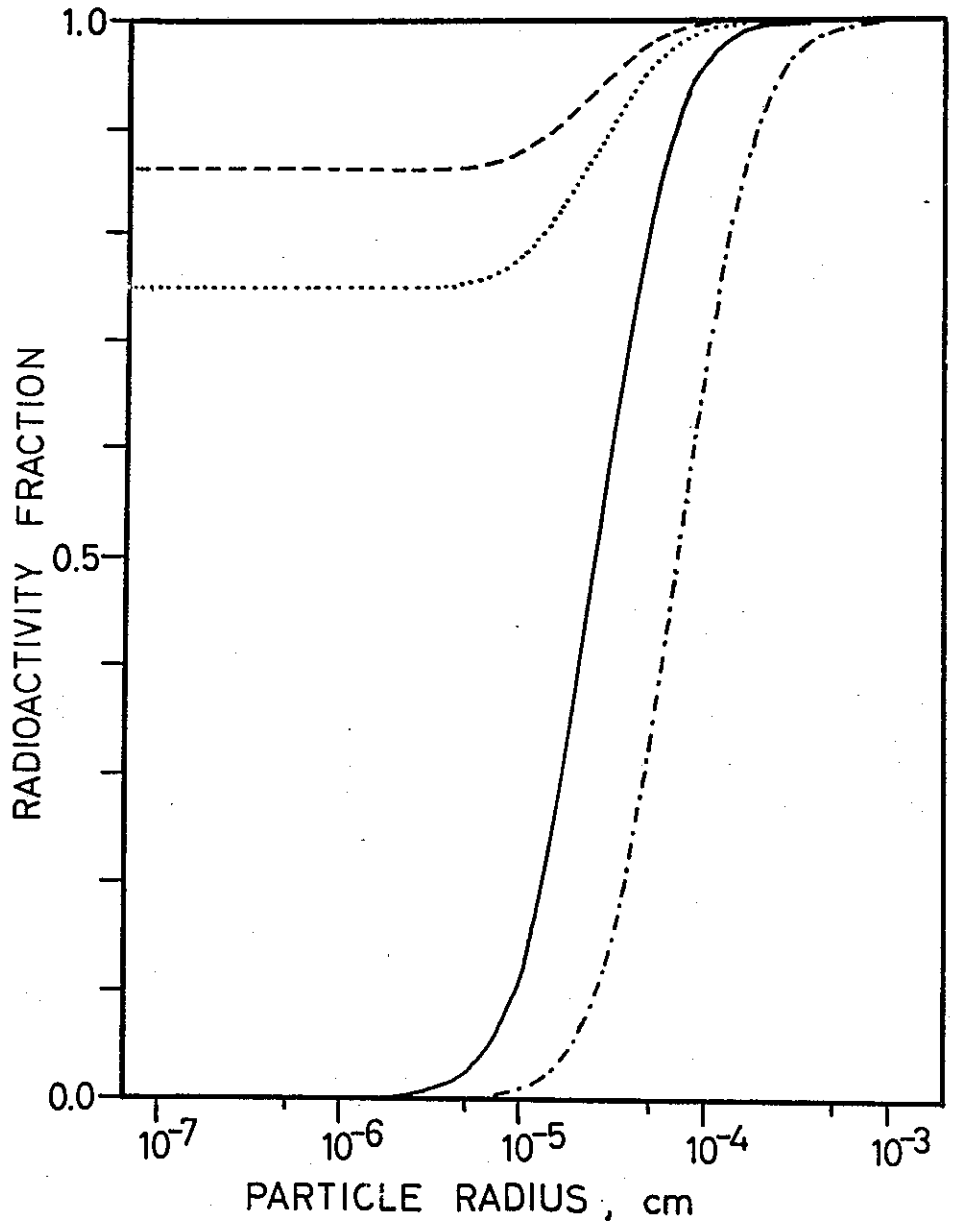

Fig. 7.8. *Cumulative distributions, fraction of individual total.* The aerosol and the environment are the same as in Fig. 7.5. Solid curve indicates deposition distribution for free nuclei, broken curve steady-state distribution for radioactivity from Tn descendants, dotted for Rn descendats. Broken/dotted curve shows aerosol mass distribution.

particles. In the thoron chain, however, this will only be true for *ThA*. Since 2/3 of the radioactivity may have ample time for deposition, the bulk of the radioactivity will be associated with larger particles than for the radon chain. Figure 7.7 is based on such conditions.

If dilution of the aerosol occurs rapidly, most *TbB* and *ThC* disappear before deposition. If now *Tn* descendants are weighted according to radioactivity, they essentially consist of *ThA*, which is not attached to particles. Figure 7.8 is based on such conditions.

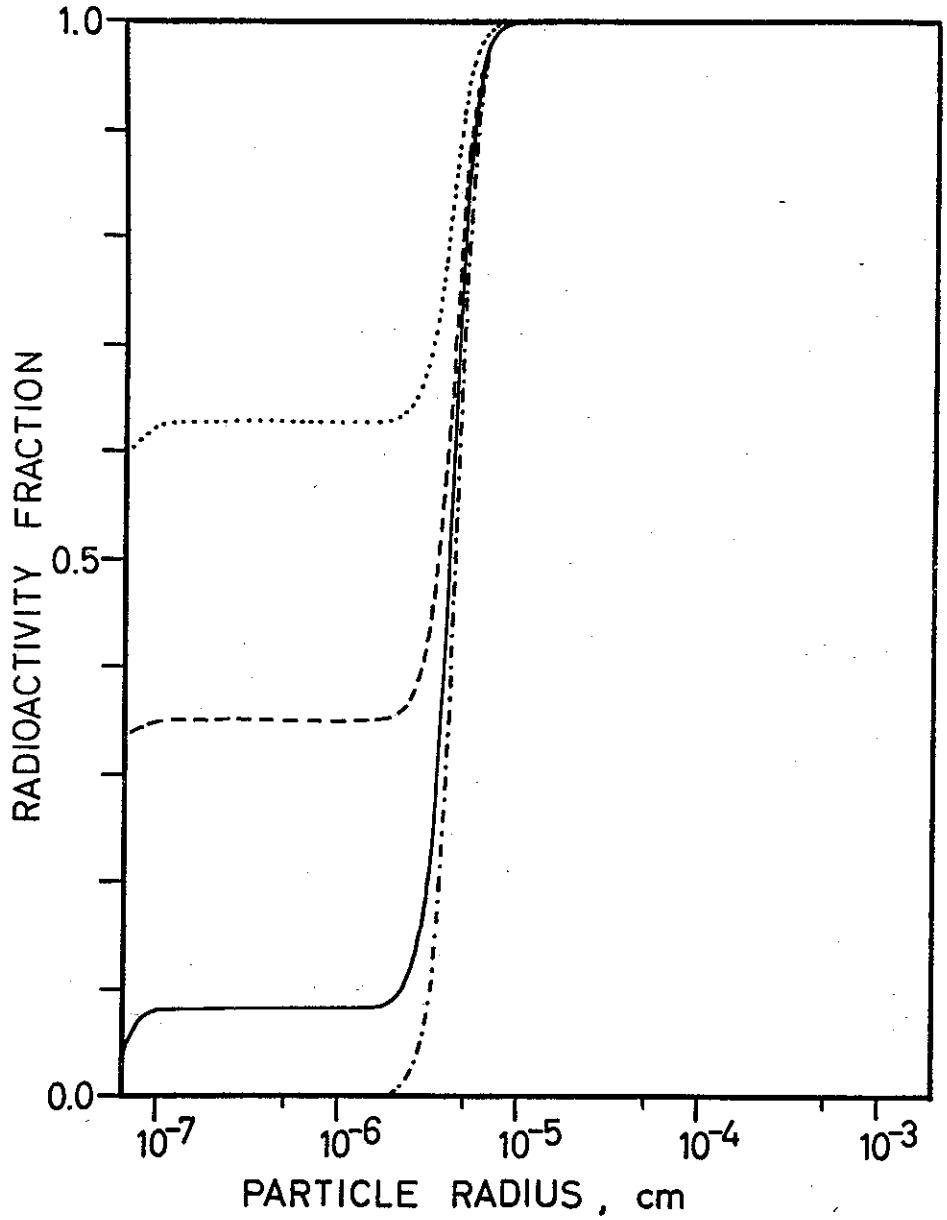

Fig. 7.9. *Cumulative distributions, fraction of individual total.* The aerosol and the environment are the same as in Fig. 7.6. Solid curve indicates deposition distribution for free nuclei, broken curve steady-state distribution for radioactivity from Tn descendants, dotted for Rn descendants. Broken/dotted curve shows aerosol mass distribution.

It is seen that the radioactivity for *Tn* descendants is associated with smaller particles than for *Rn* descendants. In an aerosol in radioactive environment, *ThB* and *ThC* would normally be close to equilibrium concentrations and the opposite order can easily be established. This is the case in Figure 7.7.

The effect of non-attached elements is to displace the radioactivity distribution curves towards small particles. Coagulation within the aerosol leads to a shift towards larger particles. When coagulation is slow, the effect is weak. When coagulation is

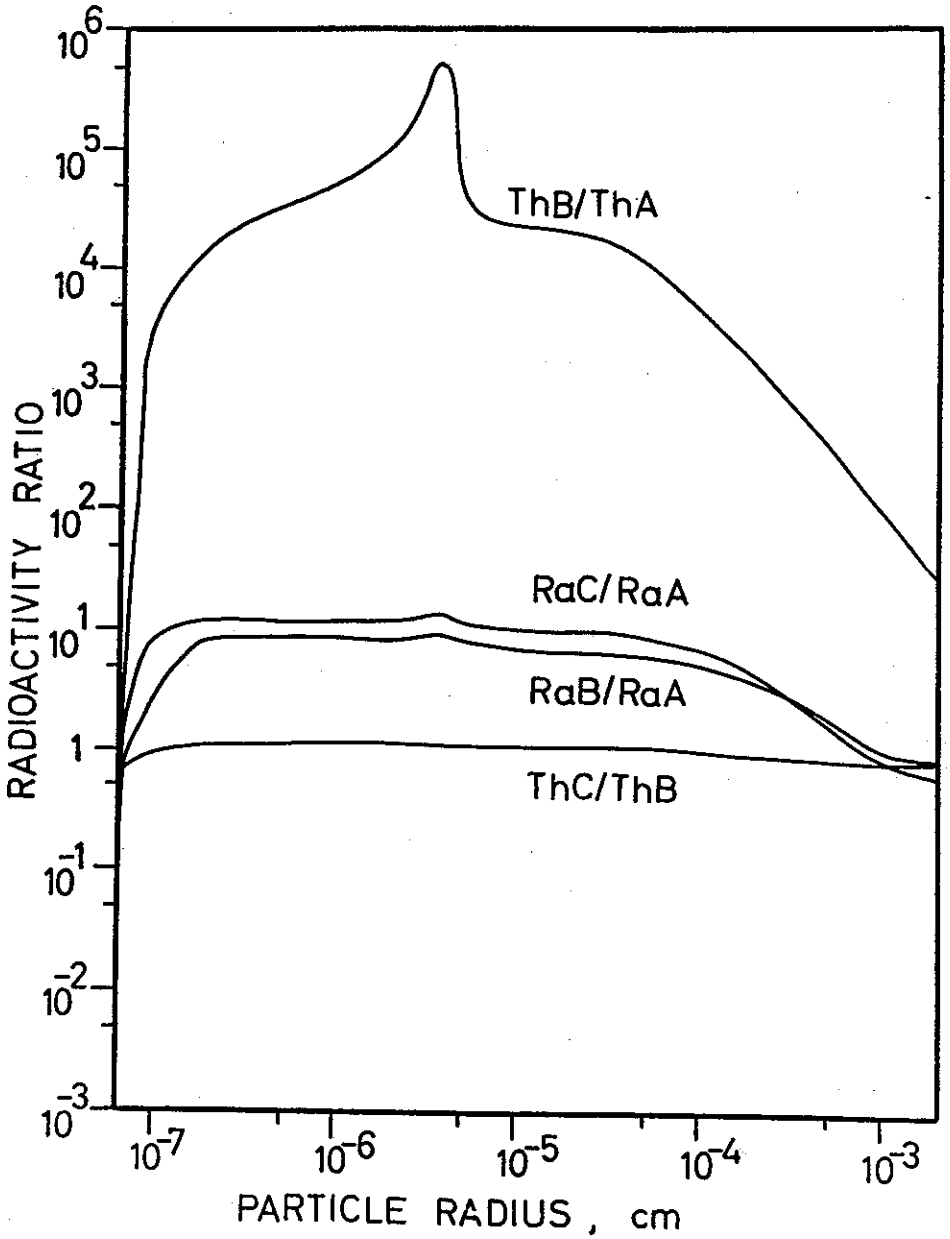

Fig. 7.10. *Radioactivity ratios for elements in the same chain of decay.* The aerosol and the environment are the same as in Fig. 7.4.

strong, the effect may outweigh the effect of non-attached elements, and radioactivity may in the steady state be associated with larger particles than indicated by the deposition distribution. Long mass turn-over time and slight dilution are favourable, since loss of particles will counteract the effect of the size shift. The phenomenon is present in Figure 7.7 for thoron. A similar effect for radon is difficult to achieve, because the time available for coagulation is so much shorter.

Ratios between the radioactivities of elements in the same decay chain show the degree of radioactive equilibrium present in the aerosol. Based on the distribution of nuclei on the different particle sizes, radioactivity ratios from nuclei attached to one

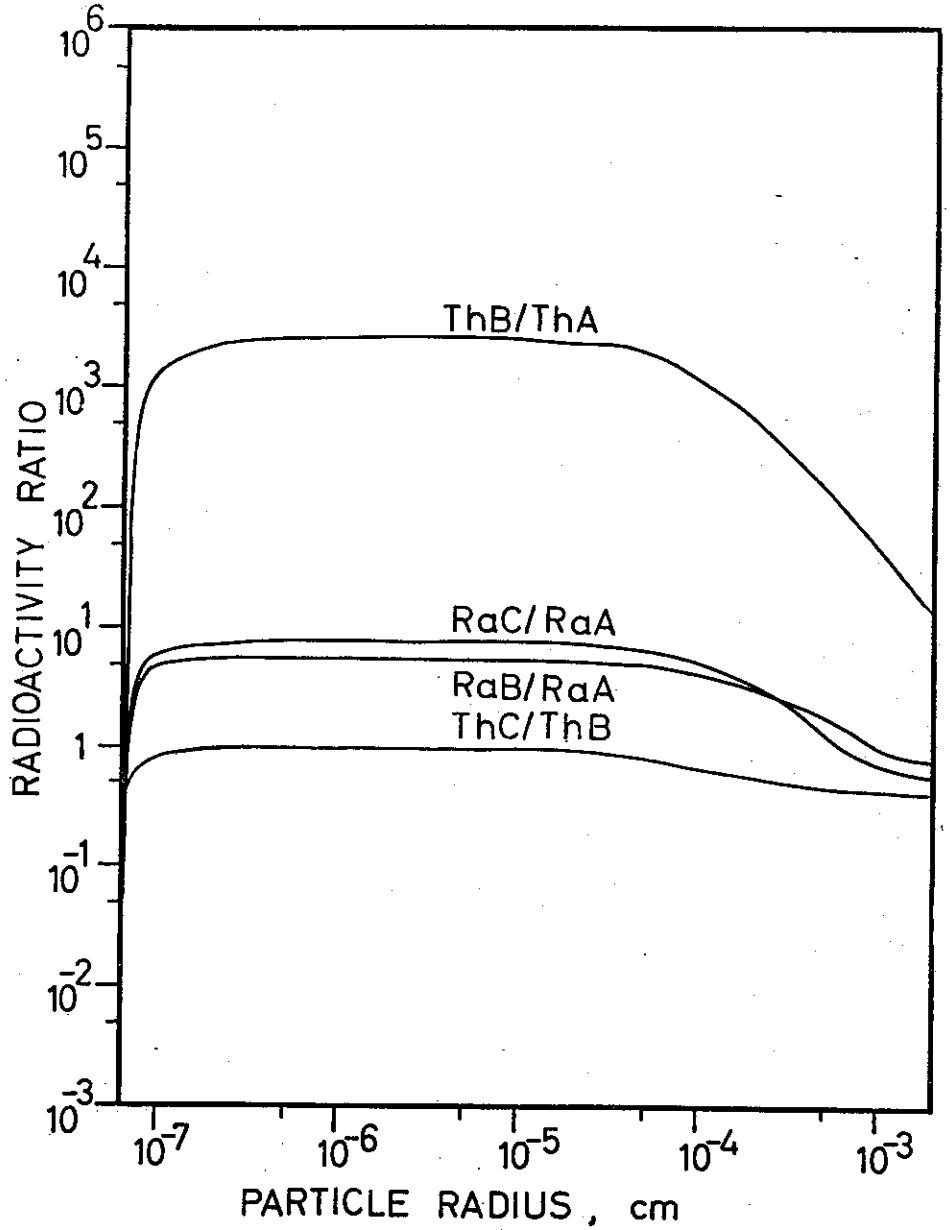

Fig. 7.11. *Radioactivity ratios for elements in the same chain of decay.* The aerosol and the environment are the same as in Fig. 7.5.

particular particle size can be studied. Figures 7.10—7.12 show ratios for certain *Tn* and *Rn* decay products. Due to the very different radioactive-lives of the elements, the *Tn* chain is illustrated by the *ThB/ThA* and *ThC/ThB* ratios, while the *Rn* chain is illustrated by *RaB/RaA* and *RaC/RaA*.

Due to the shift with time upward on the size distribution, ratios between the radioactivity from nuclei late and early in the decay chain are low for the very smallest particles. Supply of the early nuclei is ample, while later ones are older as particles and have been moved away from the region by coagulation.

For slightly larger particles the situation is changed completely. Due to an excess

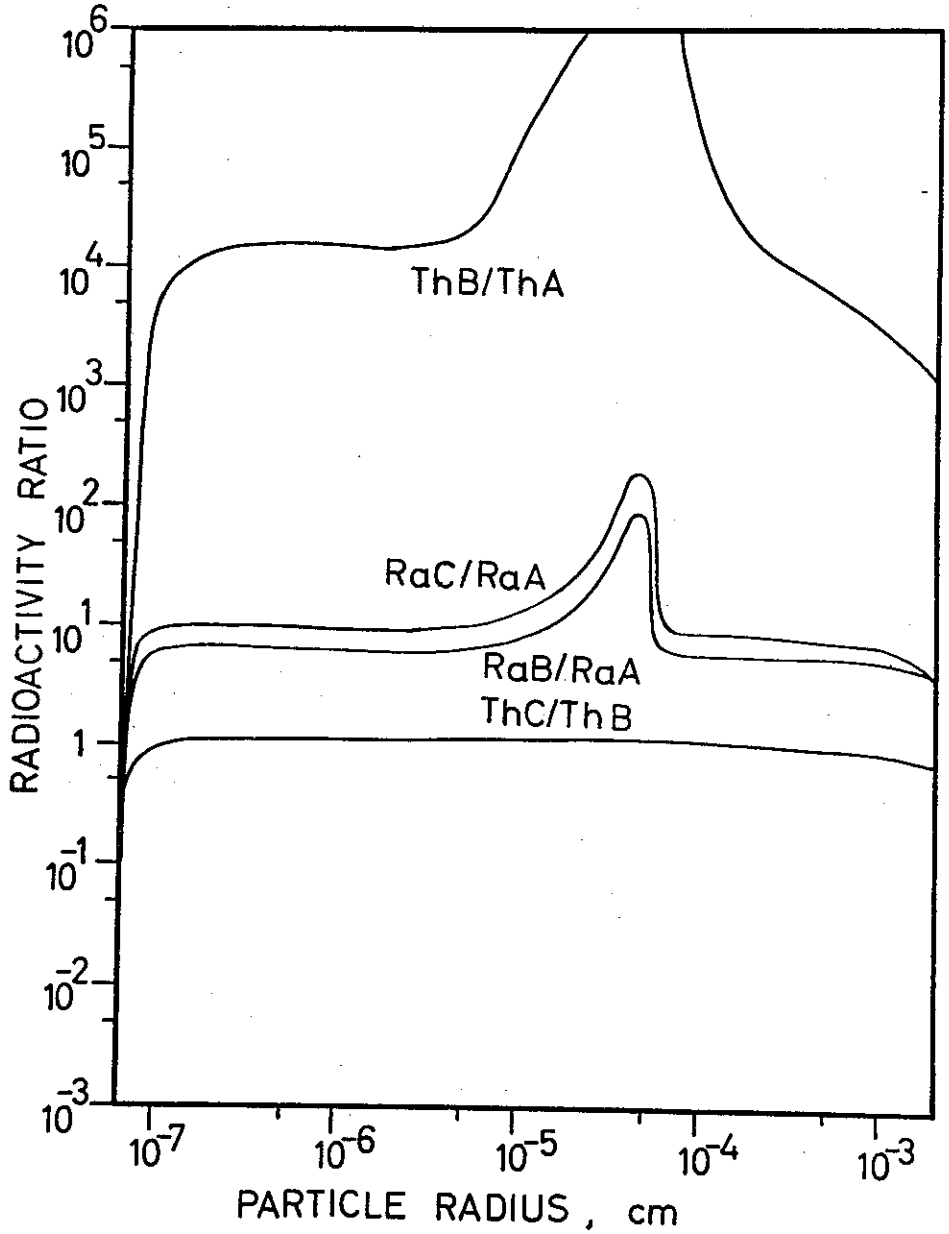

Fig. 7.12. *Radioactivity ratios for elements in the same chain of decay.* The aerosol and the environment are the same as in Fig. 7.6.

of free *ThA* and *RaA* nuclei, the nuclei associated with particles are depleted in these elements. The ratio *ThB/ThA* rises higher than 10,000, while *RaB/RaA* and *RaC/RaA*, where radioactive life-times are more of the same magnitude, rise to about 10. The radioactivity ratio *ThC/ThB* is between elements which are almost entirely deposited on particles, and the ratio never rises much above unity.

At the upper end of the size region the ratios tend to fall off. This is the region where particles are increasingly being removed from the aerosol. Since the nuclei late in the chains are, on the average, oldest, a higher fraction of the particles to which they are attached has disappeared, and radioactivity ratios fall off.

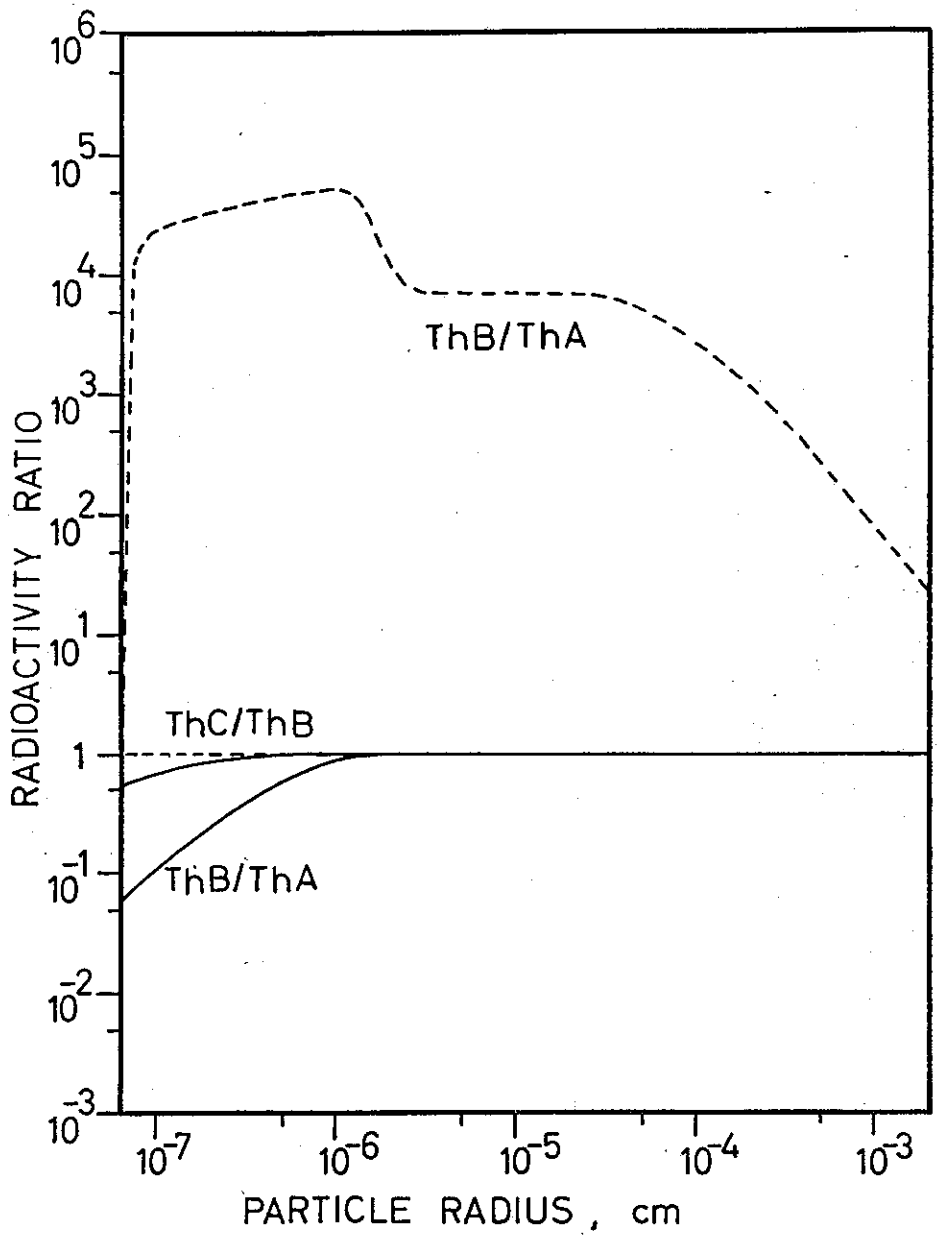

7.13.

Figs. 7.13. and 7.14. *Ratios between accumulated radioactivity on particles smaller or larger than the size indicated.* The aerosol and the environment are the same as in Fig. 7.4. Solid curves are for radioactivity accumulation from the lower end of the size distribution, broken curves from the upper end.

Even when the cumulative radioactivity associated with particles below or above a particular size is examined, some effect of the skew distributions of individual nuclei is apparent. Figures 7.13—7.18 show radioactivity ratios for accumulated nuclei below and above the reference size. The lack of radioactive equilibrium is especially striking for radioactivity associated with particle sizes *above* a certain size.

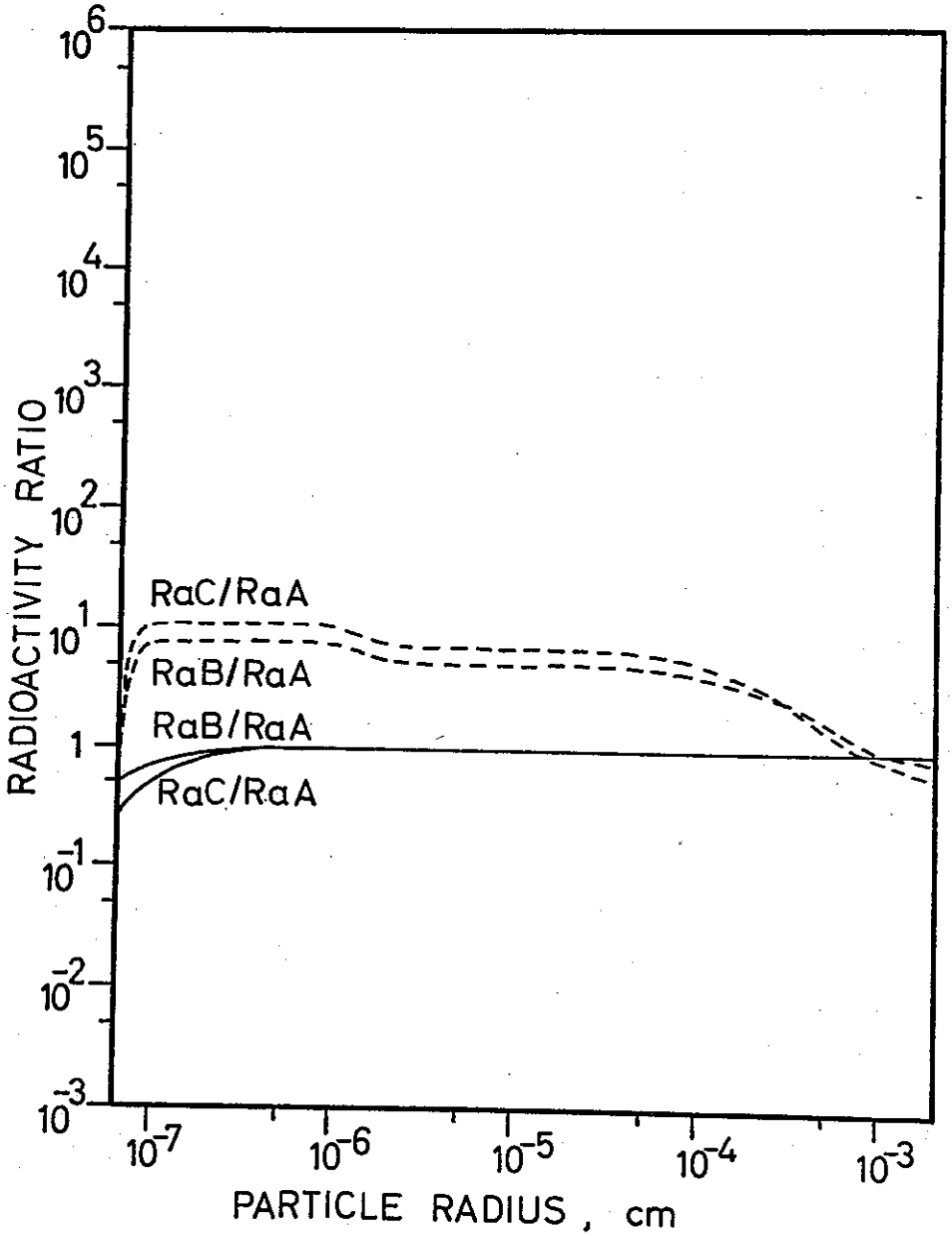
RADIOACTIVITY RATIO
PARTICLE RADIUS, cm
RaC/RaA
RaB/RaA
RaB/RaA
RaC/RaA

7.14.

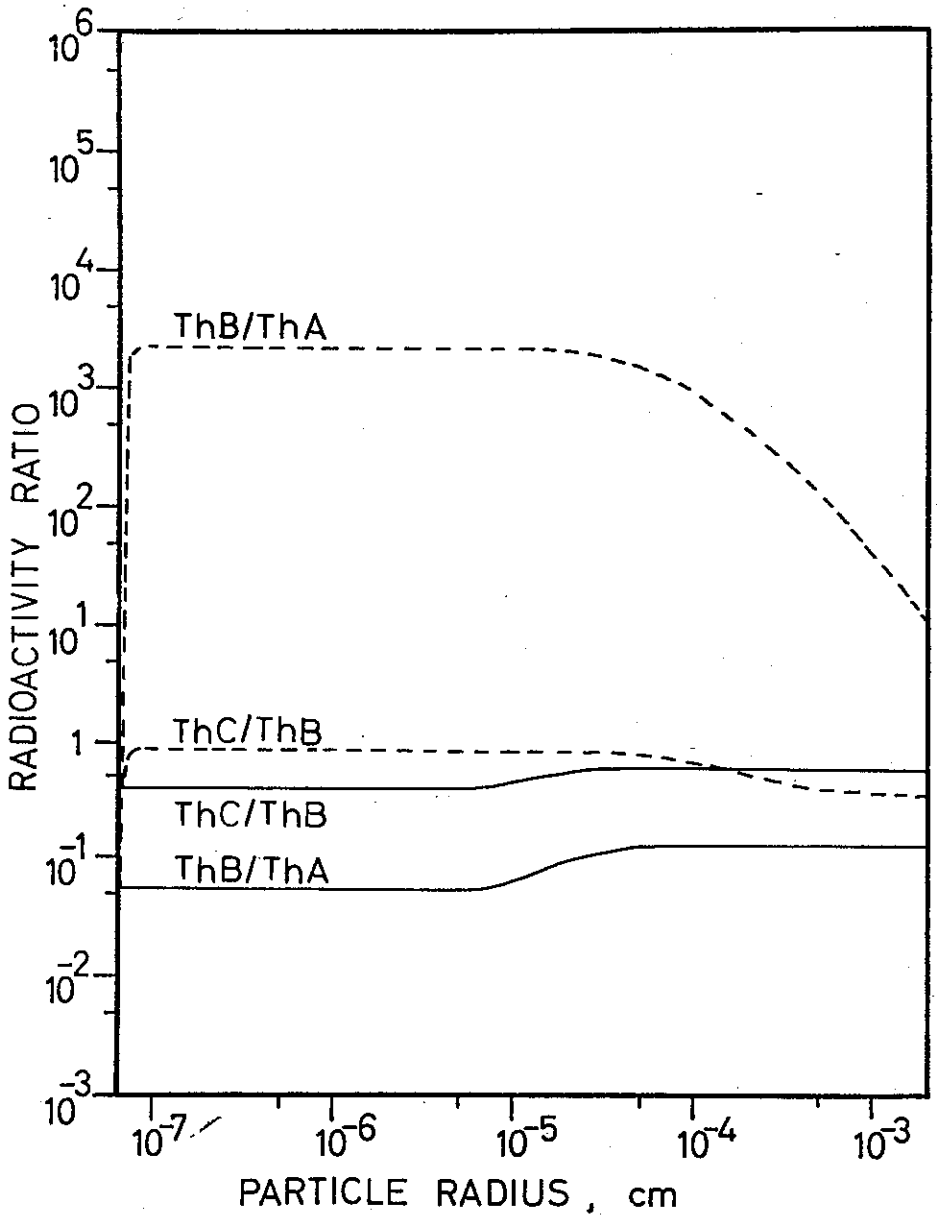

7.15.

Figs. 7.15. and 7.16. *Ratios between accumulated radioactivity on particles smaller or larger than the size indicated.* The aerosol and the environment are the same as in Fig. 7.5. Solid curves are for radioactivity accumulation from the lower end of the size distribution, broken curves from the upper end.

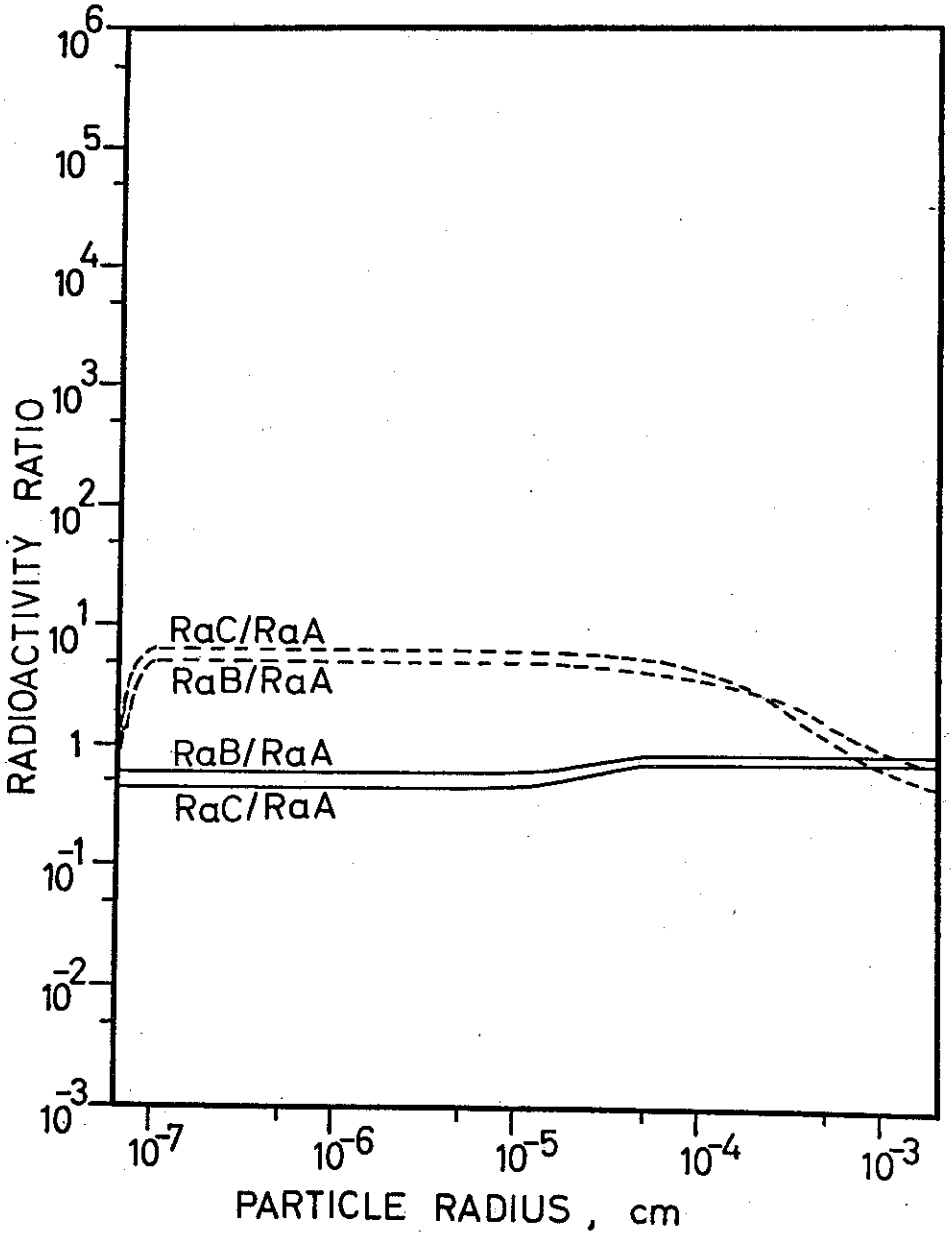
RADIOACTIVITY RATIO
PARTICLE RADIUS, cm
RaC/RaA
RaB/RaA
RaB/RaA
RaC/RaA

7.16.

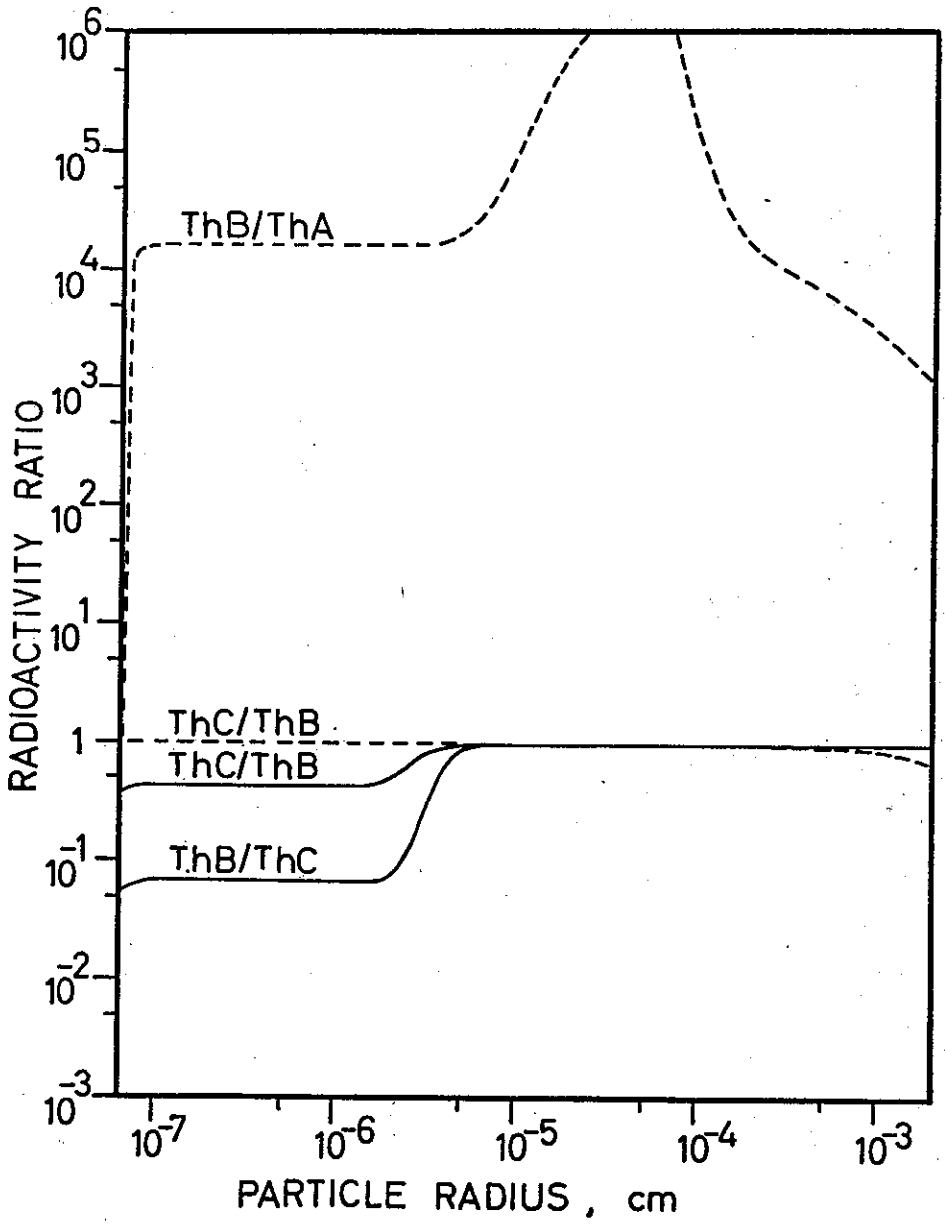

7.17.

Figs. 7.17. and 7.18. *Ratios between accumulated radioactivity on particles smaller or larger than the size indicated.* The aerosol and the environment are the same as in Fig. 7.6. Solid curves are for radioactivity accumulation from the lower end of the size distribution, broken curves from the upper end.

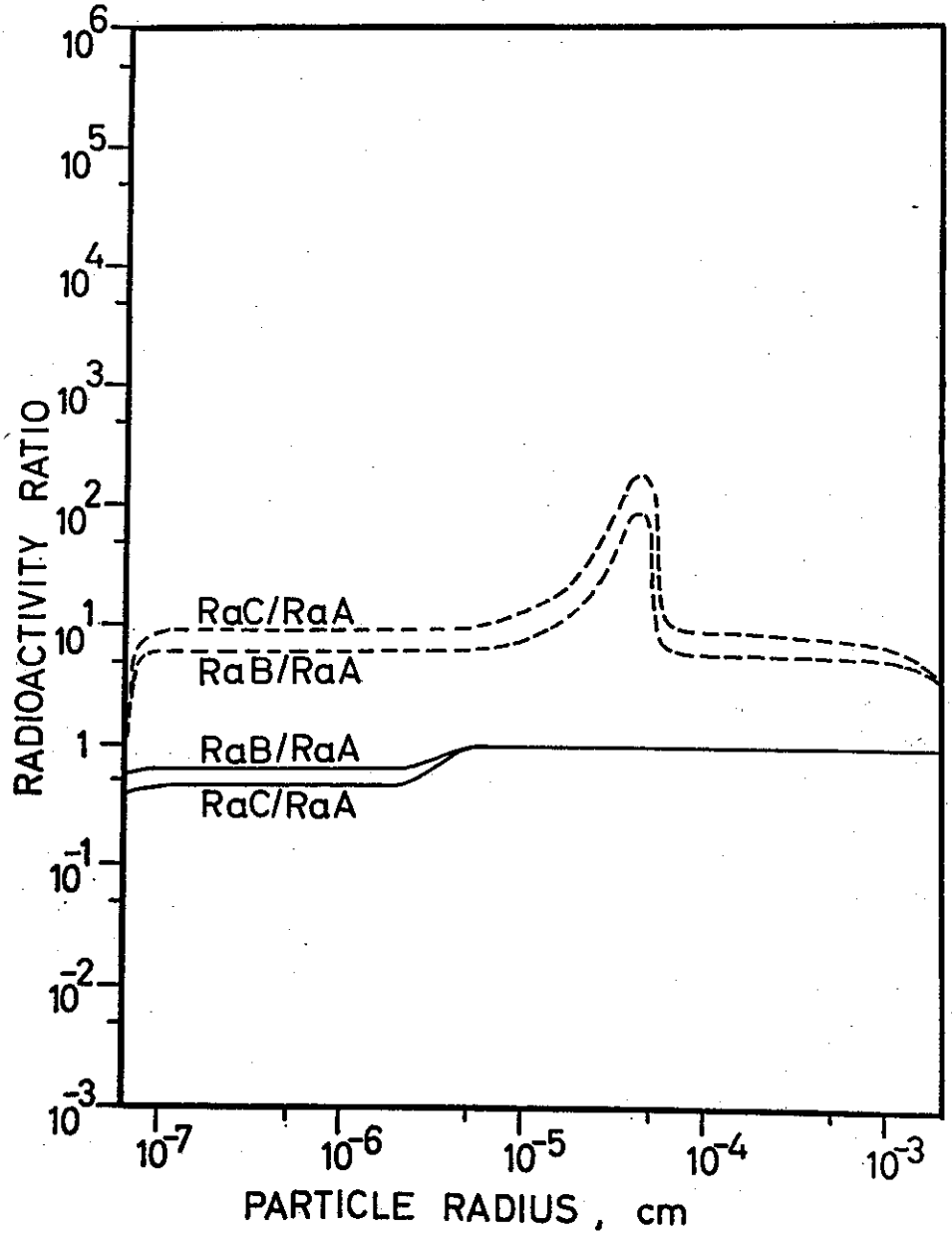
RADIOACTIVITY RATIO
PARTICLE RADIUS, cm
RaC/RaA
RaB/RaA
RaB/RaA
RaC/RaA

7.18.

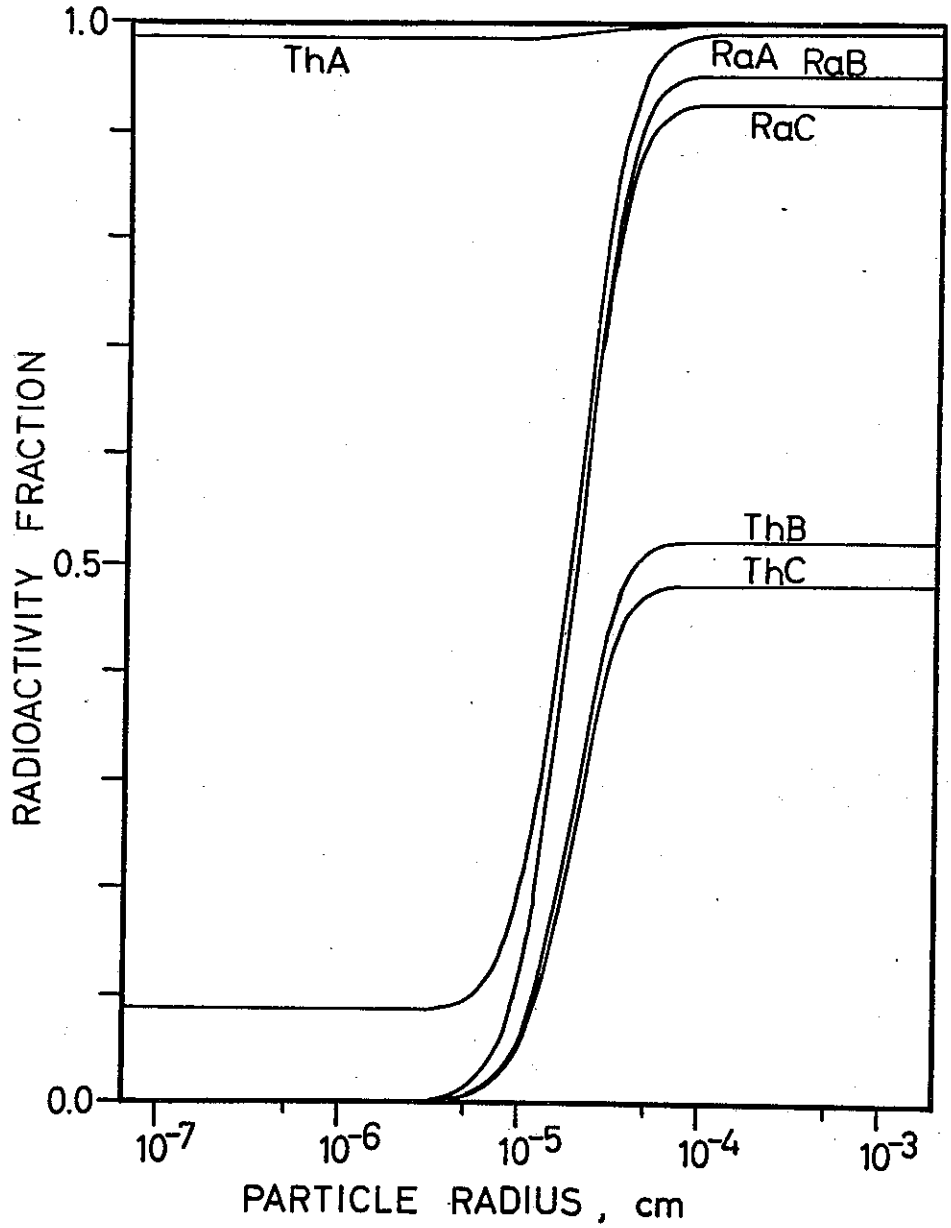

Fig. 7.19. *Normalized cumulative radioactivity distributions — Non-radioactive environment.* Parameters for the aerosol: small-particle supply 100 $cm^{-3}s^{-1}$, other supply $10^{-14}gcm^{-3}s^{-1}$ with mode 10^{-5} cm and $\sigma = 2$, removal coefficient 10^{-4} and exponent 2, air replacement time 24 hrs.

7.3 Radioactivity in denser aerosols. In a more dense aerosol, where a distribution mode at medium/large particle sizes is well developed, the time needed for attachment of the radioactive elements to the particles is fairly short. Cumulative radioactivity distributions for such aerosols are presented in Figures 7.19—7.21.

When dilution is slow, only *ThA* and *RaA* are present as free elements to a noticeable degree. When dilution is more rapid, the situation is similar as long as the aerosol environment is non-radioactive. If it is radioactive, however, free nuclei of all elements are introduced. In the steady state therefore a certain fraction of the elements, even

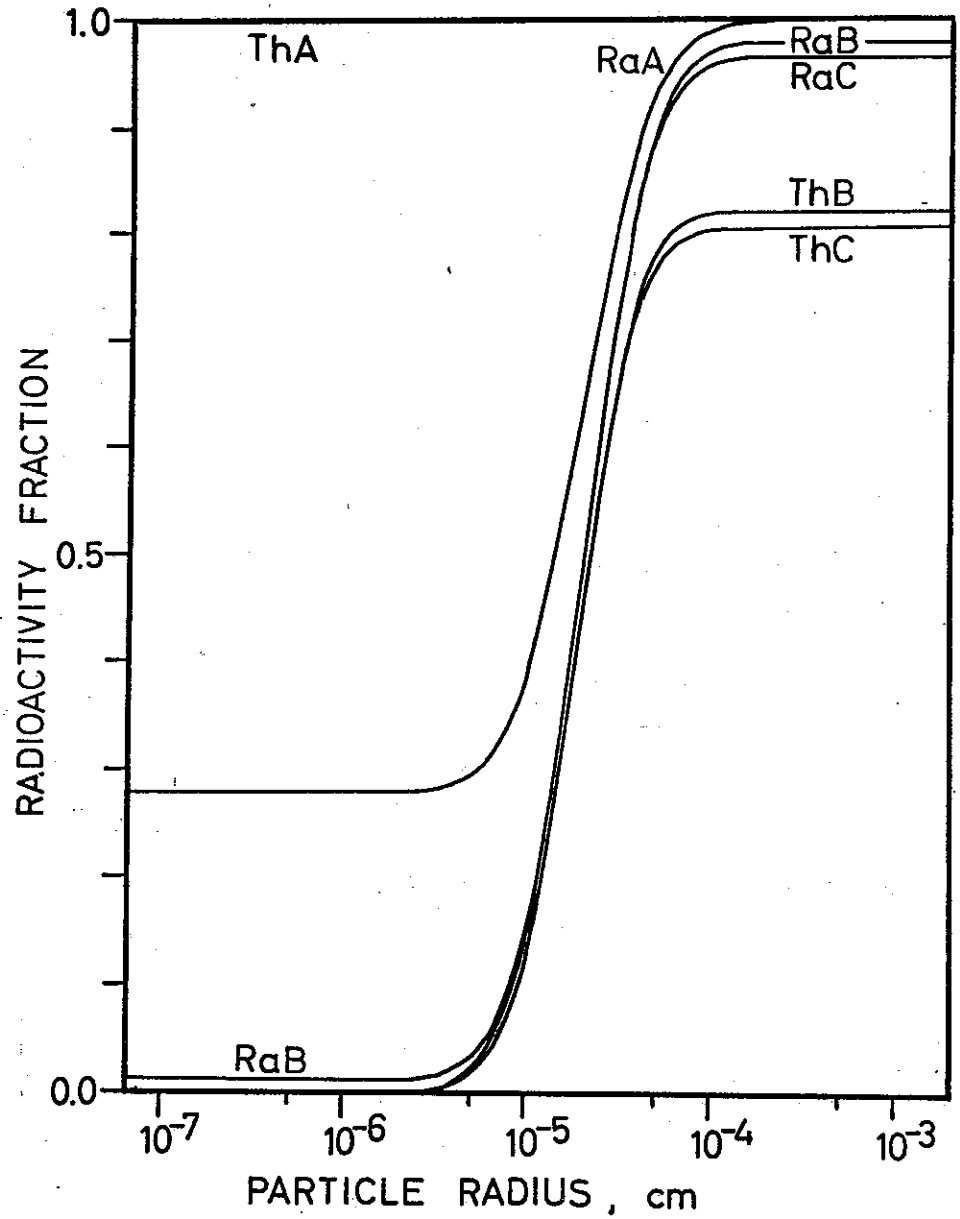

Fig. 7.20. *Normalized cumulative radioactivity distributions — Radioactive environment.* Parameters for the aerosol: small-particle supply 100 $cm^{-3}s^{-1}$, other supply $10^{-14}gcm^{-3}s^{-1}$ with mode 10^{-5} cm and $\sigma = 2.5$, removal coefficient 10^{-4} and exponent 2, air replacement time 24 hrs.

those late in the decay chain, may not be attached to particles. In Figure 7.20 this is evidently the case for *RaB*, for which the time elapsed since decay of the gaseous precurser is the next shortest. For the other elements, the time as a particulate substance increases from *RaC* through *ThB* to *ThC*, and free nuclei are increasingly scarce in this succession.

For steady-state aerosols of the type presented, lower concentrations than that of radioactive equilibrium are normal for all elements late in the decay chain. Even when dilution is strong, removal of particles by deposition is significant. Regardless

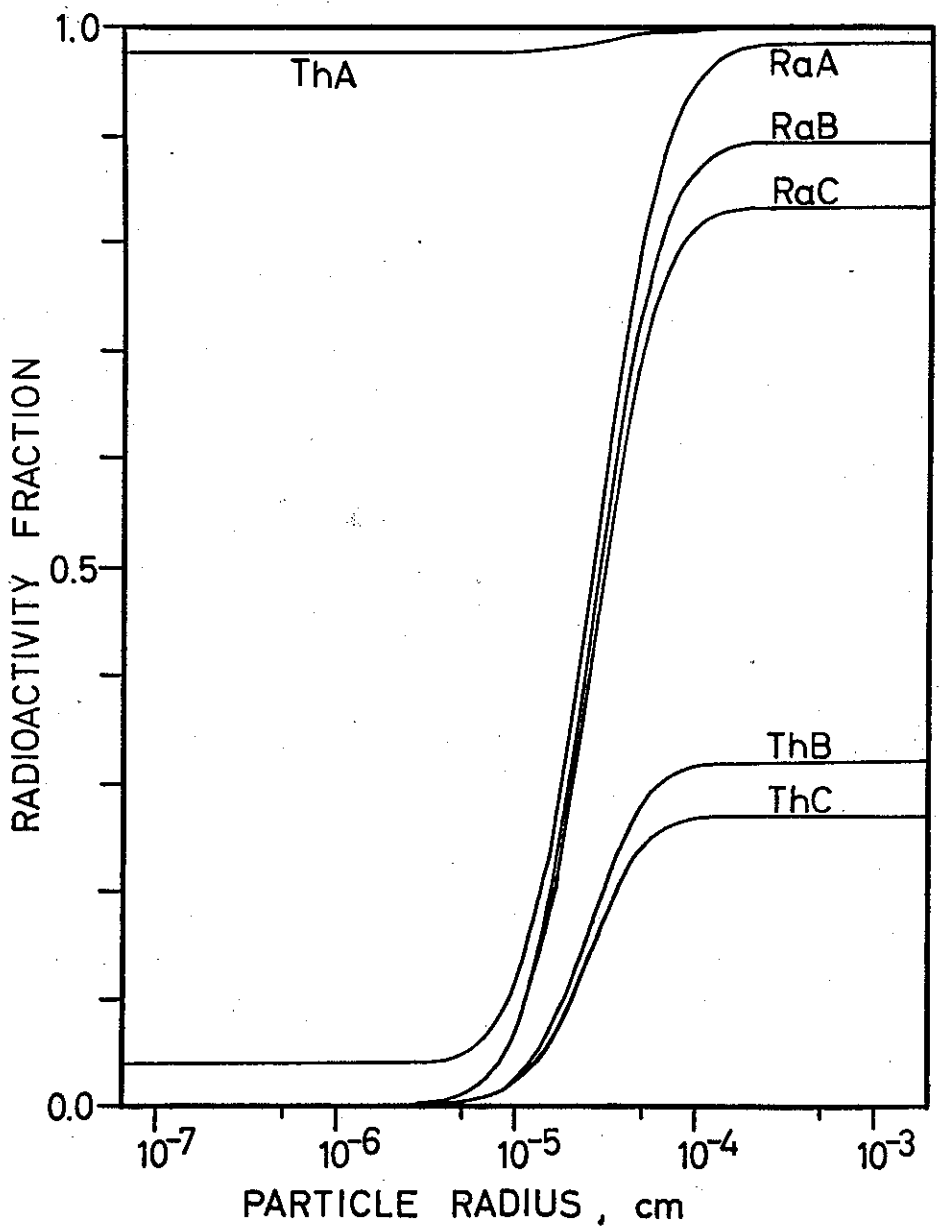

Fig. 7.21. *Normalized cumulative radioactivity distributions — Non-radioactive environment.* Parameters for the aerosol: small-particle supply 10 $cm^{-3}s^{-1}$, other supply $10^{-12}gcm^{-3}s^{-1}$ with mode 10^{-5} and $\sigma = 3$, removal coefficient 10^{-4} and exponent 1.75, air replacement time 12 hrs.

of radioactive or non-radioactive environment, the effect of removal increases with time elapsed since decay of the gaseous precurser. On all the Figures 7.18—7.21 the fraction of equilibrium concentrations falls off in the succession *ThA*, *RaA*, *RaB*, *RaC*, *ThB*, *ThC*.

The upward size shift due to coagulation is dependent on the same time quantity. In the Figures, the curves are therefore found from left to right in the succession just mentioned. For a very dense aerosol the feature becomes really pronounced. This is illustrated in Figure 7.22.

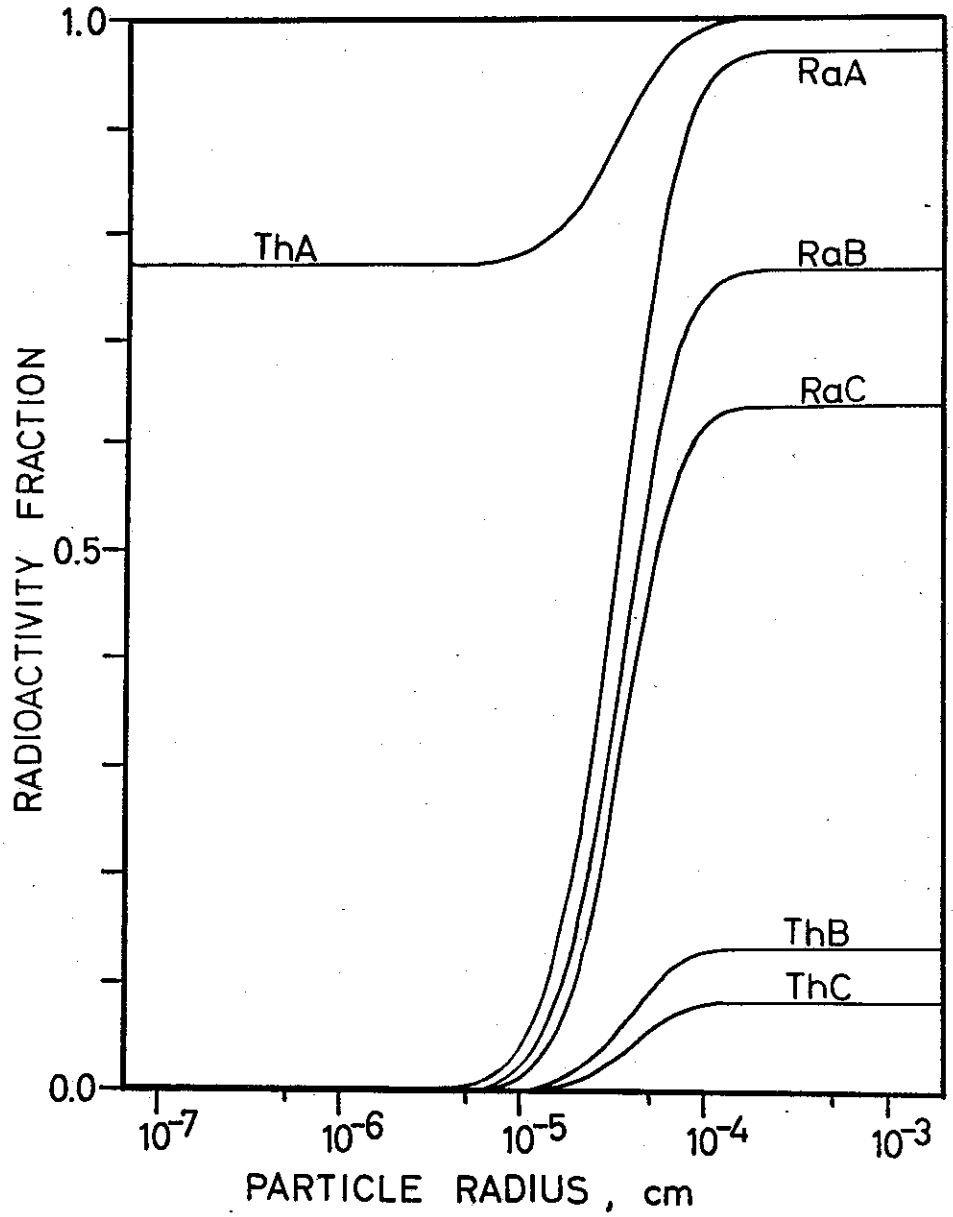

Fig. 7.22. *Normalized cumulative radioactivity distributions — Non-radioactive environment.* Parameters for the aerosol: small-particle supply 10 $cm^{-3}s^{-1}$, other supply $100^{-11}gcm^{-3}s^{-1}$ with mode 10^{-5} cm and $\sigma = 2.5$, removal coefficient 10^{-4} and exponent 1.75, air replacement time 3 hrs.

The radioactivity distributions associated with the *Rn* and *Tn* chains are shown in Figures 7.23—7.25. For the type of aerosol under consideration, deposition time is short compared to the radioactive life-times for radon descendants. Free *ThA* nuclei therefore dominate, with the result that radioactivity in the *Tn* chain is associated with the smallest particle sizes.

The distribution of nucleus deposition on particles is also shown. Normally the upward size shift by coagulation is not strong enough to outweigh the effect of non-attached nuclei, even for *Rn* decay products. Only the very dense aerosol in Figure 7.26 has a

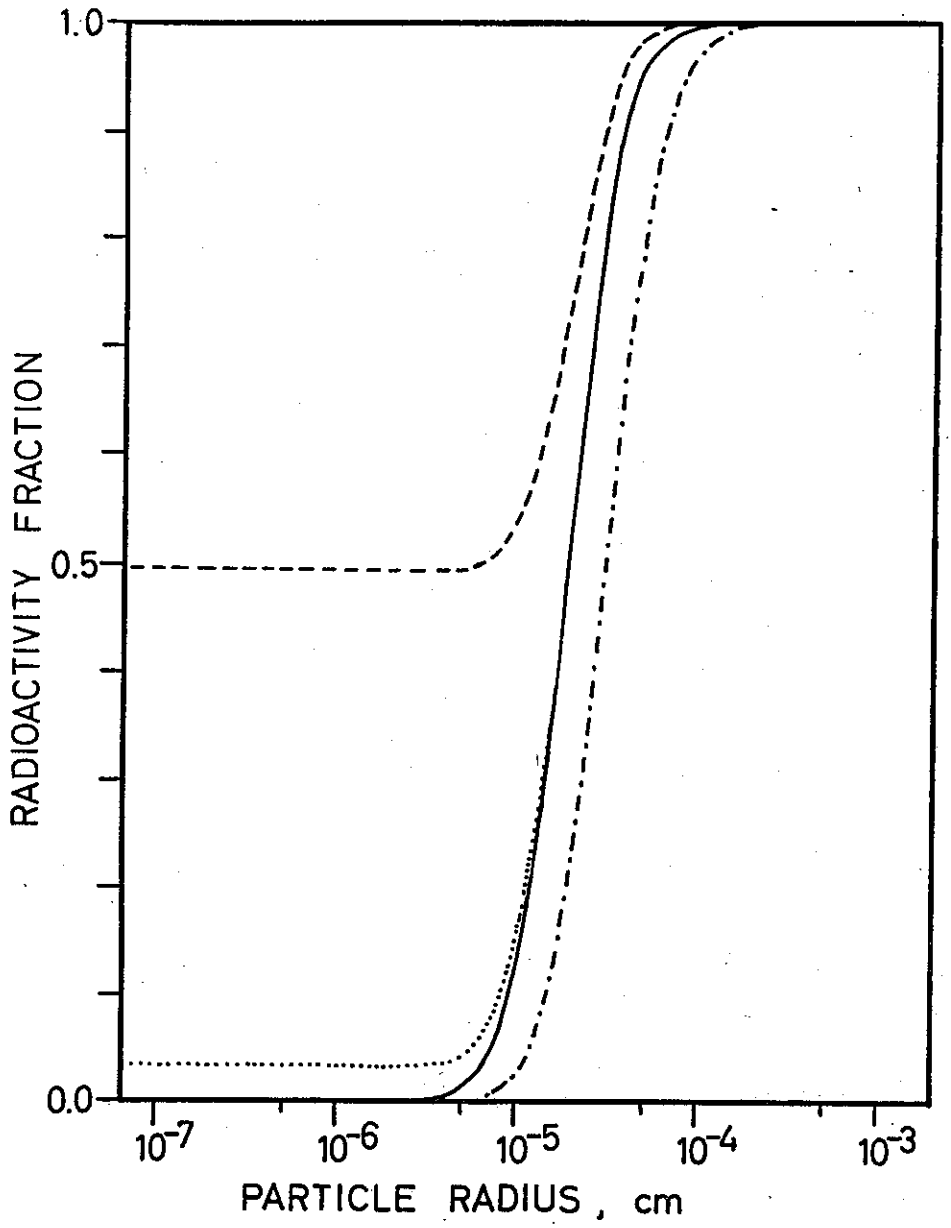

Fig. 7.23. *Cumulative distributions, fraction of individual total.* The aerosol and the environment are the same as in Fig. 7.19. Solid curve indicates deposition distribution for free nuclei, broken curve steady-state distribution for radioactivity from Tn descendants, dotted for Rn descendants. Broken/dotted curve shows aerosol mass distribution.

distribution curve for radon descendants which is partly to the right of the deposition distribution. Part of the explanation for the slow response may lie in the fact that increased removal of the radioactivity on the larger particles occurs simultaneously with an increased coagulation shift towards larger sizes. Figure 7.25 shows less radiactivity associated with large particles than that corresponding to deposition. This is due to the rapid removal of those particles.

Ratios between the radioactivities from nuclei attached to different particle sizes are shown in Figures 7.27—7.30.

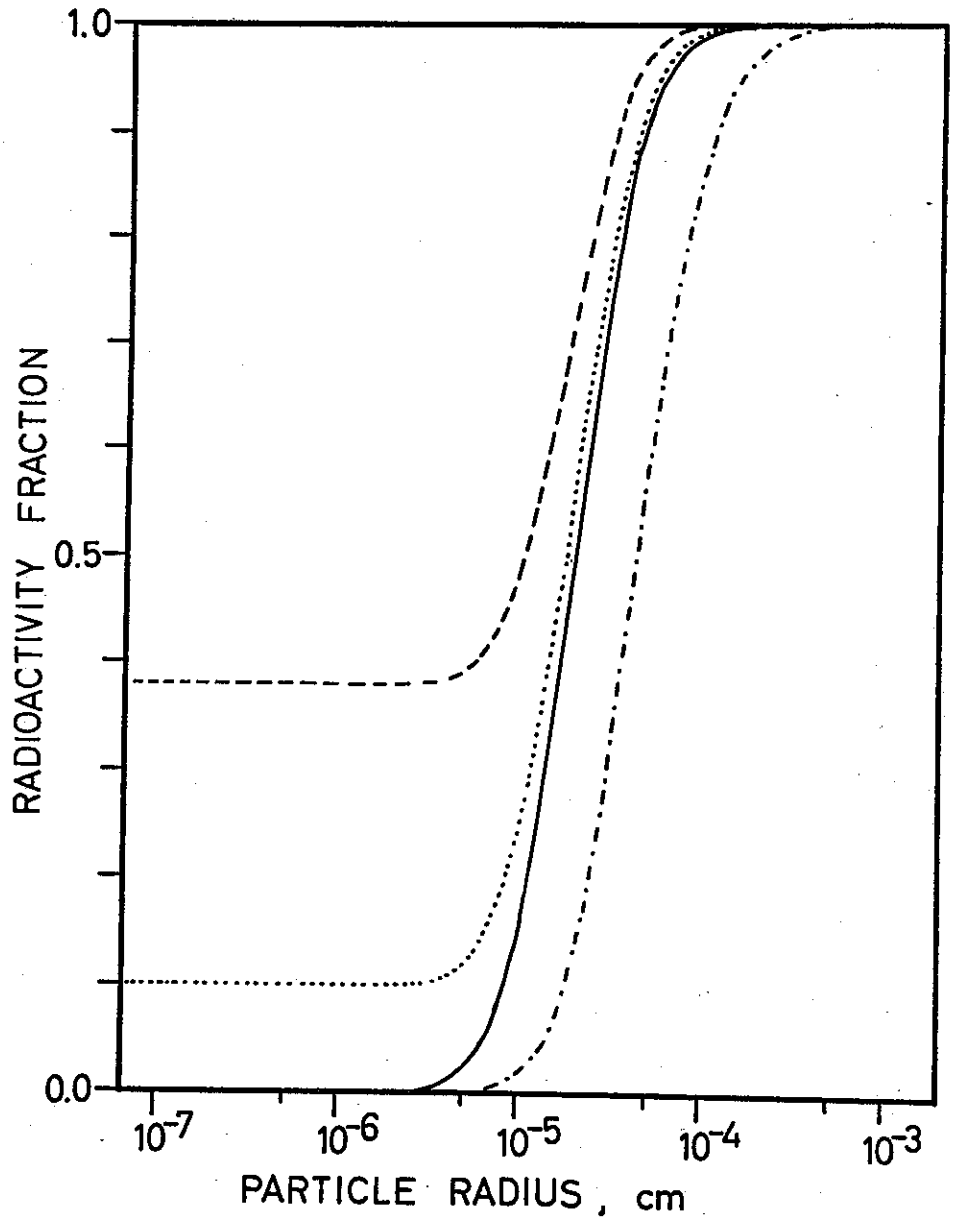

Fig. 7.24. *Cumulative distributions, fraction of individual total.* The aerosol and the environment are the same as in Figure 7.20. Solid curve indicates deposition distribution for free nuclei, broken curve steady-state distribution for radioactivity from Tn descendants, dotted for Rn descendants. Broken/dotted curve shows aerosol mass distribution.

It is evident that the ratios change more gradually with particle size than was the case for the low-mass aerosols in Figures 7.10—7.12. Neither are maximum values so high. But the trend is very much the same.

At the lower end of the size distribution the ratio between an early and an older element in a chain is low, because early elements are more concentrated on small particles than the later ones. A gradual rise takes place towards the middle part of the distribution, because coagulation has shifted the distribution of later elements towards larger sizes. For the upper end the effect of removal is dominant, mostly affecting the

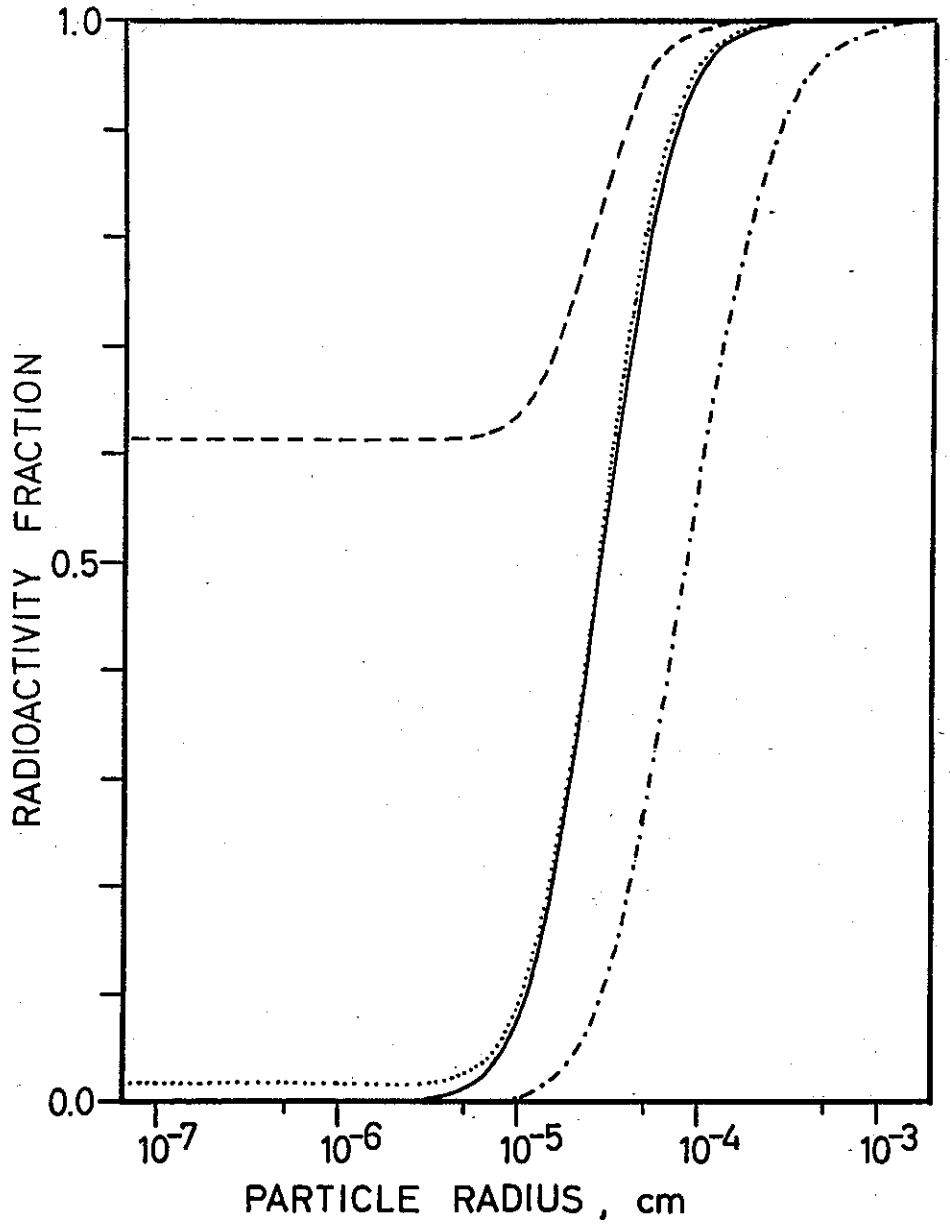

Fig. 7.25. *Cumulative distributions, fraction of individual total.* The aerosol and the environment are the same as in Fig. 7.21. Solid curve indicates deposition distribution for free nuclei, broken curve steady-state distribution for radioactivity from Tn descendants, dotted curve for Rn descendants. Broken/dotted curve shows aerosol mass distribution.

later chain elements, because they are worked upon for a longer time, and the ratios drop.

The maximum *ThB/ThA* ratio is found in Figure 7.28 and it is less than 500, compared to more than 10,000 for the low-mass aerosols. The maximum *RaB/RaA* ratio is less than 1.5 compared with 10 earlier. The drop for larger sizes carries the ratios far below 1, a value seldom reached before.

For the dense aerosol in Figure 7.30 the removal of radioactivity is so heavy that none of the ratios ever reaches 1.

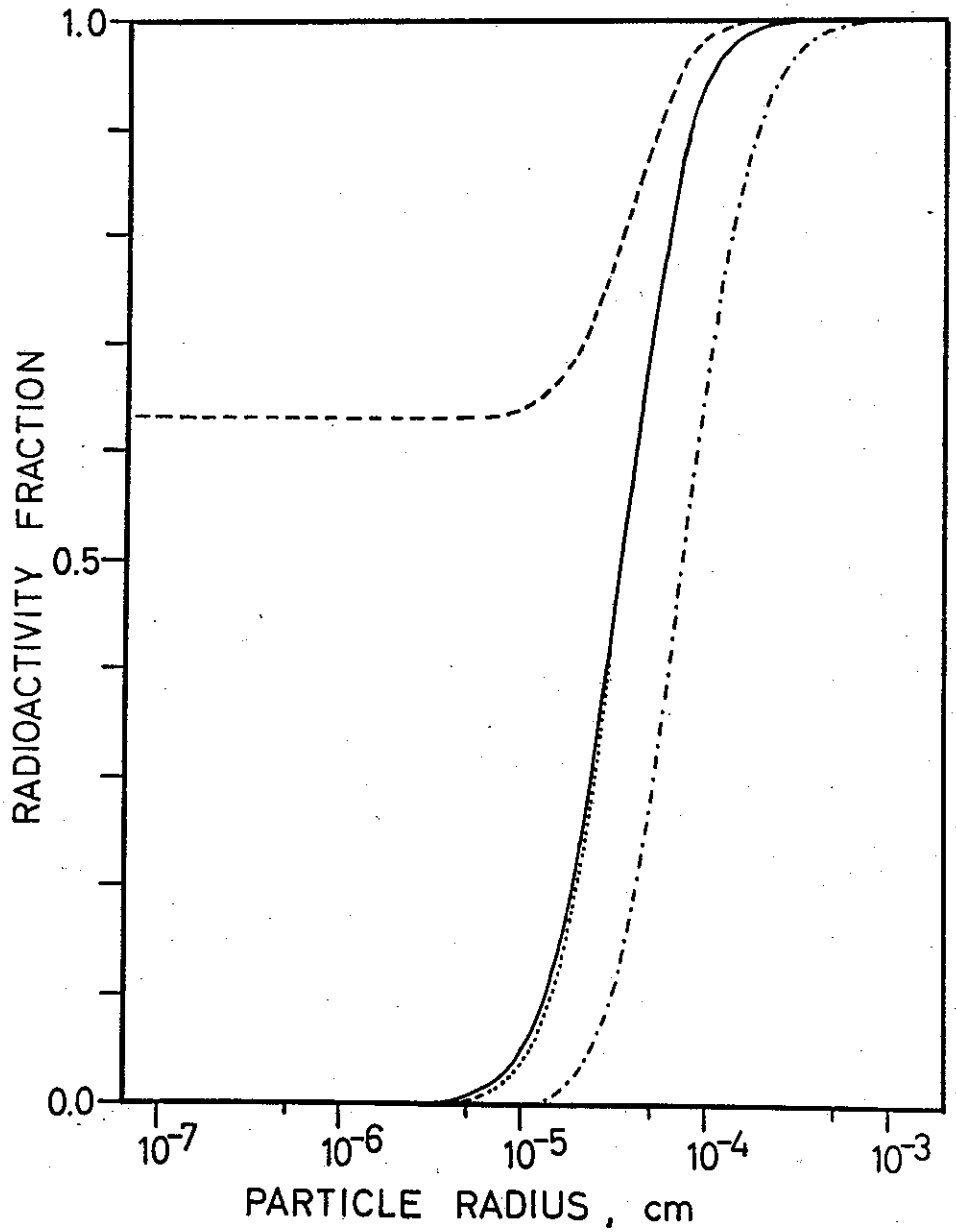

Fig. 7.26. *Cumulative distributions, fraction of individual total.* The aerosol and the environment are the same as in Fig. 7.22. Solid curve indicates deposition distribution for free nuclei, broken curve steady-state distribution for radioactivity from Tn descendants, dotted for Rn descendants. Broken/dotted curve shows aerosol mass distribution.

The ratios between the cumulative radioactivity associated with particles above and below the reference size are shown for two aerosols in Figures 7.31—7.34. The effect of uneven distributions over the size range is also evident for cumulative ratios. Many sampling instruments in use catch either small or large particles, and the diagrams may be a warning against far-reaching conclusions.

The lack of equilibrium between radioactive elements in a chain can be used as a measure for the radioactivity-indicated age of the particles in the aerosol. The equations to be used are (6.18), (6.19) and (6.20).

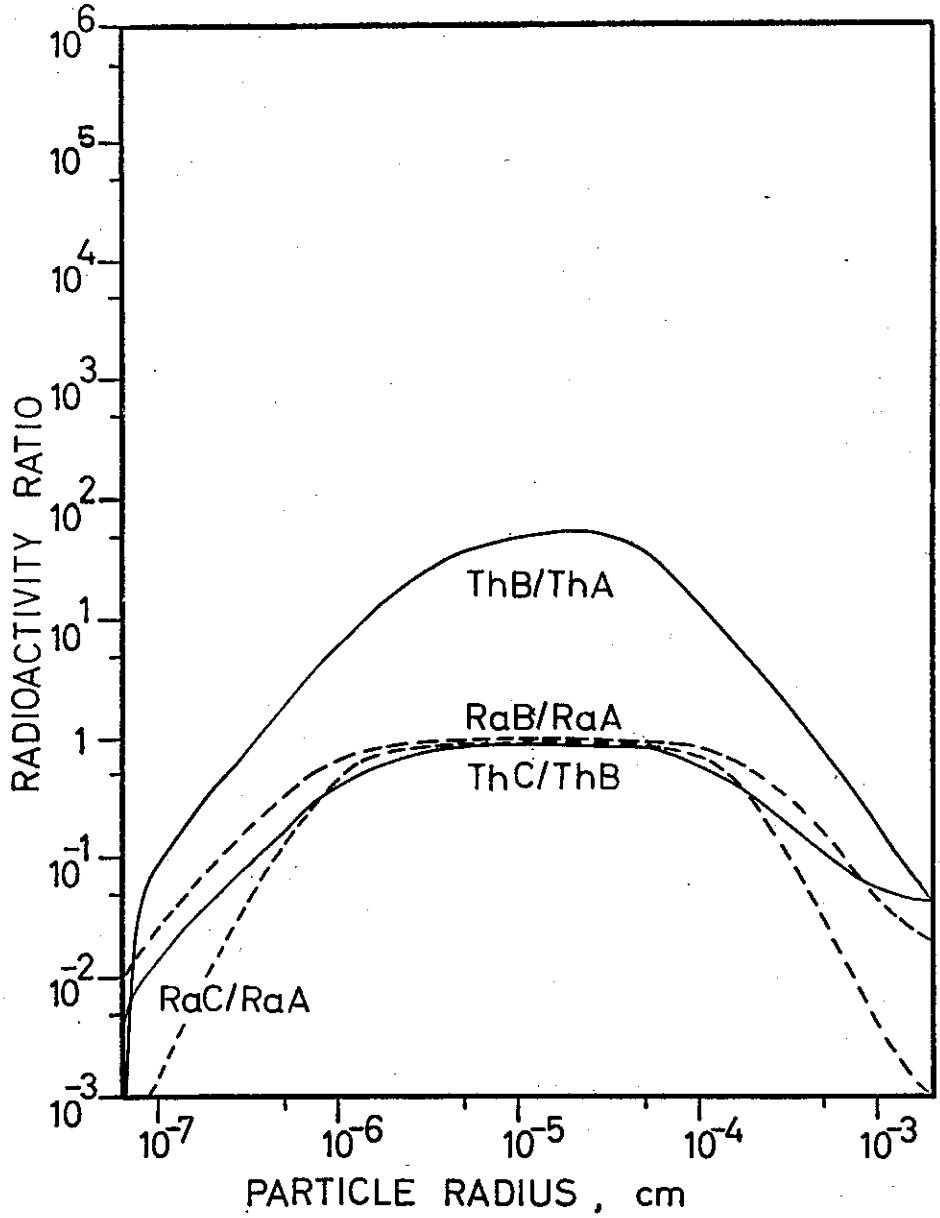

Fig. 7.27. *Radioactivity ratios for elements in the same chain of decay.* The aerosol and the environment are the same as in Fig. 7.19.

In Figure 7.35 such age estimates are shown as a function of mass turn-over time for a number of steady-state aerosols. For each set of aerosol conditions exchange with both radioactive and non-radioactive environments has been entered. In order to show the effect of dilution, several series of computations, within each of which dilution only is changed, have been indicated.

It is apparent that the radioactivity ages are higher than the mass turn-over times. The reason for this is the upward size shift from radioactivity to mass distribution, illustrated in Figures 7.19—7.22. Since the mass flow in the aerosol is towards the upper end of the distribution, from where particles are removed, the radioactive elements will as an aver-

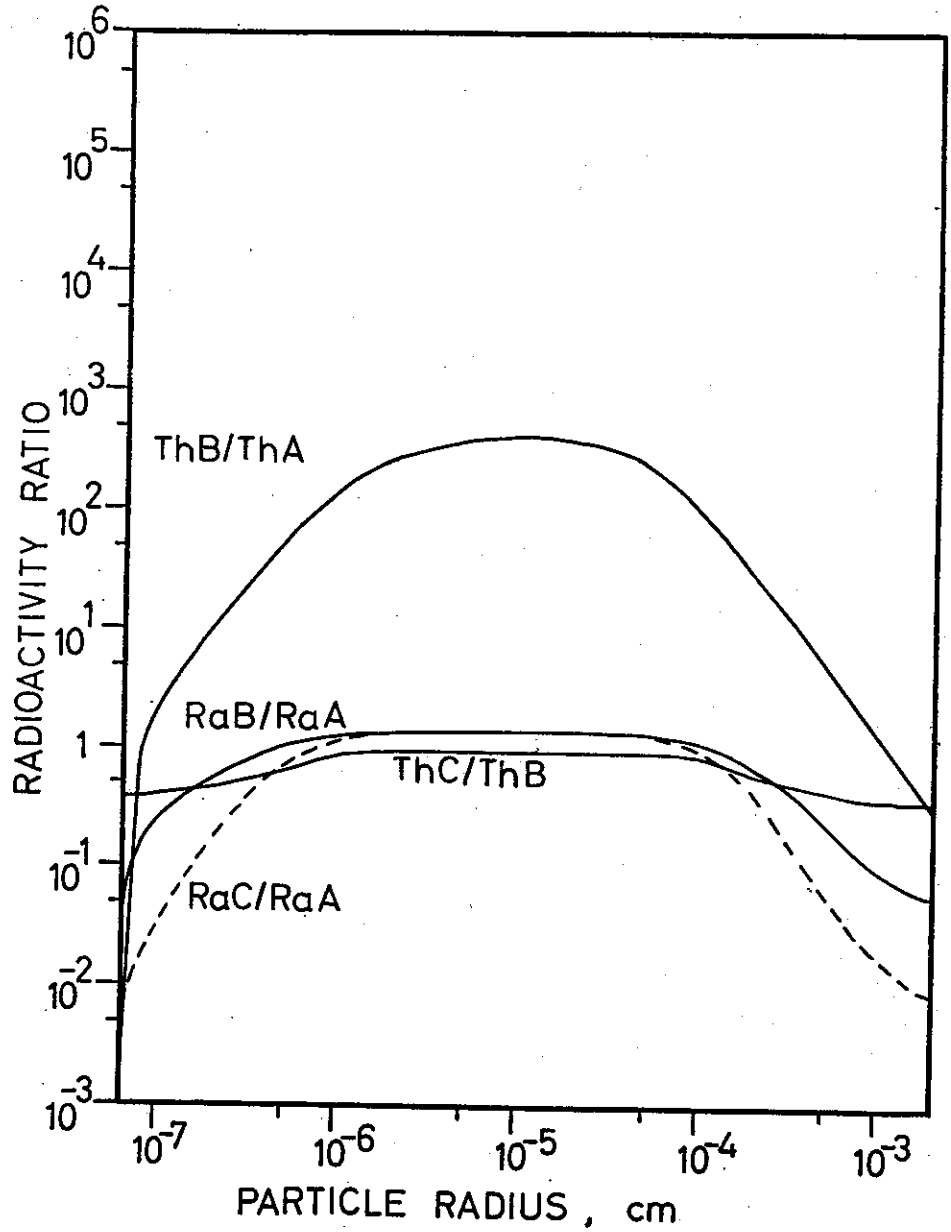

Fig. 7.28. *Radioactivity ratios for elements in the same chain of decay.* The aerosol and the environment are the same as in Fig. 7.20.

age stay in the aerosol for a longer time than the average mass element. Further, since nuclei are continuously shifted towards larger particles, age estimates where elements late in the decay chain take part, are generally the lowest. These factors are all reflected in the age computations, even though some of them are not presented in the figure.

It is also evident that if the equations based on non-radioactive environment are used on radioactive environments, the discrepancy with mass turn-over time is so big and the points are so scattered that no connection can be found. When the degree of dilution is changed, while other conditions remain unchanged, the change in indicated age is even going in a direction opposite to the change in mass turn-over time.

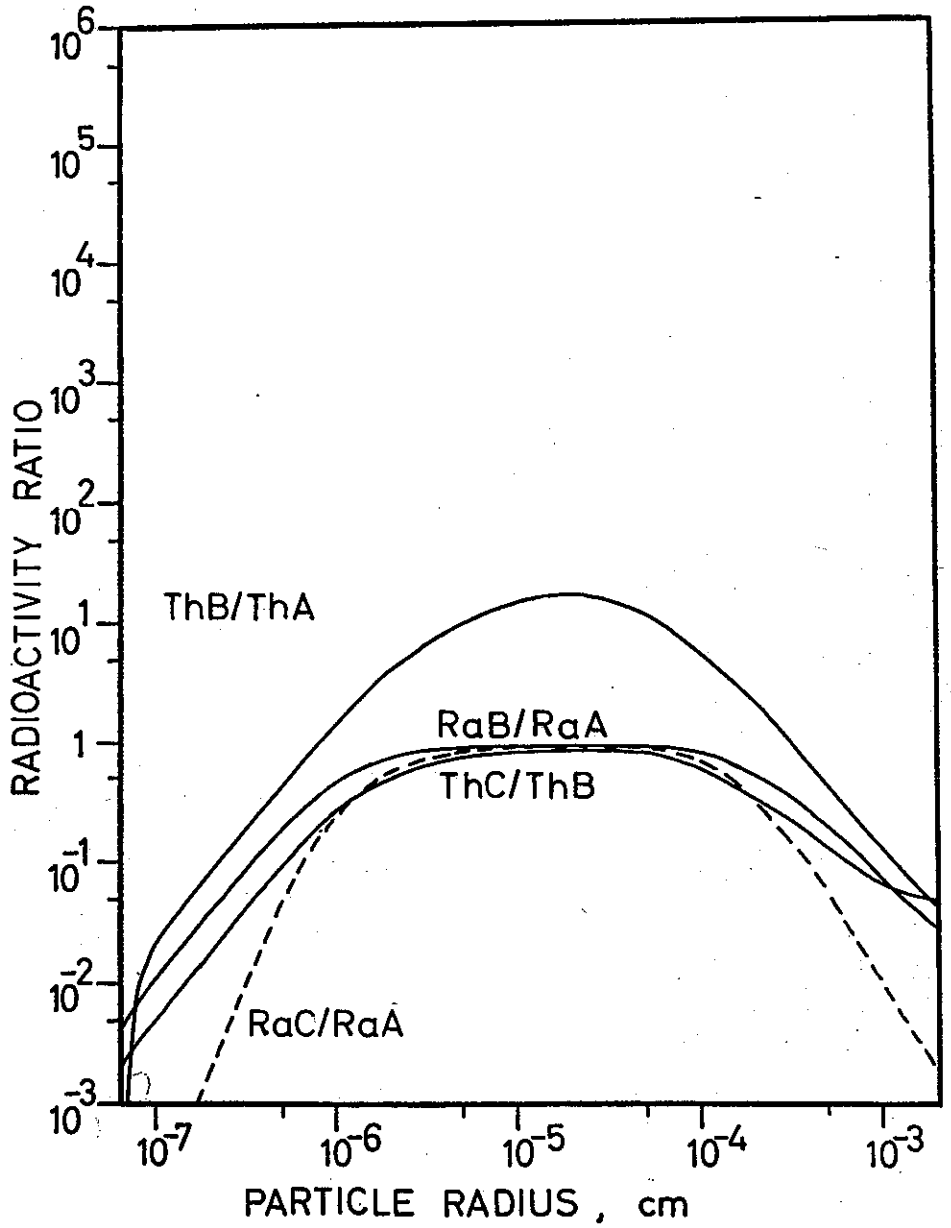

Fig. 7.29. *Radioactivity ratios for elements in the same chain of decay.* The aerosol and the environment are the same as in Fig. 7.21.

There is nothing strange or new in the observation that a set of equations cannot be used outside their terms of reference. But the equations in question, or similar ones for other ratios, are so often used under unspecified conditions that some sort of warning should be issued.

An alternative is to use double-ratio equations (e.g. (6.20)) with the effect of dilution eliminated, since they do not require knowledge about the state of the environment at the time of measurement. It is seen from Figure 7.35 that the results are close to those produced by a single-ratio equation in non-radioactive environment.

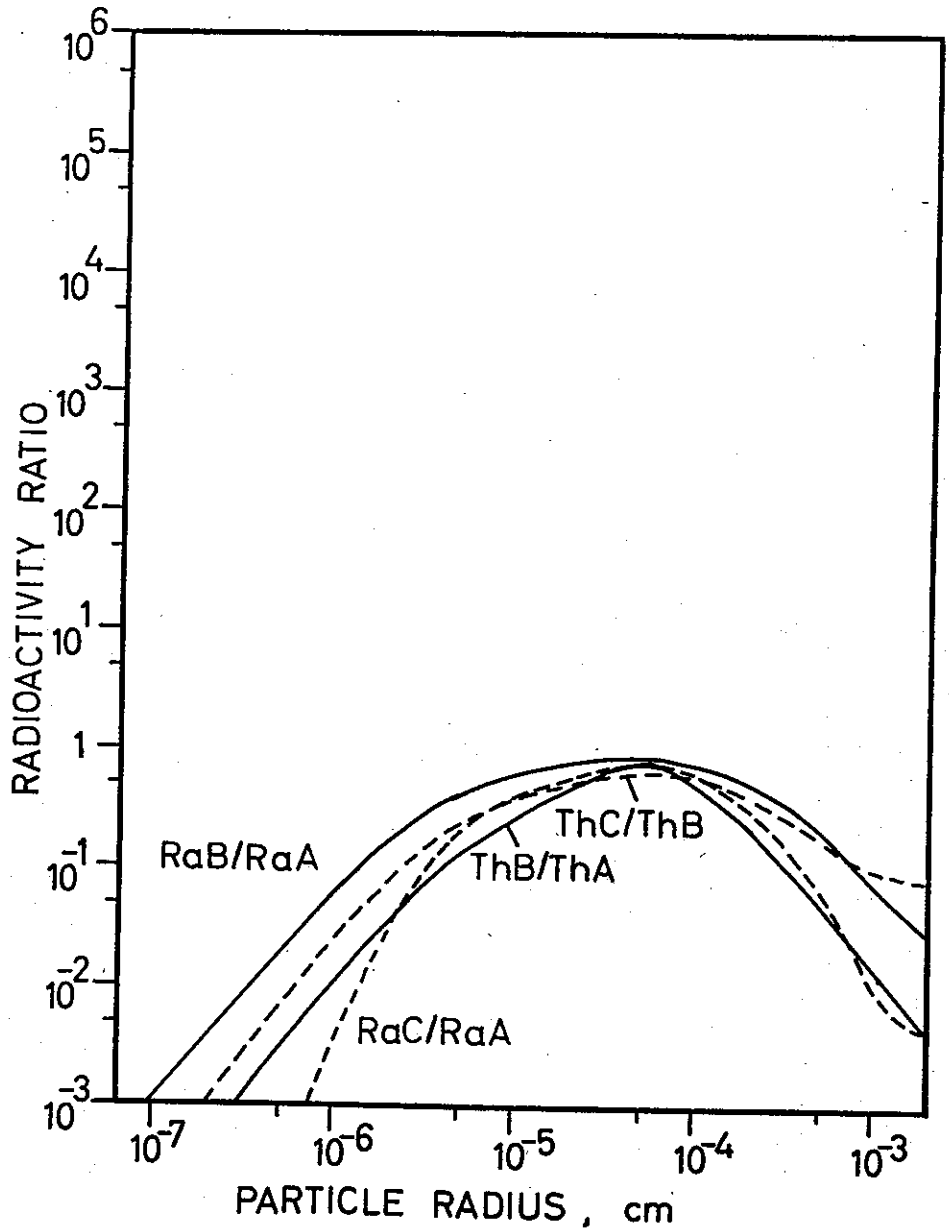

Fig. 7.30. *Radioactivity ratios for elements in the same chain of decay.* The aerosol and the environment are the same as in Fig. 7.22.

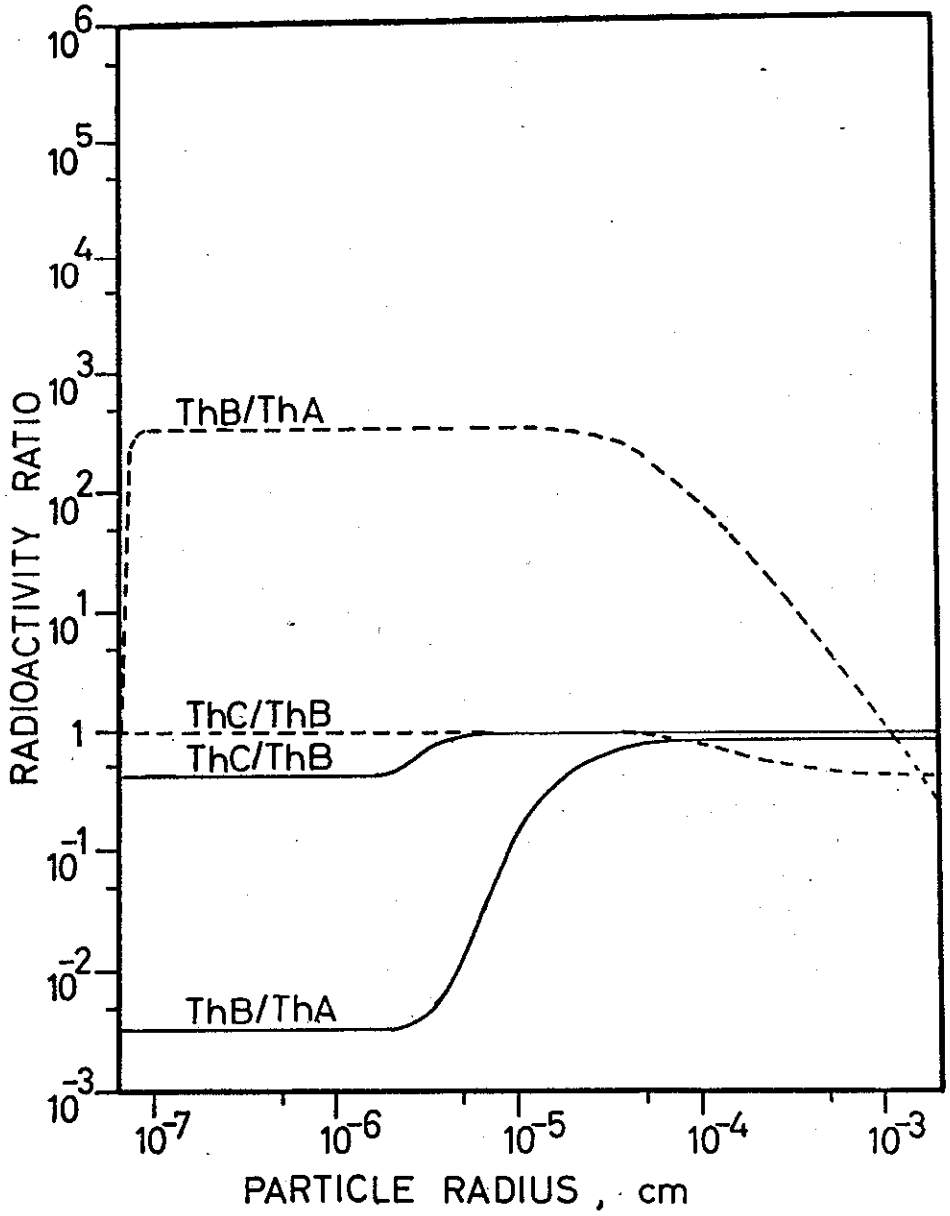

7.31.

Figs. 7.31 and 7.32. *Ratios between accumulated radioactivity on particles smaller or larger than the size indicated.* The aerosol and the environment are the same as in Fig. 7.20 Solid curves are for radioactivity accumulation from the lower end of size distribution, broken curves from the upper end.

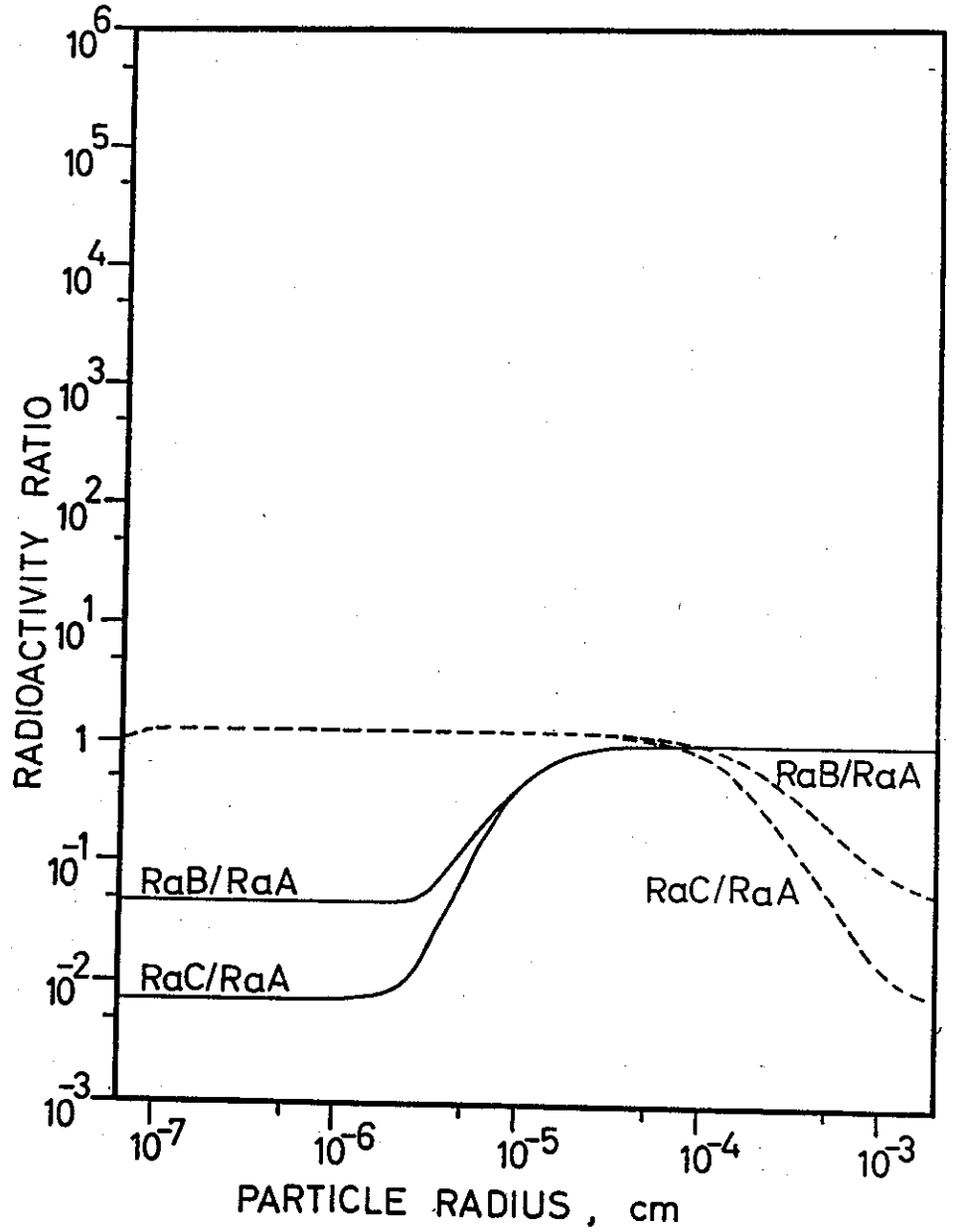
RADIOACTIVITY RATIO
PARTICLE RADIUS, cm
RaB/RaA
RaC/RaA
RaB/RaA
RaC/RaA

7.32.

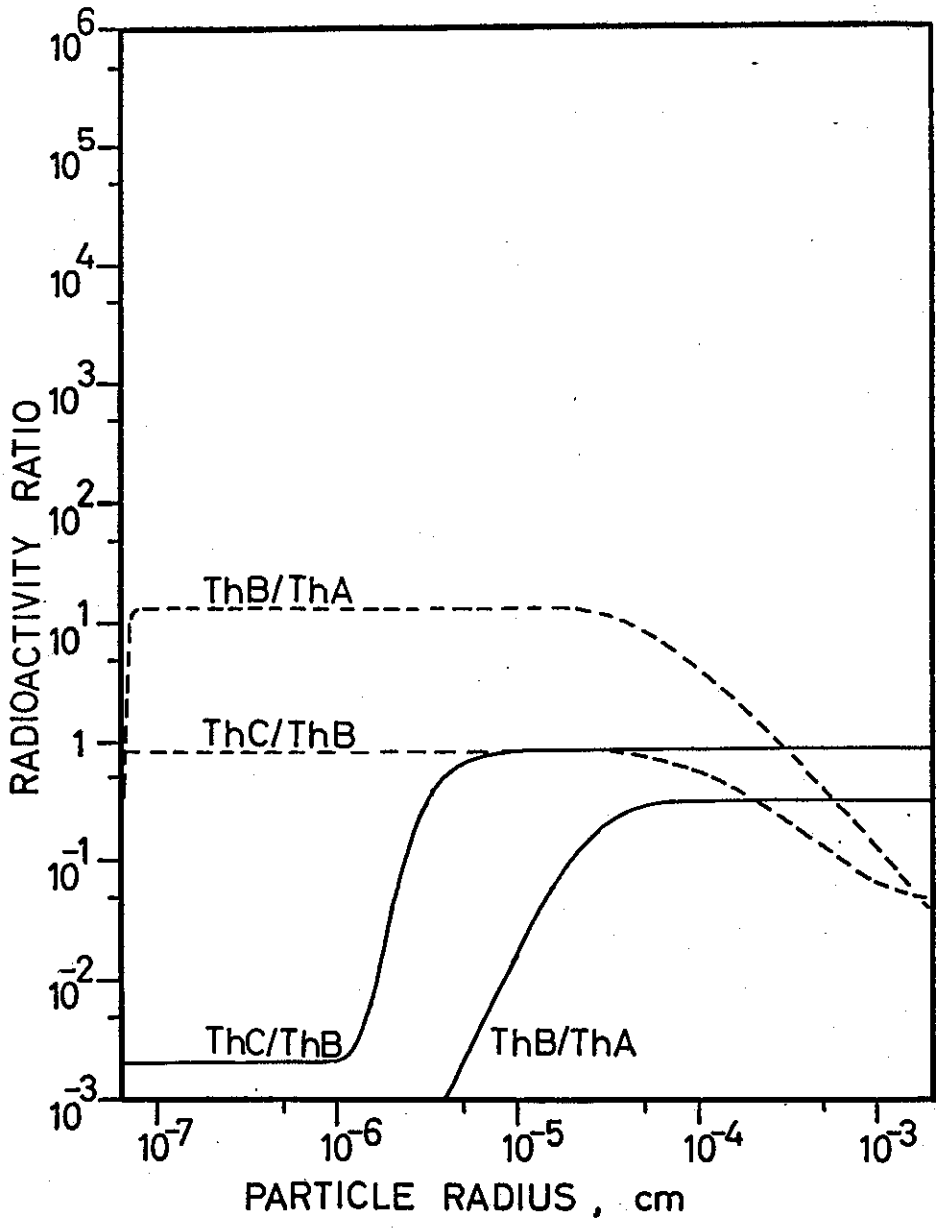

7.33.

Figs. 7.33 and 7.34. *Ratios between accumulated radioactivity on particles smaller or larger than the size indicated.* The aerosol and the environment are the same as in Fig. 7.21. Solid curves are for radioactivity accumulation from the lower end of the size distribution, broken curves from the upper end.

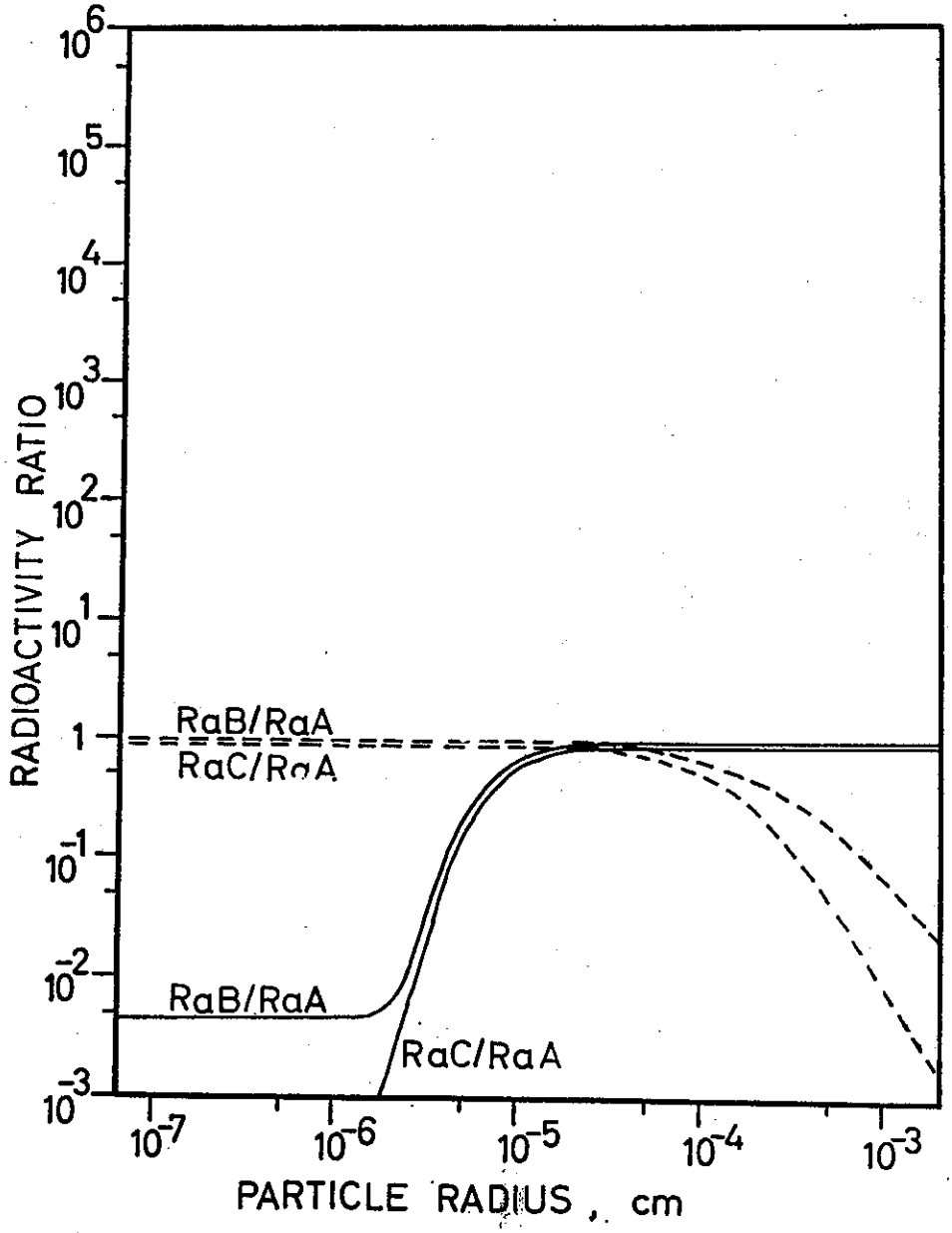
RADIOACTIVITY RATIO
PARTICLE RADIUS, cm
RaB/RaA
RaC/RaA
RaB/RaA
RaC/RaA

7.34.

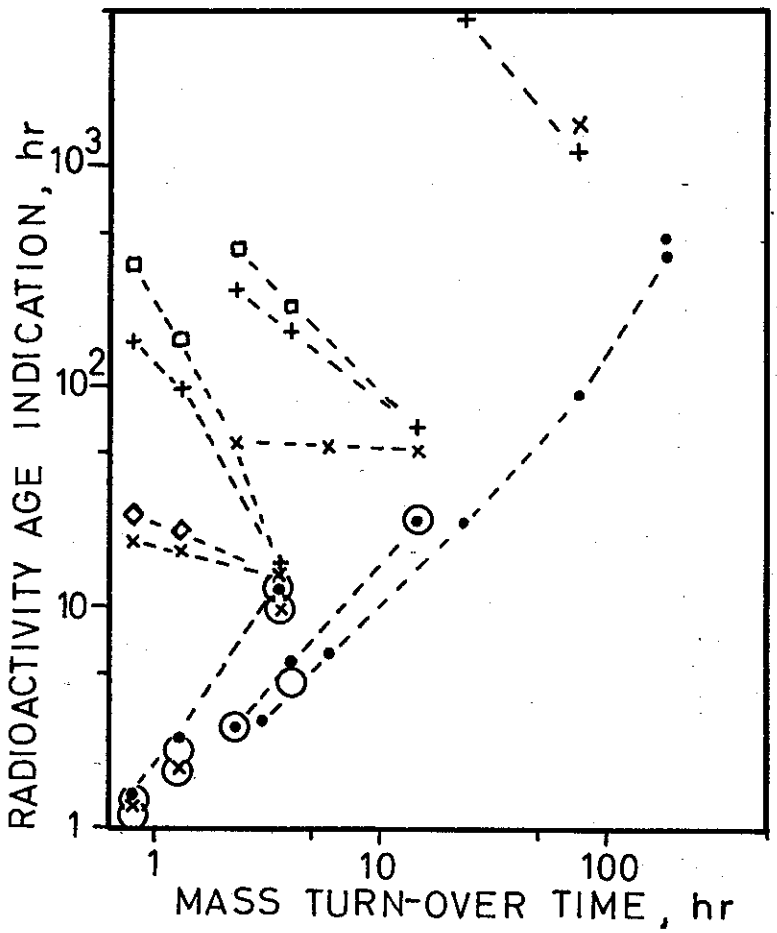

Fig. 7.35. *Age based on total aerosol radioactivity.* Dots show results of equations (6.18) in aerosols with non-radioactive environments. Used for radioactive environments results for ThB/ThA are indicated by +, ThC/ThB by squares, RaB/RaA by × and RaC/RaA by diamonds. The open circles are results from equation (6.20), regardless of type of environment. Curves connect series of results for which dilution only is varied.

8. Conclusion. The most important subject treated in this paper, together with the preceding one (7), is probably coagulation effects in an aerosol. Coagulation computations have been performed for all particle combinations in the aerosols, and as a result the interdependence of different particle size regions has been studied. It is evident that no size region can be studied separately, since the influence of the whole distribution is present everywhere. One interesting consequence is the completely different size distribution for thin and dense aerosols.

Generally accepted results of measurements are not in disagreement with the present results. On the other hand, the measured results are seldom specific enough to act as a test of the theory. The conclusions drawn are restricted to steady-state aerosols in dry weather, but it is expected that similar features are present in most aerosols. Quantitative results are of course bound to the degree of approximation achieved by Fuchs treatment of coagulation. Possible electric effects are also neglected. These points may be improved.

The distribution of short-lived natural radioactivity in the aerosol has also been studied in detail. Since individual elements are treated and general conclusions about their ratios are drawn, it is hoped that a foundation has been laid for further exploration of the field. It is the author's opinion that radioactivity mesurements, properly evaluated, can be a simple and rapid means of examining the state of an aerosol.

REFERENCES

(1) Abel, N., P. Winkler, C. E. Junge: Studies of size distributions and growth with humidity of natural aerosol particles, Final report, Max-Planck-Institut für Chemie, Mainz (1959).
(2) Blifford, J. H., Jr., L. B. Lockhart, Jr., B. H. Rosenstock: On the natural radioactivity in the air, J. Geophys. Res. **57**, 499—509 (1952).
(3) Fuchs, N. A.: The mechanics of aerosols, Pergamon Press, Oxford (1964).
(4) Haxel, O., G. Schumann: Selbstreinigung der Atmosphäre, Z. Physik, **142**, 127—32 (1955).
(5) Junge, C. E.: Air chemistry and radioactivity, Pergamon Press, New York (1963).
(6) Madelaine, G.: Comportement des descendants du radon et du thoron en atmosphere depoussiérée, Tellus **18**, 593, (1966).
(7) Storebø, P. B., C. Rho: Formation of a dense aerosol size distribution, J. Geophys. Res. **75**, 2931—8 (1970).

APPENDIX

Survey over related diagrams

Rather than introducing new aerosols when new aspects were to be discussed, care was taken to use only a limited selection of aerosols throughout the paper. Many aerosols therefore appear in a number of different diagrams. The following list over related diagrams may be of interest.

1) 4.1, 4.4, 4.10, 7.4, 7.7, 7.10, 7.13, 7.14
2) 4.1, 4.6, 4.8, 4.13, 5.20
3) 4.1, 4.4, 5.33, 7.6, 7.9, 7.12, 7.17, 7.18
4) 4.2, 4.4, 4.7, 4.11, 5.2, 7.19, 7.23, 7.27
5) 4.2, 5.13, 5.19, 7.20, 7.24, 7.28, 7.31, 7.32
6) 4.2, 5.15, 7.2, 7.3, 7.21, 7.25, 7.29, 7.33, 7.34
7) 4.3, 5.1
8) 4.3, 5.2
9) 4.3, 4.5, 4.12, 5.3, 7.22, 7.26, 7.30
10) 4.6, 5.3, 5.20
11) 4.6, 4.9, 4.14, 5.20, 7.5, 7.8, 7.11, 7.15, 7.16
12) 5.1, 5.24, 5.31
13) 5.9, 5.26
14) 5.9, 5.27
15) 5.13, 5.32, 5.39
16) 5.26, 5.33
17) 5.34, 5.38

Papers published in *Geofysiske Publikasjoner* may be obtained from: Universitetsforlaget, Blindern Oslo 3, Norway.

Vol. XXIII.

No. 1. Bernt Mæhlum: The sporadic E auroral zone. 1962.
» 2. Bernt Mæhlum: Small scale structure and drift in the sporadic E layer as observed in th auroral zone. 1962.
» 3. L. Harang and K. Malmjord: Determination of drift movements of the ionosphere at hig latitudes from radio star scintillations. 1962.
» 4. Eyvind Riis: The stability of Couette-flow in non-stratified and stratified viscous fluids. 196
» 5. E. Frogner: Temperature changes on a large scale in the arctic winter stratosphere and thei probable effects on the tropospheric circulation. 1962.
» 6. Odd H. Sælen: Studies in the Norwegian Atlantic Current. Part II: Investigations durin the years 1954—59 in an area west of Stad. 1963.

Vol. XXIV.

In memory of Vilhelm Bjerknes on the 100th anniversary of his birth. 1962.

Vol. XXV.

No. 1. Kaare Pedersen: On the quantitative precipitation forecasting with a quasi-geostrophic mode 1963.
» 2. Peter Thrane: Perturbations in a baroclinic model atmosphere. 1963.
» 3. Eigil Hesstvedt: On the water vapor content in the high atmosphere. 1964.
» 4. Torbjørn Ellingsen: On periodic motions of an ideal fluid with an elastic boundary. 196
» 5. Jonas Ekman Fjeldstad: Internal waves of tidal origin. 1964.
» 6. A. Eftestøl and A. Omholt: Studies on the excitation of N_2 and N_2^+ bands in aurora. 196

Vol. XXVI.

No. 1. Eigil Hesstvedt: Some characteristics of the oxygen-hydrogen atmosphere. 1965.
» 2. William Blumen: A random model of momentum flux by mountain waves. 1965.
» 3. K. M. Storetvedt: Remanent magnetization of some dolerite intrusions in the Egersund Area Southern Norway. 1966.
» 4. Martin Mork: The generation of surface waves by wind and their propagation from a storm area. 1966.
» 5. Jack Nordø: The vertical structure of the atmosphere. 1965.
» 6. Alv Egeland and Anders Omholt: Carl Størmer's height measurements of aurora. 1966.
» 7. Gunnvald Bøyum: The energy exchange between sea and atmosphere at ocean weather station M, I and A. 1966.
» 8. Torbjørn Ellingsen and Enok Palm: The energy transfer from submarine seismic waves t the ocean. 1966.
» 9. Torkild Carstens: Experiments with supercooling and ice formation in flowing water. 196
» 10. Jørgen Holmboe: On the instability of stratified shear flow. 1966.
» 11. Lawrence H. Larsen: Flow over obstacles of finite amplitude. 1966.

Vol. XXVII.

No. 1. Arne Grammeltvedt: On the nonlinear computational instability of the equations of one dimensional flow. 1967.
» 2. Jørgen Holmboe: Instability of three-layer models in the atmosphere. 1968.
» 3. Einar Høiland and Eyvind Riis: On the stability of shear flow of a stratified fluid. 1968.
» 4. Eigil Hesstvedt: On the effect of vertical eddy transport on atmospheric composition in th mesosphere and lower thermosphere. 1968.
» 5. Eigil Hesstvedt: On the photochemistry of ozone in the ozone layer. 1968.
» 6. Arnt Eliassen: On meso-scale mountain waves on the rotating earth. 1968.
» 7. Kaare Pedersen and Knut Erik Grønskei: A method of initialization for dynamical weathe forecasting, and a balanced model. 1969.

A.s John Griegs Boktrykkeri